Published for SISSA by Springer

Received: *February 28, 2022*
Revised: *April 11, 2022*
Accepted: *April 25, 2022*
Published: *May 17, 2022*

Four-point functions with multi-cycle fields in symmetric orbifolds and the D1-D5 CFT

Andre Alves Lima,[a] **G.M. Sotkov**[a] **and M. Stanishkov**[b]

[a] *Department of Physics, Federal University of Espírito Santo, 29075-900, Vitória, Brazil*

[b] *Institute for Nuclear Research and Nuclear Energy, Bulgarian Academy of Sciences, 1784 Sofia, Bulgaria*

E-mail: andrealves.fis@gmail.com, gsotkov@gmail.com, marian@inrne.bas.bg

Abstract: We study S_N-invariant four-point functions with two generic multi-cycle fields and two twist-2 fields, at the free orbifold point of the D1-D5 CFT. We derive the explicit factorization of these functions following from the action of the symmetric group on the composite multi-cycle fields. Apart from non-trivial symmetry factors that we compute, the function with multi-cycle operators is reduced to a sum of connected correlators in which the composite fields have, at most, two cycles. The correlators with two double-cycle and two single-cycle fields give the leading order contribution in the large-N limit. We derive explicit formulas for these functions, encompassing a large class of choices for the single- and the double-cycle fields, including generic Ramond ground states, NS chiral fields and the marginal deformation operator. We are thus able to extract important dynamical information from the short-distance OPEs: conformal dimensions, R-charges and structure constants of families of BPS and non-BPS fields present in the corresponding light-light and heavy-light channels. We also discuss properties of generic multi-cycle Q-point functions in M^N/S_N orbifolds, using a technology due to Pakman, Rastelli and Razamat.

Keywords: Scale and Conformal Symmetries, Conformal Field Models in String Theory, Discrete Symmetries

ArXiv ePrint: 2202.12424

https://doi.org/10.1007/JHEP05(2022)106

JHEP05(2022)106

Contents

JHEP05(2022)106

1 Introduction and summary

The AdS/CFT correspondence has been a two-way lane leading to insights both into quantum gravity and into aspects of the strong coupling structure of quantum field theories. Significant computational (and conceptual) developments have sprung from modern technologies devised to compute correlation functions using the full resource of the symmetries of holographic CFTs. Progress has been notable, in particular, in the context of four-dimensional $\mathcal{N}=4$ SYM dual to $\mathrm{AdS}_5\times\mathbb{S}^5$, with some results extending to other instances of $\mathrm{AdS}_{d+1}/\mathrm{CFT}_d$ with $d>2$. Meanwhile, the study of correlation functions in $\mathrm{AdS}_3/\mathrm{CFT}_2$ has progressed at a somewhat different pace. Methods such as Witten diagrams and Mellin transforms meet some technical difficulties when faced with the idiosyncrasies of two-dimensional CFTs [1–3]. On the other hand, it is precisely the exceptional nature of CFT_2 and of $\mathrm{AdS}_3\times\mathbb{S}^3$ that makes $\mathrm{AdS}_3/\mathrm{CFT}_2$ special [4–7], and correlation functions in the holographic symmetric orbifold CFT particularly relevant.

1.1 On the problem of computing four-point functions in the D1-D5 CFT

One of the ongoing programs for computing four-point functions in $\mathrm{AdS}_3/\mathrm{CFT}_2$ uses 'microstate geometries' as a tool [1, 2, 8–14]. Microstate geometries are horizonless solutions of Type IIB supergravity that are asymptotically $\mathrm{AdS}_3\times\mathbb{S}^3\times M$. They are part of the conjectured 'fuzzball' resolution of black holes formed by bound D1-D5 branes wrapping $\mathbb{T}\times M$, with M being $\mathbb{T}^4$ or K3 [15, 16]. The dual CFT_2, called 'the D1-D5 CFT', is a $\mathcal{N}=(4,4)$ superconformal theory in the moduli space of the symmetric orbifold M^N/S_N. A vast collection of such geometries has now been found, largely due to the development of the fuzzball program. In particular, $\frac{1}{4}$-BPS geometries have been completely classified, being dual to superpositions of Ramond ground states; classes of $\frac{1}{8}$-BPS geometries are known as well [15–20]. In the semi-classical limit where $N\gg 1$, the central charge of the D1-D5 CFT, $c=6N$, is very large. As $c\to\infty$, an operator is said to be 'heavy' if its conformal weight scales as $h_H\sim c$, or 'light' if its weight h_L is fixed and finite. Operators dual to specific (microstate) geometries are heavy: for example, the Ramond ground states have $h_H=\frac{1}{24}c$. On the other hand, probe-like fields in the bulk are light. If O_H and O_L are heavy and light, respectively, the four-point function

$$\left\langle \bar{O}_H(\infty)\,\bar{O}_L(1)\,O_L(z,\bar{z})\,O_H(0)\right\rangle \tag{1.1}$$

can be regarded as a two-point function of O_L in the state $|O_H\rangle$. In the bulk, this corresponds to the propagator of the light field dual to O_L in the asymptotically $\mathrm{AdS}_3\times\mathbb{S}^3$ geometry dual to $|O_H\rangle$.

Relating the bulk and CFT descriptions requires, first of all, that one knows the precise translation of O_H into a microstate geometry, and of O_L into a bulk field. Pages of the holographic dictionary were written some time ago [16–21], others more recently [22–24]. From the bulk perspective, several examples of heavy-light correlators based on microstate geometries [1, 2, 8–10, 12–14] have been studied, the computation of (1.1) amounting to solving a wave equation in the fixed space-time background. One of the interesting uses of these correlators is to contrast them against known universal semi-classical properties

JHEP05(2022)106

of correlators in AdS. At large c, the form of conformal blocks of heavy-light four-point functions is constrained by AdS symmetries [25–32], resulting in phenomena associated with the thermality of AdS black holes, such as "spurious singularities" outside of OPE limits, that contradict the unitarity of the CFT. It has been argued that these paradoxical properties should be resolved by corrections appearing at order $1/c$, but in [8, 10] explicit computations with known microstate geometries revealed examples of heavy-light correlators that are unitary already at leading order in c.

The holographic dictionary between SUGRA and the D1-D5 CFT in the free orbifold point is based on the proper identification of protected states, BPS operators, their OPE algebra, and the corresponding three-point functions [20–24]. Now, *four*-point functions are not guaranteed to be protected when the free CFT is deformed in moduli space, even if they involve only protected operators. This is because four-point functions typically depend also on non-BPS (i.e. non-protected) fields that might appear in channels of the OPEs between pairs of twisted operators. This is true, in particular, of the deformation modulus, which has twist 2. Thus, while the holographic dictionary allows us to identify which heavy/light SUGRA fields correspond to which heavy/light CFT operators, there is generally a mismatch between computing the heavy-light function (1.1) in terms of linear fluctuations around microstate geometries, or as the corresponding correlator in the free CFT. Explicit examples of this can be found, for instance, in refs. [8, 9]; the correlators computed in [8] in the SUGRA and in the free CFT descriptions match, but those computed in [9], involving less symmetric heavy fields, do not. So, to completely fix the dictionary between four-point functions, it is necessary to determine the conditions that select contributions (at leading order) only from OPE channels containing BPS operators. The computation of (1.1) in the free orbifold point, as well as a study of the non-BPS content of the different OPE channels, appears to be an important step towards this goal.

Computing functions like (1.1), even at the free point, is not always easy. The twisted boundary conditions of the symmetric orbifold M^N/S_N often causes correlation functions to be rather complicated. The orbifold has twisted sectors corresponding to permutations $\prod_n (n)^{N_n} \in S_N$, where (n) is a cycle of length n, and the multiplicities $[N_n]$ form a partition $\sum_n nN_n = N$. The fact that permutations are uniquely decomposable into disjoint cycles can be interpreted as saying that multi-cycle fields are "composite", while single-cycle fields are indecomposable. In this sense, single- and multi-cycleness in the orbifold CFT_2 is analogous to single- and mutli-traceness in four-dimensional $\mathcal{N} = 4$ SYM. Heavy fields, such as the Ramond ground states, are multi-cycle, while light fields, and in particular "elementary" fields, are generically single-cycle. Typically, Ramond ground states are in fact made of many cycles, also known as 'strands', with different lengths and "spins". Hence (1.1) is typically a complicated function, with all the S_N monodromy properties and selection rules that ensue. One way to still have a not-very-complicated function is to take the light fields in (1.1) to be *un*twisted. This simplifies the permutations to such an extent that one does not even need to resort to covering surfaces. Examples of such computations have been considered in many places [1, 8–10, 14], leading to very interesting results as mentioned above. It is well known, however, that the complete holographic bulk-boundary

JHEP05(2022)106

dictionary — for, say, light NS chiral fields with conformal dimension one or two — must include both untwisted *and* twisted (with twist 2) fields with equal conformal dimensions.

1.2 A summary of our results

In the present paper we consider examples of four-point functions with the simplest configuration of *twisted* light NS fields. That is, our goal is to study correlators where *all fields are non-trivially twisted* and, besides, some of the fields (e.g. the heavy Ramond ground states) can be *multi*-cycle.

The paper can be divided in two parts. In sections 2–3, we study general properties of correlation functions with multi-cycle fields in M^N/S_N orbifolds. In section 4, we apply our general results to the D1-D5 CFT, computing a collection of four-point functions with Ramond ground states, NS chiral fields and the deformation modulus.

More precisely, in section 2 we study generic Q-point functions of twisted fields, and extract their decomposition into components associated with equivalence classes of permutations in S_N. (To improve clarity, detailed derivations of the results of section 2 are presented appendix B.) We follow the work of [33], but with some relevant differences. First, we keep the twists generic, not restricted to single cycles. Second, the derivation, in ref. [33], of the N-dependence of twisted correlators relies heavily on a diagrammatic interpretation of connected functions, while ours does not. Instead, we use a construction of equivalence classes of twist permutations entering in a given Q-point function. This is also a technology developed in [33]: the equivalence classes are in one-to-one correspondence with diagrams for connected correlators. Hence, although we do not resort to the diagrammatic interpretation, our analysis is in fact an application of the methodology of [33] to (often disconnected) correlation functions with generic, multi-cycle fields. That is a powerful technique, relating an orbifold CFT to the geometry of coverings of the Riemann sphere, via the conjugacy classes of twists, being thus related to 'Hurwitz theory' (see e.g. [34]). Here we try to outline how this language can be used explore symmetries of twisted correlation functions.

Specifically, we want to compute four-point functions involving (light) fields $Z_{[\ell]}$ with single-cycle twists of length $\ell = 2$, and (heavy) multi-cycle fields $[\prod_{\zeta,n}(\bar{X}^{\zeta}_{[n]})^{N^{\zeta}_n}]$, with *arbitrary* twist given by a partition of N,

$$\Big\langle \Big[\prod_{\zeta,n}(\bar{X}^{\zeta}_{[n]})^{N^{\zeta}_n}\Big](\infty)\,\bar{Z}_{[2]}(1)\,Z_{[2]}(v,\bar{v})\Big[\prod_{\zeta,n}(X^{\zeta}_{[n]})^{N^{\zeta}_n}\Big](0)\Big\rangle, \qquad \text{where} \quad \sum_{n,\zeta} N^{\zeta}_n\, n = N. \tag{1.2}$$

Here we use an index ζ to possibly distinguish between distinct components of the multicycle field which have the same cycle length n. For example, in the case where the multicycle field is a Ramond ground state, ζ indicates the R-charges of the strands. We focus on twists $\ell = 2$ for the single-cycle Z fields for two reasons. First, it is the simplest non-trivial twist. Second, the interesting moduli that deform the free orbifold CFT into an interacting theory dual to SUGRA solutions lie in the twisted sector with $\ell = 2$ [35, 36]. We will specifically consider the marginal deformation operator $O^{(\text{int})}_{[2]}$ which is a scalar under all

JHEP05(2022)106

SU(2) symmetries of the $\mathcal{N} = (4, 4)$ superconformal algebra. We also consider NS chirals with $\ell = 2$ which include, in particular, another set of operators with dimension one, the "middle-cohomology" NS chirals.

The function (1.2) is typically *disconnected*. By this, we mean that it factorizes into products of functions involving only some of the operators that compose the multi-cycle field — not only products of two-point functions, but also of three- and four-point functions with "smaller" composite fields. In other words, the *'disconnected four-point functions'* addressed in this paper are not "bubble diagrams"; in fact, they are still dynamical objects. It is well-known that twisted correlation functions are associated with ramified covering surfaces of the Riemann sphere [37, 38]. The nomenclature 'disconnected' also agrees with the fact that, since the correlator factorizes, its associated covering surface can be seen as a product of disconnected surfaces.

One important information to be extracted from correlation functions is how they depend on N or, at least, how they scale with large N. For connected correlators, the exact dependence found in [33] reproduces the result of [37],

$$\text{Connected single-cycle } Q\text{-point function} \sim \sum_{\mathbf{g}} N^{-\mathbf{g}+1-\frac{1}{2}Q} \tag{1.3}$$

where $\mathbf{g}$ is the genus of the covering surface. For multi-cycle fields, the disconnected functions are associated with disconnected covering surfaces, for which the $\mathbf{g}$ is not well-defined. Still, we find a natural generalization of (1.3), featuring the Euler invariant χ instead of $\mathbf{g}$,

$$\left[\begin{array}{c}\text{Disconnected* multi-cycle } Q\text{-point function} \\ \text{with } R \geq Q \text{ cycles}\end{array}\right] \sim \sum_{\chi} N^{\frac{1}{2}(\chi-R)}. \tag{1.4}$$

The Euler invariant χ *is* a well-defined, additive property of disconnected surfaces. For connected surfaces/correlators, it reduces to $\chi = 2 - 2\mathbf{g}$, and, if the fields are single-cycle, i.e. $R = Q$, eq. (1.4) reduces to (1.3). The reason for the * in eq. (1.4) is that the formula requires some assumptions about the twists: the number of cycles and their lengths must both be kept *fixed* when $N \to \infty$. These assumptions are very natural for connected single-cycle functions, but they do not hold for some of the most important examples of multi-cycle fields. In particular, they do not hold for functions like (1.2), unless $N_1^{\zeta} \to \infty$. To find how functions that do not fulfill the assumptions of (1.4) depend on N can be a rather difficult problem in general, that is strictly dependent on the twists of all fields entering the correlator. Let us note that many results that we derive in section 2 were previously found by Dei and Eberhardt in [39].

In section 3, we apply the language developed in section 2 for generic Q-point functions, to study (1.2) in full detail. Generalizing our previous works [40, 41], where similar functions were considered, here we work at the level of M^N/S_N orbifolds, i.e. focusing only on the twists, not on the specific form of the fields $X^{\zeta}_{[n]}$ and $Z_{[2]}$. Because transpositions are the simplest non-trivial elements of S_N, we are able to derive in detail the structure of these four-point functions, including the explicit way it factorizes into connected parts

$$\left\langle \left[\bar{X}^{\zeta_1}_{[n_1]}\bar{X}^{\zeta_2}_{[n_2]}\right](\infty)\, \bar{Z}_{[2]}(1)\, Z_{[2]}(v,\bar{v})\, \left[\bar{X}^{\zeta_1}_{[n_1]}\bar{X}^{\zeta_2}_{[n_2]}\right](0)\right\rangle, \tag{1.5}$$

JHEP05(2022)106

containing only double-cycle components of the original multi-cycle field, multiplied by "symmetry factors". The double-cycle functions (1.5) always appear in the factorization of (1.2) in association with a covering surface of genus zero. While, for connected correlators with the same number of twists, the genus-zero contributions always dominate over higher genera, in the factorization of (1.2) there are also genus-one contributions, but with only one single-cycle component $X^{\zeta}_{[n]}$, instead of the composite double-components seen in (1.5). By themselves these single-cycle, genus-one functions contribute at order N^{-2}, which is the same as the double-cycle, genus-zero functions (1.5). But we show that, when multiplied by their symmetry factors, the genus-zero contributions do dominate when N is large.

Let us note that, apart from the argument that the genus-zero functions dominate at large N, we will not take N to be large in our formulas, so most of our formulas are exact at *finite* N. This is why, through most of the paper, we avoid the nomenclature 'heavy' and 'light' fields, preferring 'multi-cycle' and 'single-cycle' fields instead. It should be kept in mind, nevertheless, that, in the D1-D5 CFT examples we consider, the multi-cycle fields are almost always heavy (Ramond) fields, the single-cycle fields are always light, and that heavy-light correlators in the semi-classical limit are an important part of our motivations.

Focusing on (1.5), the appropraite genus-zero covering map was derived in [40]. Here we present a detailed analysis of the geometry of the covering surfaces, and the relation between coverings and permutation classes. The goal is to understand how the geometry dictated by the twists controls the form of the correlation functions. The connected functions can be decomposed into **H** 'Hurwitz blocks', where **H** is the Hurwitz number of different coverings of the sphere.[1] These blocks are defined by the roots of an algebraic equation, which cannot be found in closed form when $n_1 \neq n_2$, but nevertheless fix many properties of the correlation functions. In particular, they determine the twists of the fields appearing in the OPE channels,

$$\begin{aligned} \bar{Z}_{[2]} \times Z_{[2]} &= C_{Z\bar{Z}U}\ \{U_{[1]}\} + C_{Z\bar{Z}S}\ \{S_{[3]}\} \\ Z_{[2]} \times [X^{\zeta_1}_{[n_1]} X^{\zeta_2}_{[n_2]}] &= C_{[\bar{X}\bar{X}]\bar{Z}Y}\ \{Y_{[n_1+n_2]}\} \\ &\quad + C_{\bar{X}\bar{Z}[WX]} B_{\bar{X}X}\ \left\{ [W_{[n_1-n_2]} X^{\zeta_2}_{[n_2]} X^{\zeta_2}_{[n_2]}] \right\} \end{aligned} \tag{1.6}$$

where Cs are structure constants, B a two-point function normalization, and curly brackets indicate conformal families. The appearance of the composite field containing the operator $W_{[n_1-n_2]}$, with twist length $n_1 - n_2$, is the result of an interesting interaction between the twist permutations in the $v \to 0$ channel, which was previously overlooked in our papers [40, 41], and is now analyzed in detail within this more general context of M^N/S_N orbifolds. When $n_1 = n_2$, we also find a special symmetry between covering surfaces (or equivalence classes, or Hurwitz blocks), that allow us to compute the correlators in closed form on the base sphere, while "reducing the Hurwitz number by half".

In section 4 we turn our attention from M^N/S_N orbifolds in general to the D1-D5 CFT (at the free-orbifold point) specifically. We derive a pair of "master formulas" that encompass many different choices for the operators in (1.2)–(1.5). The multi-cycle fields

[1] Hurwitz blocks correspond to diagrams in the language of [33].

JHEP05(2022)106

can be Ramond ground states or composite NS chirals, and the single-cycle fields can be Ramond fields, NS chirals or the scalar deformation modulus taking the CFT away from the free-orbifold point. With these functions, we can use the technology of section 3 to extract conformal data. Besides the twists, we can find the dimensions of the operators and the structure constants in the OPEs (1.6). In refs. [40, 41] this analysis was performed when $Z_{[2]}$ is the interaction modulus $O^{(\mathrm{int})}_{[2]}$, and the $X^{\zeta}_{[n]}$ are Ramond ground states of the n-twisted sector. Here, with our general functions, we can extend these results to find the OPEs between $O^{(\mathrm{int})}_{[2]}$ and NS chirals, between NS chirals and Ramond ground states, and also between single-cycle and composite NS chirals themselves. In the latter case, we note that the form of the correlation functions is restricted by the NS chiral ring, and show that we can recover some known structure constants [42–44] by taking $n_2 = 1$, reducing the composite field to a single-cycle one.

The D1-D5 CFT's $\mathcal{N} = (4, 4)$ superconformal algebra has a symmetry under 'spectral flow' [45], that changes weights and R-charges of fields, and relates states in the NS and Ramond sectors. In section 4.4, we discuss the effect of spectral flow on four-point functions, and show how it connects specific pairs of functions derived with our master formulas.

We close with a brief discussion of our results and a few comments concerning the derivation of a new family of four-point functions related to D1-D5-P superstrata. These four-point functions, which involve excitations of the left-moving twisted Ramond ground states, can be found in terms of the correlators calculated in the present paper, using standard $\mathcal{N} = 4$ super-conformal Ward identities.

2 Multi-cycle correlators on S_N orbifolds

The M^N/S_N orbifold is made by N identical copies of a "seed theory" in M, each copy labeled by an index $I = 1, \cdots, N$, and all independent, so that the total central charge is $c = Nc_{\mathrm{seed}}$. The Hilbert space decomposes into twisted sectors created by 'bare twist fields' $\sigma_g(z)$. The permutation g acts on copy indices of operators going around the twist, $O_I(e^{2\pi i}z)\sigma_g(0) = O_{g(I)}(z)\sigma_g(0)$. Every $g \in S_N$ can be uniquely decomposed as a product of disjoint cycles of different lengths n_i, $(n_i) = (I_1, \cdots, I_{n_i}) \in \mathbb{Z}_{n_i}$,

$$g = \textstyle\prod_n (n)^{N_n}, \qquad \sum_n nN_n = N. \tag{2.1}$$

The conformal weight of σ_g, with g given in (2.1), is the sum

$$h^{\sigma}_{[N_n]} = \sum_n N_n h^{\sigma}_n, \quad h^{\sigma}_n = \frac{1}{4}\Big(n - \frac{1}{n}\Big) = \tilde{h}^{\sigma}_n \tag{2.2}$$

where h^{σ}_n is the dimension of the single-cycle components [37, 46]. The same is true for anti-holomorphic weight $\tilde{h}^{\sigma}_{[N_n]}$, and the total dimension is $\Delta^{\sigma}_{[N_n]} = h^{\sigma}_{[N_n]} + \tilde{h}^{\sigma}_{[N_n]}$. The weight (2.2) is the same for any g in the conjugacy class $[g] = \{hgh^{-1} \,|\, h \in S_N\}$, associated with the partition

$$[N_n] \equiv \{N_n \in \mathbb{N} \mid \textstyle\sum_n nN_n = N\}. \tag{2.3}$$

Twists corresponding to individual permutations are not invariant under actions of S_N. An invariant field can be built by summing over the orbit of $g \in S_N$ under the action

JHEP05(2022)106

of S_N by conjugacy,

$$\sigma_{[g]} \equiv \frac{1}{\mathscr{S}_{[g]}} \sum_{h \in S_N} \sigma_{hgh^{-1}}. \tag{2.4}$$

The factor $\mathscr{S}_{[g]}$ ensures that the S_N-invariant two-point function normalization is the same as that of its (non-S_N-invariant) components. In section B.1 we show that

$$\mathscr{S}_{[g]} = \sqrt{N!|\mathrm{Cent}[g]|} \tag{2.5}$$

where the order of the centralizer of g in S_N is[2]

$$|\mathrm{Cent}[g]| = \prod_n N_n!\, n^{N_n} \quad \text{for} \quad g = \prod_n (n)^{N_n}, \quad \sum_n N_n n = N. \tag{2.6}$$

The result (2.5) was previously found in [39]. For single cycles $g = (n)(1)^{N-n}$, it yields the usual normalization factor [33, 37, 48] which we will denote by $\mathscr{S}_n$, and for double cycles $g = (n_1)(n_2)(1)^{N-n_1-n_2}$ we obtain a normalization denoted by $\mathscr{S}_{n_1,n_2}$,

$$\mathscr{S}_n = \sqrt{N!(N-n)!n}, \qquad \mathscr{S}_{n_1,n_2} = \sqrt{N!(N-n_1-n_2)!n_1 n_2}. \tag{2.7}$$

Excited twisted fields can also be combined into S_N-invariant operators, in the same way as (2.4), and with the same normalization (2.5).

2.1 Twisted Q-point functions

Q-point functions of twisted operators are subject to selection rules associated with the permutations carried by the fields. A fundamental property of a twisted correlator, possibly with a collection $\mathscr{X}$ of excitations, is that the permutations must compose to the identity $\mathrm{id} \in S_N$,

$$\Big\langle \mathscr{X} \prod_{i=1}^{Q} \sigma_{g_i}(z_i) \Big\rangle \neq 0 \quad \text{only if} \quad g_1 \cdots g_Q = \mathrm{id} \tag{2.8}$$

otherwise the function would have ill-defined monodromy. If the g_i can be separated into two disjoint sets $\{g_i\} = \{g_k\} \sqcup \{g_\ell\}$, such that one set commutes with the other, the function factorizes,

$$\Big\langle \mathscr{X} \prod_i \sigma_{g_i}(z_i) \Big\rangle = \Big\langle \mathscr{Y} \prod_k \sigma_{g_k}(z_k) \Big\rangle \Big\langle \mathscr{Y}' \prod_\ell \sigma_{g_\ell}(z_\ell) \Big\rangle \tag{2.9}$$

where $\mathscr{Y}$ and $\mathscr{Y}'$ are excitations of the respective sets of bare twists. A function which cannot be factorized in such a way is called 'connected'. In this section, we will be interested only on the S_N-related properties of twisted correlators, so we now consider functions of bare twists $\sigma_{[g]}$ only. The Q-point function of invariant operators is the sum

$$\Big\langle \sigma_{[g_1]}(z_1) \cdots \sigma_{[g_Q]}(z_Q) \Big\rangle = \frac{1}{\prod_i \mathscr{S}_{[g_i]}} \sum_{\substack{h_1 \in S_N \\ \cdots \\ h_Q \in S_N}} \Big\langle \sigma_{h_1 g_1 h_1^{-1}}(z_1) \cdots \sigma_{h_Q g_Q h_Q^{-1}}(z_Q) \Big\rangle. \tag{2.10}$$

[2] We recall the definition of $\mathrm{Cent}[g]$ in (B.5). See e.g. [47] for a derivation of formula (2.4).

JHEP05(2022)106

Many terms of the sum of the r.h.s. vanish because they do not satisfy the condition (2.8). It is convenient to replace the individual sums over the orbits of the $\{g_i\}$ by sums of different equivalence classes of permutations that do satisfy (2.8). Let $p_i = h_i g_i h_i^{-1}$ be the permutations in the r.h.s. of (2.10), and consider an ordered sequence $\{p_1, \cdots, p_Q\}$ that satisfies (2.8),

$$p_1\, p_2\, \cdots\, p_Q = \mathrm{id}. \tag{2.11}$$

This will also be satisfied by every other sequence in the *equivalence class* α defined by

$$\alpha: \quad \{p_1, p_2, \cdots, p_Q\} \sim \{k p_1 k^{-1}, k p_2 k^{-1}, \cdots, k p_Q k^{-1}\}, \tag{2.12}$$

i.e. a *global* conjugation of every p_i by the *same* $k \in S_N$. Moreover, all correlators $\langle \sigma_{p_1}(z_1) \cdots \sigma_{p_Q}(z_Q)\rangle$ with the $\{p_i\}$ in a given class α will be equal by symmetry, because the global conjugation only relabels every copy in the twists, and all copies are identical. If we denote the set of all such conjugacy classes by Cl, the sum over orbits in (2.10) can be replaced by a sum over all $\alpha \in \mathrm{Cl}$, where we take one representative correlator for each class α, and multiply it by a "symmetry factor" $\mathcal{N}_\alpha$, counting the number of permutations in α. It is convenient to separate the classes according to the number $\mathbf{c}$ of distinct copies that participate in *non-trivial* cycles (i.e. cycles of length $n > 1$).[3] This number is, of course a class property, so we can decompose $\mathrm{Cl} = \cup_{\mathbf{c}} \mathrm{Cl}_{\mathbf{c}}$. In the end, the r.h.s. of eq. (2.10) becomes

$$\Big\langle \sigma_{[g_1]}(z_1) \cdots \sigma_{[g_Q]}(z_Q) \Big\rangle = \frac{1}{\prod_i \mathscr{S}_{[g_i]}} \sum_{\mathbf{c}} \sum_{\alpha_{\mathbf{c}} \in \mathrm{Cl}_{\mathbf{c}}} \mathcal{N}_{\alpha_{\mathbf{c}}} \Big\langle \sigma_{p_1^{\alpha_{\mathbf{c}}}}(z_1) \cdots \sigma_{p_Q^{\alpha_{\mathbf{c}}}}(z_Q) \Big\rangle \tag{2.13}$$

In appendix B we give several examples of classes α and discuss the set Cl in detail. Some of the classes are made of permutations that factorize, as in (2.9), one or more times. The type of factorization is, also, a class property. In appendix B we show that the symmetry factor $\mathcal{N}_{\alpha_{\mathbf{c}}}$ is basically the same for every class $\alpha_{\mathbf{c}} \in \mathrm{Cl}_{\mathbf{c}}$,

$$\mathcal{N}_{\alpha_{\mathbf{c}}} = \frac{N!}{(N-\mathbf{c})!} \left(\prod_{i=1}^{Q} |\mathrm{Cent}[g_i]| \right) \nu_{\alpha_{\mathbf{c}}}. \tag{2.14}$$

The only class-dependent factor, $\nu_{\alpha_{\mathbf{c}}}$, is given by eq. (B.18). In classes $\alpha_{\mathbf{c}}$ where no two-point function factorizes, $\nu_{\alpha_{\mathbf{c}}} = 1$; in classes $\alpha_{\mathbf{c}}$ where there is a factorization of d two-point functions with cycles n_j, $j = 1, \cdots, d$, we have $\nu_{\alpha_{\mathbf{c}}} = 1/\prod_j n_j$. eqs. (2.13) and (2.14) contain the exact N-dependence of the twisted Q-point function,

$$\Big\langle \prod_{i=1}^{Q} \sigma_{[g_i]}(z_1) \Big\rangle = \left[\prod_{i=1}^{Q} \sqrt{\frac{|\mathrm{Cent}[g_i]|}{N!}} \right] \sum_{\mathbf{c}} \frac{N!}{(N-\mathbf{c})!} \sum_{\alpha_{\mathbf{c}} \in \mathrm{Cl}_{\mathbf{c}}} \nu_{\alpha_{\mathbf{c}}} \Big\langle \prod_{i=1}^{Q} \sigma_{p_i^{\alpha_{\mathbf{c}}}}(z_i) \Big\rangle \tag{2.15}$$

This formula generalizes a result of [33], which only considers connected functions. The *connected* classes $\alpha \in \mathrm{Cl}_{\mathbf{g}}$ can be described in a diagrammatic language developed in [33]; each class α corresponds to a different diagram, and the sum in eq. (2.22) is a "sum over diagrams".

[3] For example, for $N = 9$, the permutation $(1,2,3)(5,6)$, has $\mathbf{c} = 5$ non-trivial copies, namely copies $I = 1, 2, 3, 5, 6$. Copies $I = 4, 7, 9$ are trivial, as they do not participate in any non-trivial cycle. See the discussion below (B.12) for examples of *classes* of permutations with different $\mathbf{c}$.

JHEP05(2022)106

2.1.1 The large-N limit

The way eq. (2.15) depends on N seems to dwell solely in the coefficients multiplying the last sum over $\alpha_{\mathbf{c}} \in \mathrm{Cl}_{\mathbf{c}}$. If this was the case, it would suffice to expand these coefficients as functions of N to find scaling of the function as $N \to \infty$. This works for single-cycle correlators with cycles of fixed length [33], but when we consider multi-cycle fields, there are subtleties. A multi-cycle twist may be allowed to have a large number of cycles; an important example is $g_i = (n)^{N/n} \in S_N$. So the centralizers of g_i may depend on N, in eq. (2.15). Also, the number of terms in the sum over $\alpha_{\mathbf{c}} \in \mathrm{Cl}_{\mathbf{c}}$ may be very large, scaling with N. In summary, determining the scaling of a multi-cycle Q-point function in the large-N limit is a problem that depends intrinsically on the specific properties of the twists involved. The detailed analysis of a relatively simple case is the subject of section 2.1 below.

But, under certain assumptions, we can find an interesting generalization of the results of [33]. Let us isolate trivial cycles in the twist permutations,

$$g_i = (1)^{N-\sum_j N_j^{(i)} n_j^{(i)}} \prod_j (n_j^{(i)})^{N_j^{(i)}}, \qquad n_j^{(i)} > 1 \tag{2.16}$$

such that the order of the centralizers are

$$|\mathrm{Cent}[g_i]| = \left(N - \textstyle\sum_j N_j^{(i)} n_j^{(i)}\right)! \prod_j N_j!\; n_j^{N_j}. \tag{2.17}$$

If we now *assume that the cycle lengths* $n_j^{(i)}$ *and their multiplicities* $N_j^{(i)}$ *are fixed as* $N \to \infty$, we can use Stirling's formula to find

$$\sqrt{\frac{|\mathrm{Cent}[g_i]|}{N!}} \approx \sqrt{\textstyle\prod_j N_j^{(i)}!\; (n_j^{(i)})^{N_j^{(i)}}}\; e^{-\frac{1}{2}\sum_j N_j^{(i)} n_j^{(i)}}\; N^{-\frac{1}{2}\sum_j N_j^{(i)} n_j^{(i)}} \tag{2.18}$$

expanding the factor $N!/(N-\mathbf{c})!$ as well, eq. (2.15) becomes, up to order $1/N$,

$$\left\langle \prod_{i=1}^{Q} \sigma_{[g_i]}(z_1) \right\rangle \approx \sum_{\mathbf{c}} N^{\mathbf{c} - \frac{1}{2}\sum_i \sum_j N_j^{(i)} n_j^{(i)}}\, \varpi \sum_{\alpha_{\mathbf{c}} \in \mathrm{Cl}_{\mathbf{c}}} \nu_{\alpha_{\mathbf{c}}} \left\langle \sigma_{p_1^{\alpha_{\mathbf{c}}}}(z_1) \cdots \sigma_{p_Q^{\alpha_{\mathbf{c}}}}(z_Q) \right\rangle \tag{2.19}$$

The factor

$$\varpi = e^{\mathbf{c} - \frac{1}{2}\sum_i \sum_j N_j^{(i)} n_j^{(i)}} \sqrt{\textstyle\prod_i \prod_j N_j^{(i)}!\; (n_j^{(i)})^{N_j^{(i)}}} \tag{2.20}$$

is the same for all classes $\alpha_{\mathbf{c}}$, depends on the lengths n_r and on $\mathbf{c}$ but not on N. Let R be the total number of non-trivial cycles in *all* the permutations g_i, and $n_r > 1$, $r = 1, \cdots, R$, be their lengths, in such a way that we can write the sum in the exponent of N in eq. (2.19) as $\sum_i \sum_j N_j^{(i)} n_j^{(i)} \equiv \sum_{r=1}^{R} n_r$. Inserting this into eq. (2.19) leads to eq. (2.21).

$$\left\langle \prod_{i=1}^{Q} \sigma_{[g_i]}(z_1) \right\rangle = \sum_{\mathbf{c}} N^{\mathbf{c} - \frac{1}{2}\sum_{r=1}^{R} n_r} \left[1 + \mathrm{O}\left(\frac{1}{N}\right)\right] \varpi \sum_{\alpha_{\mathbf{c}} \in \mathrm{Cl}_{\mathbf{c}}} \nu_{\alpha_{\mathbf{c}}} \left\langle \prod_{i=1}^{Q} \sigma_{p_i^{\alpha_{\mathbf{c}}}}(z_i) \right\rangle \tag{2.21}$$

Note that the total number of these cycles is $R \geq Q$, and if all g_i are *single*-cycle permutations, $R = Q$. If we further assume that the sum over classes $\alpha_{\mathbf{c}} \in \mathrm{Cl}_{\mathbf{c}}$ in eq. (2.21)

JHEP05(2022)106

also do not depend on N, then we have found the leading large-N scaling of the function. This assumption about the sum over classes is not unrelated to the assumption used to derive (2.18). If there is a finite number of cycles with fixed (and finite) lengths n_r, then it is reasonable to expect a finite number of non-vanishing classes satisfying the condition (2.11). (This is true, for example, in the case of single-cycle fields.)

Eq. (2.21) can be written as

$$\left\langle \prod_{i=1}^{Q} \sigma_{[g_i]}\left(z_1\right) \right\rangle = \sum_{\chi} N^{\frac{1}{2}(\chi-R)} \left[1+\mathrm{O}\left(\frac{1}{N}\right)\right] \varpi\left(n_r\right) \sum_{\alpha_\chi \in \mathrm{Cl}_\chi} \nu_{\alpha_\chi} \left\langle \prod_{i=1}^{Q} \sigma_{p_i^{\alpha_\chi}}\left(z_i\right) \right\rangle \tag{2.22}$$

if we define the number

$$\chi\left(\mathbf{c}\right) \equiv 2\mathbf{c} + R - \sum_{r=1}^{R} n_r. \tag{2.23}$$

We can interpret χ as the *Euler characteristic of covering surfaces*, as follows. It is well-known that a connected twisted correlator is associated with a ramified covering surface Σ of the 'base sphere' $\mathbb{S}^2_{\text{base}}$ [37]. In a *connected* correlator, the number R of non-trivial cycles is the number of ramification points of Σ, the number $\mathbf{c}$ of distinct copies entering these cycles is the number of sheets of Σ, and the order of the ramification point associated with the cycle (n_r) is its length n_r. With this ramification data, the Riemann-Hurwitz formula gives the *genus* of the (connected) covering surface Σ to be

$$\mathbf{g} = 1 - \mathbf{c} - \frac{1}{2}R + \frac{1}{2}\sum_{r=1}^{R} n_r \tag{2.24}$$

which is compatible with (2.23), i.e. $\chi = 2 - 2\mathbf{g}$. But some of the classes $\alpha_{\mathbf{c}}$ may give *disconnected* correlators, which are products of ℓ connected functions. The latter are each associated with a covering surface Σ_i, and we can assoaciate the factorized correlator with their disjoint union $\Sigma_1 \sqcup \cdots \sqcup \Sigma_\ell$. The $\mathbf{c}$ non-trivial copies and the non-trivial cycles will be split among the factorized correlators in such a way that eq. (2.23) gives, schematically

$$\chi(\Sigma_1 \sqcup \cdots \sqcup \Sigma_\ell) = \chi(\Sigma_1) + \cdots + \chi(\Sigma_\ell), \tag{2.25}$$

which is the appropriate behavior of the Euler characteristic. Note that the maximum value of the Euler invariant is $\chi = 2$ when the covering surfaces have $\mathbf{g} = 0$, followed by $\chi = 0$ for $\mathbf{g} = 1$, and for higher genera $\chi < 0$. So, in eq. (2.22), as in the standard case, the leading-N contribution to the correlator comes from (possibly disconnected) the zero-genus covering surfaces.

Eq. (2.22) is a natural generalization, for disconnected functions, of the well-known scaling of connected Q-point functions as $\sim \sum_{\mathbf{g}} N^{-\mathbf{g}+1-\frac{1}{2}Q}$ [37]. Of course, for single-cycle, connected functions, our derivation above can be reduced to that of [33]. See also the more general results of [39].

Let us stress that formulas (2.21) and (2.22) for the large-N scaling only hold under certain assumptions about the twists of the multi-cycle fields. Essentially, we are assuming that, when $N \to \infty$, the number of cycles in the correlation function does not proliferate — hence, although the function may be disconnected, it disconnects into a product of a finite number of connected functions/covering surfaces.

JHEP05(2022)106

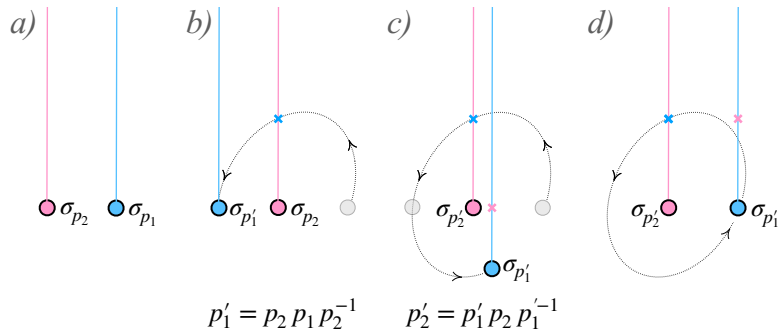

Figure 1. Moving twist operators on $\mathbb{S}^2_{\text{base}}$. Each twist creates a branch cut (dotted lines). Whenever a twist crosses a branch cut, its permutation changes.

2.1.2 The monodromy of classes

The twist $\sigma_p(z)$ creates a branch cut at $z \in \mathbb{S}^2_{\text{base}}$. When an operator crosses it, the copy indices are permuted by the action of p. If σ_{p_1} crosses the branch cut of σ_{p_2} counterclockwise (figure 1b), p_2 acts on p_1 by left conjugation, and σ_{p_1} becomes $\sigma_{p_1'}$ where $p_1' = p_2 p_1 p_2^{-1}$. (If the branch cut is crossed clockwise, p_2 acts by right conjugation on $p_1 \mapsto p_2^{-1} p_1 p_2$.) Completing the circular movement of the first twist, the second one crosses a branch cut and is also affected (figure 1c). The final configuration (figure 1d) has two different twists than the initial one (figure 1a), but the product of the permutations is preserved:

$$p_2' p_1' = p_2 p_1. \tag{2.26}$$

Thus, when we rotate the $\sigma_{p_i}(z_i)$ around each other inside a Q-point function we obtain a function with different twists. The condition (2.8) is, however, preserved, as a result of (2.26).

Suppose we start with a twisted Q-point function whose permutations belong to the equivalence class α. After rotating the twists as in figure 1, the final permutations belong to a different class $\alpha' \neq \alpha$. The fact that moving twist fields around each other moves between the different equivalence classes $\alpha \in \text{Cl}$ was called "channel crossing symmetry" in [33]. (Since each class is associated with a diagram, "channel crossing" is a symmetry of the set of all diagrams under the monodromies of a connected correlation function [33].)

In summary, correlation functions of individual permutations, such as (2.8), do not have well-defined monodromies, because individual twists are altered when they go around another twist. But the S_N-invariant functions (2.10) do have well-defined monodromies, because they are a sum over all equivalence classes α, hence explicitly channel-crossing symmetric.

2.2 Untwisted operators

When the correlation function contains operators in the untwisted sector, the discussion above must be modified. In this case, the sum over conjugacy orbits of (2.4) is not a good definition for an S_N-invariant untwisted operator. Instead, it should be replaced by a fully

JHEP05(2022)106

symmetrized tensor product

$$[\prod_i (X^{\zeta_i}_{[1]})^{p_i}] \equiv \frac{1}{\mathscr{S}} \mathrm{Sym}[\otimes_i (X^{\zeta_i}_{I^{(i)}_1} \otimes \cdots \otimes X^{\zeta_i}_{I^{(i)}_{p_i}})], \quad \mathscr{S} = \sqrt{\frac{N!}{(N-\sum_i p_i)! \prod_i (p_i!)}}. \tag{2.27}$$

Here it should be understood that the copies I entering the symmetrized tensor product are all different. The normalization factor $\mathscr{S}$, whose structure is different from the one in (2.4), counts the number of equivalent terms in the symmetrized product, and is derived in section B.4. When there is only one untwisted field, we have a simple sum over copies: $X_{[1]} \equiv N^{-\frac{1}{2}} \sum_{I=1}^{N} X_I$. For the N-fold product of two components $X^{\zeta_1}_I = X_I$ and $X^{\zeta_2}_I = Y_I$, we have

$$[\prod_{i=1}^{2} (X^{\zeta_i}_{[1]})^{p_i}] = \frac{1}{\mathscr{S}} \mathrm{Sym}[X^{\otimes p} Y^{\otimes (N-p)}], \quad \mathscr{S} = \sqrt{\binom{N}{p}}. \tag{2.28}$$

Fields with this structure appear, for example, in [9].

There is a way to extend the definition (2.27) to products of composite *twisted* fields, which is widely used in the literature concerned with fuzzballs and microstate geometries. A detailed derivation of the normalization factor analogous to the one in (2.27) can be found e.g. in [12]. This type of construction of S_N-invariant twisted fields is different from the sum over orbits that we use here, and the normalization factor in [12] differs from the one in eq. (2.4).[4] We note that, although it seems perhaps less intuitive than the straightforward symmetrization of copies, the sum over orbits is particularly useful for correlators whose fields are all twisted, as it is amenable to the equivalence-class decomposition of [33, 44, 49] discussed in section 2.1.

3 Four-point functions with two fields of twist two

From now on, we will be interested in four-point functions of the type

$$A(v, \bar{v}) = \left\langle \bar{\mathscr{X}}_{[N^\zeta_n]}(\infty) \bar{Z}_{[2]}(1) Z_{[2]}(v, \bar{v}) \mathscr{X}_{[N^\zeta_n]}(0) \right\rangle \tag{3.1}$$

where v is a anharmonic ratio. $Z_{[2]}$ is an S_N-invariant single-cycle field of length 2, and $\mathscr{X}_{[N^\zeta_n]}$ is a generic multi-cycle field with $\left[N^\zeta_n\right] = \left\{N^\zeta_n \in \mathbb{N} \,|\, \sum_{\zeta,n} n N^\zeta_n = N\right\}$

$$\mathscr{X}_{[N^\zeta_n]} \equiv \frac{1}{\mathscr{S}\left[N^\zeta_n\right]} \sum_{h \in S_N} \left[\prod_{\zeta,n} \left(X^\zeta_{h(n)h^{-1}}\right)^{N^\zeta_n}\right] \equiv \left[\prod_{\zeta,n} \left(X^\zeta_{[n]}\right)^{N^\zeta_n}\right] \tag{3.2}$$

It is usual to interpret single-cycle fields as "winding stands", see e.g. [15, 50]. In this language, $Z_{(2)}$ and $X^\zeta_{(n)}$ are excitations of a 2-wound and an n-wound strand, respectively. The index ζ labels possibly different excitations of the multiple strands that make up $\mathscr{X}_{[N^\zeta_n]}$, and the bar over $\bar{X}^\zeta_{(n)}$ indicates a field with opposite charges. For example, in the D1-D5

[4] The sum over the orbits in S_N has many "repeated" terms because the centralizer of the permutation is non-empty, as discussed extensively in appendix B; these repeated terms are duly accounted for in the normalization factor. In contrast, following [12] we sum over less terms.

JHEP05(2022)106

CFT, ζ labels different SU(2) charges.[5] In the D1-D5 CFT, we will mostly be interested in the case where $Z_{[2]}$ is a NS chiral or the interaction operator, and $X^{\zeta}_{(n)}$ are Ramond ground states, but, at this point, we focus only on the twist structure, which rules the factorization properties of the full correlator.

3.1 Factorization

The correlation function (3.1) factorizes because the cycles of $Z_{[2]}$ and $\bar{Z}_{[2]}$ can overlap with at most four of the cycles of $\mathscr{X}_{[N_n^{(s)}]}$ and $\bar{\mathscr{X}}_{[N_n^{(s)}]}$. To find the exact way the factorization occurs, recall that the r.h.s. of (3.1) is a multiple sum over orbits, and, apart from normalization factors, each term has the structure

$$A_{\alpha_{\mathbf{c}}} = \Big\langle [\prod_{\zeta,n} (\bar{X}^{\zeta}_{(n)})^{N^{\zeta}_n}](\infty)\ \bar{Z}_{(2)}(1)\ Z_{(2)}(v,\bar{v})\, [\prod_{\zeta,n} (X^{\zeta}_{(n)})^{N^{\zeta}_n}](0) \Big\rangle. \tag{3.3}$$

The term (3.3) factorizes in two different ways, depending on how the cycles of the four operators overlap. The first is a four-point function with only one component of each heavy field (we omit position dependences for brevity)

$$\Big\langle \bar{X}^{\zeta_1}_{(n_1)}\ \bar{Z}_{(2)}\ Z_{(2)}\ X^{\zeta_1}_{(n_1)} \Big\rangle, \tag{3.4a}$$

and the other possibility is a four-point function with double-cycle fields

$$\Big\langle [\bar{X}^{\zeta_1}_{(n_1)} \bar{X}^{\zeta_2}_{(n_2)}]\ \bar{Z}_{(2)}\ Z_{(2)}\ [X^{\zeta_1}_{(n_1)} X^{\zeta_2}_{(n_2)}] \Big\rangle. \tag{3.4b}$$

This restricted factorization follows because in both eqs. (3.4) there is, implicit, a product of factorized two-point functions $\langle \bar{X}^{\zeta}_{(n)}(\infty) X^{\zeta}_{(n)^{-1}}(0)\rangle = 1$, and the fields $X^{\zeta}_{(n)}$ and $\bar{X}^{\zeta}_{(n)}$ whose cycles do not overlap with $Z_{(2)}$ nor $\bar{Z}_{(2)}$ must all match in such a way that none of these two-point function vanishes, see section B.3.[6]

Besides (3.4) there is, sometimes, a third possible type of factorization of (3.3), resulting in a product of three-point functions. This only happens for some special configurations of the cycles in the composite field $[\prod_{\zeta,n}(X^{\zeta}_{(n)})^{N^{\zeta}_n}]$, and for special configurations of the R-charges, including that of $Z_{[2]}$. Since this type of factorization is not generically present, we will ignore it in the remaining of this paper, and henceforth it should be always understood that the composite fields are not such that this factorization occurs. Still, we note that, in the cases where it does occur, the contribution of the factorized three-point functions can be determined in a similar way as we derive the contributions of the connected four-point functions below. We give a more detailed discussion of this case in section B.3.

Applying eq. (2.15) to the four-point function (3.1), we get

$$A(v,\bar{v}) = \frac{|\mathrm{Cent}[g]||\mathrm{Cent}[(2)]|}{N!} \sum_{\mathbf{c}} \frac{1}{(N-\mathbf{c})!} \sum_{\alpha_{\mathbf{c}} \in \mathrm{Cl}_{\mathbf{c}}} \nu_{\alpha_{\mathbf{c}}} A_{\alpha_{\mathbf{c}}}(v,\bar{v}). \tag{3.5}$$

[5] We use X to denote arbitrary fields. They are not to be confused with the bosons $X_I^{\dot{A}A}$ of the seed CFT defined in appendix A, which do not appear in the main text.

[6] See also [41]. Here we derive the factorization in a slightly different way.

JHEP05(2022)106

Here $g = \prod_n (n)^{N_n}$, with $\sum_n nN_n = N$, is the permutation in the multi-cycle field. The number of active copies is constrained by the conjugacy class of g. We now assume, for simplicity, that $N_1 = 0$, i.e. that all cycles entering the correlation function are non-trivial. Then all N copies enter the correlation function non-trivially, and[7]

$$\mathbf{c} = N \qquad (\text{if } g = \textstyle\prod_n (n)^{N_n}, \text{ with all } n > 1). \tag{3.6}$$

Assuming (3.6), and using (2.6),

$$\begin{aligned} A(v,\bar v) &= \frac{(\prod_{n>1} N_n! n^{N_n})(N-2)!2}{N!} \sum_{\alpha\in \mathrm{Cl}} \nu_\alpha A_\alpha(v,\bar v) \\ &= \frac{2(N-2)!\prod N_n!}{N!}\Bigg[\sum_{\alpha_0} n_1 n_2 \Big\langle [\bar X^{\zeta_1}_{(n_1)} \bar X^{\zeta_2}_{(n_2)}]\, \bar Z_{(2)} Z_{(2)} [X^{\zeta_1}_{(n_1)} X^{\zeta_2}_{(n_2)}] \Big\rangle_{\alpha_0} \\ &\qquad + \sum_{\alpha_1} n \Big\langle \bar X^{\zeta}_{(n)} \bar Z_{(2)} Z_{(2)} X^{\zeta}_{(n)} \Big\rangle_{\alpha_1} \Bigg]. \end{aligned} \tag{3.7}$$

The classes α can be divided into two subgroups, denoted α_0 and α_1, according to whether they factorize as in (3.4a) or (3.4b), respectively. In each case, many two-point functions factorize, and inserting the factors ν_α given by (B.18) we find the final result in (3.7). Among the terms in the classes α_0, are all possible pairings of components $\bar X^{\zeta_i}_{(n_i)}$, and of components $X^{\zeta_i}_{(n_i)}$, from the multi-cycle fields. The classes with the same pairing reconstruct the connected part of the S_N-invariant function with double-cycles and with the number of colors restricted to $\mathbf{c} = n_1 + n_2$, that is

$$\begin{aligned} &\Big\langle [\bar X^{\zeta_1}_{[n_1]} \bar X^{\zeta_2}_{[n_2]}](\infty)\, \bar Z_{[2]}(1)\, Z_{[2]}(v,\bar v)\, [X^{\zeta_1}_{[n_1]} X^{\zeta_2}_{[n_2]}](0) \Big\rangle_0 \\ &\quad \equiv \Bigg[\frac{2(N-2)!(N-n_1-n_2)! n_1 n_2}{N!} \\ &\qquad \times \sum_{\mathbf{c}} \frac{1}{(N-\mathbf{c})!} \sum_{\alpha_{\mathbf{c}}} \Big\langle [\bar X^{\zeta_1}_{(n_1)} \bar X^{\zeta_2}_{(n_2)}]\ \bar Z_{(2)}\ Z_{(2)}\ [X^{\zeta_1}_{(n_1)} X^{\zeta_2}_{(n_2)}] \Big\rangle_{\alpha_{\mathbf{c}}} \Bigg]_{\mathbf{c}=n_1+n_2} \\ &\quad = \frac{2(N-2)! n_1 n_2}{N!} \sum_{\alpha_0} \Big\langle [\bar X^{\zeta_1}_{(n_1)} \bar X^{\zeta_2}_{(n_2)}]\ \bar Z_{(2)}\ Z_{(2)}\ [X^{(\zeta_1)}_{(n_1)} X^{\zeta_2}_{(n_2)}] \Big\rangle_{\alpha_0}. \end{aligned} \tag{3.8}$$

We assumed $n_1 \neq n_2$; for $n_1 = n_2 = n$, the overall coefficient in the r.h.s. must be multiplied by 2!. The index 0 in the function $\langle\cdots\rangle_0 \sim \sum_{\alpha_0}\langle\cdots\rangle_{\alpha_0}$ indicates that its associated covering-surfaces have genus $\mathbf{g} = 0$, as given by the Riemann-Hurwitz formula (2.24) with $\mathbf{c} = n_1 + n_2$. Similarly, the classes α_1, which have $\mathbf{c} = n$, reconstruct the connected function

$$\Big\langle \bar X^{\zeta}_{[n]}(\infty)\, \bar Z_{[2]}(1)\, Z_{[2]}(v,\bar v) X^{\zeta}_{[n]}(0) \Big\rangle_1 = \frac{2(N-2)!n}{N!} \sum_{\alpha_1} \Big\langle \bar X^{\zeta}_{(n)} \bar Z_{(2)} Z_{(2)} X^{\zeta}_{(n)} \Big\rangle_{\alpha_1} \tag{3.9}$$

whose index indicates that the associated covering surfaces have genus $\mathbf{g} = 1$.

[7] If $N_1 > 0$, then (in a given class $\alpha_{\mathbf{c}}$) $\mathbf{c} = N - N_1 + \lambda$, where λ is the number of copies which are trivial in g, but participate in the cycles of $Z_{(2)}$ and/or of $\bar Z_{(2)}$.

JHEP05(2022)106

Combining everything, we gather that eq. (3.7) gives

$$
\begin{aligned}
A(v,\bar v) &= \Big\langle \Big[\prod_{\zeta,n} (\bar X^{\zeta}_{[n]})^{N^{\zeta}_n}\Big](\infty)\, \bar Z_{[2]}(1)\, Z_{[2]}(v,\bar v) \Big[\prod_{\zeta,n} (X^{\zeta}_{[n]})^{N^{\zeta}_n}\Big](0)\Big\rangle \\
&= \Big(\prod_n N_n!\Big)\Bigg[\sum_{\substack{n_1\neq n_2\\ \zeta_1\neq\zeta_2}} \Big(N^{\zeta_1}_{n_1} N^{\zeta_2}_{n_2}\Big)^2 \Big\langle \Big[\bar X^{\zeta_1}_{[n_1]} \bar X^{\zeta_2}_{[n_2]}\Big]\, \bar Z_{[2]}\, Z_{[2]} \Big[X^{\zeta_1}_{[n_1]} X^{\zeta_2}_{[n_2]}\Big]\Big\rangle_0 \\
&\qquad + \sum_{\substack{n_1=n_2=n\\ \zeta_1\neq\zeta_2}} \Big(N^{\zeta_1}_{n} N^{\zeta_2}_{n}\Big)^2 \Big\langle \Big[\bar X^{\zeta_1}_{[n]} \bar X^{\zeta_2}_{[n]}\Big]\, \bar Z_{[2]}\, Z_{[2]} \Big[X^{\zeta_1}_{[n]} X^{\zeta_2}_{[n]}\Big]\Big\rangle_0 \\
&\qquad + \sum_{n,\zeta} \mathscr{P}^2(N^{\zeta}_n) \Big\langle \Big[\bar X^{\zeta}_{[n]} \bar X^{\zeta}_{[n]}\Big]\, \bar Z_{[2]}\, Z_{[2]} \Big[X^{\zeta}_{[n]} X^{\zeta}_{[n]}\Big]\Big\rangle_0 \\
&\qquad + \sum_{n,\zeta} (N^{\zeta}_n)^2 \Big\langle \bar X^{\zeta}_{[n]}\, \bar Z_{[2]}\, Z_{[2]} X^{\zeta}_{[n]}\Big\rangle_1 \Bigg].
\end{aligned}
\tag{3.10}
$$

The coefficients in each sum are 'symmetry factors', given by the number of equivalent ways of forming pairs of components from the original multi-cycle fields; see [41]. (They are squared because there are two multi-cycle fields.) The function $\mathscr{P}(q)$ is the number of ways to pair q objects,

$$
\mathscr{P}(2p) = \frac{(2p)!}{p!2^p}, \qquad \mathscr{P}(2p+1) = \frac{(2p)!}{p!2^p} + 2p. \tag{3.11}
$$

We have reduced the four-point function with two full multi-cycle fields to a sum of connected four-point functions with, at most, double-cycle fields. Note that to arrive at eq. (3.10) we have not used the large-N approximation. Although the connected functions $\langle\cdots\rangle_0$ and $\langle\cdots\rangle_1$ have genera $\mathbf{g}=0$ and $\mathbf{g}=1$, respectively, we see from eq. (2.22) that, for large N, *both* scale as $\sim N^{-2}$. This is because $\langle\cdots\rangle_0$ has an extra pair of cycles giving an extra pair of ramification points to the covering surface. The symmetry factors, which depend on the multiplicities N^{ζ}_n, also depend on N because they are constrained by $\sum_{n,\zeta} N^{\zeta}_n\, n = N$. Hence, depending on the configuration of this partition, and on how the large-N limit is taken (e.g. leaving the cycle's lengths fixed or not), the symmetry factors can also become large. It is to be expected that if some of the N^{ζ}_n grow parametrically with N, the terms with $\mathscr{P}(N^{\zeta}_n)$ dominate the r.h.s. of (3.10), as they contain factorials. In this case, the genus-one functions end up being subleading.

As a concrete example, consider the multi-cycle field[8]

$$
\mathscr{X} = \Big[\Big(X^{\zeta_1}_{[n_1]}\Big)^{2p} \Big(X^{\zeta_2}_{[n_2]}\Big)^{2q}\Big]; \quad 2p\,n_1 + 2q\,n_2 = N; \quad n_1 > n_2 > 1, \quad \zeta_1 \neq \zeta_2. \tag{3.12}
$$

[8] We tacitly assume that $\max(n_1,n_2) \neq 2\min(n_1,n_2)$, so that the type of three-point function factorization discussed below (3.4) does not exist.

JHEP05(2022)106

In this case, the second sum in (3.10) is void:

$$\begin{aligned}\Big\langle \Big[\big(\bar{X}^{\zeta_1}_{[n_1]}\big)^{2p}\big(\bar{X}^{\zeta_2}_{[n_2]}\big)^{2q}\Big]\,\bar{Z}_{[2]}Z_{[2]}\Big[\big(X^{\zeta_1}_{[n_1]}\big)^{2p}\big(X^{\zeta_2}_{[n_2]}\big)^{2q}\Big]\Big\rangle \\ = (2p)!\,(2q)!\Bigg[(4pq)^2\Big\langle\big[\bar{X}^{\zeta_1}_{[n_1]}\bar{X}^{\zeta_2}_{[n_2]}\big]\,\bar{Z}_{[2]}\,Z_{[2]}\big[X^{\zeta_1}_{[n_1]}X^{\zeta_2}_{[n_2]}\big]\Big\rangle_0 \\ + \Big(\frac{(2p)!}{p!2^p}\Big)^2\Big\langle\big[\bar{X}^{\zeta_1}_{[n_1]}\bar{X}^{\zeta_1}_{[n_1]}\big]\,\bar{Z}_{[2]}\,Z_{[2]}\big[X^{\zeta_1}_{[n_1]}X^{\zeta_1}_{[n_1]}\big]\Big\rangle_0 \\ + \Big(\frac{(2q)!}{q!2^q}\Big)^2\Big\langle\big[\bar{X}^{\zeta_2}_{[n_2]}\bar{X}^{(\zeta_2)}_{[n_2]}\big]\,\bar{Z}_{[2]}\,Z_{[2]}\big[X^{\zeta_2}_{[n_2]}X^{\zeta_2}_{[n_2]}\big]\Big\rangle_0 \\ + (2p)^2\Big\langle\bar{X}^{\zeta_1}_{[n_1]}\,\bar{Z}_{[2]}\,Z_{[2]}X^{\zeta_1}_{[n_1]}\Big\rangle_1 + (2q)^2\Big\langle\bar{X}^{\zeta_2}_{[n_2]}\,\bar{Z}_{[2]}\,Z_{[2]}X^{\zeta_2}_{[n_2]}\Big\rangle_1\Bigg].\end{aligned} \tag{3.13}$$

Since $n_1(p/N)+n_2(q/N)=\frac{1}{2}$, if we keep the cycles' lengths fixed in the large-N limit, there must be a large number of both components, i.e. $p,q\gg 1$. Using Stirling's formula, we see that the $\mathbf{g}=1$ terms in the last line are subleading to all terms with double-cycle fields.

An even simpler example is a field with only one type of component,

$$\mathscr{X}=\Big[(X^{\zeta}_{[n]})^{2p}\Big],\quad 2p=N/n. \tag{3.14}$$

The four-point function simplifies further,

$$\begin{aligned}\Big\langle\Big[(\bar{X}^{\zeta}_{[n]})^{\frac{N}{n}}\Big]\bar{Z}_{[2]}Z_{[2]}\Big[(X^{\zeta}_{[n]})^{\frac{N}{n}}\Big]\Big\rangle = \big(\frac{N}{n}\big)!\Bigg[\Bigg(\frac{\big(\frac{N}{n}\big)!}{\big(\frac{N}{2n}\big)!2^{\frac{N}{2n}}}\Bigg)^2\Big\langle\big[\bar{X}^{\zeta}_{[n]}\bar{X}^{\zeta}_{[n]}\big]\,\bar{Z}_{[2]}\,Z_{[2]}\big[X^{\zeta}_{[n]}X^{\zeta}_{[n]}\big]\Big\rangle_0 \\ + \Big(\frac{N}{n}\Big)^2\Big\langle\bar{X}^{\zeta}_{[n]}\,\bar{Z}_{[2]}\,Z_{[2]}X^{\zeta}_{[n]}\Big\rangle_1\Bigg].\end{aligned} \tag{3.15}$$

For $N/n\gg 1$, we find again that the genus-one term is strongly suppressed.

3.2 Genus-zero covering surfaces and Hurwitz blocks

We have seen that the main ingredient of the four-point functions (3.10) are the connected functions

$$A^{\zeta_1,\zeta_2}_{n_1,n_2}(v,\bar{v})\equiv\Big\langle[\bar{X}^{\zeta_1}_{[n_1]}\bar{X}^{\zeta_2}_{[n_2]}](\infty)\,\bar{Z}_{[2]}(1)\,Z_{[2]}(v,\bar{v})\,[X^{\zeta_1}_{[n_1]}X^{\zeta_2}_{[n_2]}](0)\Big\rangle_0. \tag{3.16}$$

From now on we omit the label 0, and always assume that we are dealing with the connected function with a genus-zero covering surface, which is obtained with the covering map [40]

$$z(t)=\Big(\frac{t}{t_1}\Big)^{n_1}\Big(\frac{t-t_0}{t-t_\infty}\Big)^{n_2}\Big(\frac{t_1-t_\infty}{t_1-t_0}\Big)^{n_2}. \tag{3.17}$$

The ethos of a covering map [38] is to cover the "base Riemann sphere" $\mathbb{S}^2_{\text{base}}\ni z$, where (3.16) is evaluated, with a ramified surface $\Sigma_{\mathbf{g}}\ni t$ of genus $\mathbf{g}$, whose ramification points have the property of trivializing the twists in (3.16). The map (3.17) defines

JHEP05(2022)106

such a covering surface with $\mathbf{g}=0$, i.e. a covering of the sphere by the sphere. The pair of (disjoint) twist insertions at $z=0$ lift to the pair of ramification points $t=0$ and $t=t_0$ with ramifications n_1 and n_2. The same happens to the pair of twists at $z=\infty$. The single-cycle twists at $z=1$ and $z=v$ must, each, be lifted to one ramification point, which we call $t=t_1$ and $t=x$, respectively. At these points, the map must have the correct monodromy, i.e. the derivative must be factorizable as $z'(t)\sim(t-t_1)(t-x)$. This imposes relations among the parameters t_0,t_1,t_∞ and x, that can be satisfied by choosing

$$t_0=x-1,\qquad t_1=\frac{(x-1)\left(x-1+\frac{n_1}{n_2}\right)}{x+\frac{n_1}{n_2}},\qquad t_\infty=\frac{x\left(x-1+\frac{n_1}{n_2}\right)}{x+\frac{n_1}{n_2}}. \tag{3.18}$$

The asymmetry between n_1 and n_2 in eqs. (3.17)–(3.18) is "fictitious": it stems from a freedom in parametrizing the covering map [40]. Without loss of generality, we will consider $n_1\geq n_2$.

The covering surfaces with the same ramification data, i.e. the same number of ramification points with fixed orders and positions on $\mathbb{S}^2_{\text{base}}$, are not unique. The number $\mathbf{H}$ of such surfaces it is a Hurwitz number [33, 44]. It is the number of inverses of

$$v=z(x)=\left(\frac{x+\frac{n_1}{n_2}}{x-1}\right)^{n_1+n_2}\left(\frac{x}{x+\frac{n_1-n_2}{n_2}}\right)^{n_1-n_2} \tag{3.19}$$

found by inserting (3.18) into (3.17). This is equivalent to the algebraic equation

$$v\,(x-1)^{n_1+n_2}\left(x\frac{n_1-n_2}{n_2}\right)^{n_1-n_2}-\left(x+\frac{n_1}{n_2}\right)^{n_1+n_2}x^{n_1-n_2}=0, \tag{3.20}$$

with

$$\mathbf{H}=2\max\left(n_1,n_2\right) \tag{3.21}$$

roots $x_{\mathfrak{a}}(v)$, $\mathfrak{a}=1,\cdots,\mathbf{H}$. Also, as explained in [33] (see also [44]), there is also a correspondence between covering surfaces and the equivalence classes α that compose the S_N-invariant function (3.16), cf. (3.8),

$$\begin{aligned}A^{\zeta_1,\zeta_2}_{n_1,n_2}(v,\bar v)&=\frac{2n_1n_2(N-2)!}{N!}\sum_{\substack{\alpha\in\mathrm{Cl}\\ \mathbf{g}=0}}\left\langle[\bar X^{\zeta_1}_{(n_1)_\alpha}\bar X^{\zeta_2}_{(n_2)_\alpha}]\bar Z_{(2)_\alpha}Z_{(2)_\alpha}[X^{\zeta_1}_{(n_1)_\alpha}X^{\zeta_2}_{(n_2)_\alpha}]\right\rangle\\&=\frac{2n_1n_2(N-2)!}{N!}\sum_{\mathfrak{a}=1}^{\mathbf{H}}\left|A^{\zeta_1,\zeta_2}_{n_1,n_2}(x_{\mathfrak{a}}(v))\right|^2\end{aligned} \tag{3.22}$$

In other words, in the first line there are $\mathbf{H}$ different equivalence classes α with $\mathbf{g}=0$, each class associated to one of the solutions $x_{\mathfrak{a}}(u)$ in the second line. So the sum in (3.22) is over the $\mathbf{H}=2\max(n_1,n_2)$ topologically distinct covering surfaces with $R=6$ ramification points of orders given by the twists, and $\mathbf{c}=n_1+n_2$ sheets, as per the Riemann-Hurwitz equation (2.24).

As v sweeps $\mathbb{S}^2_{\text{base}}$, each function $x_{\mathfrak{a}}(v)$ fills one out of $\mathbf{H}$ disjoint regions, which compose again the entire Riemann sphere. We will call this regions *'Hurwitz regions'*. Eq. (3.22)

JHEP05(2022)106

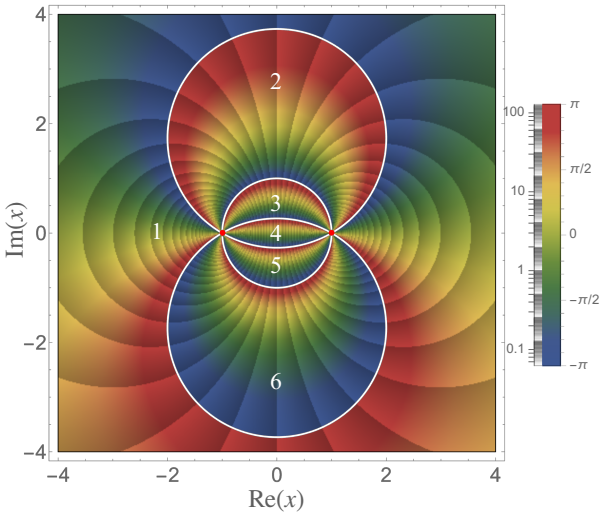

Figure 2. Plot of $v(x)$ for $n_1 = n_2 = 3$. Colors depicts the phase of $v(x)$, and the shading follows the curves of constant $|v(x)|$, as indicated by the scales. The x-plane is divided into $\mathbf{H} = 6$ regions, $v(x)$ taking all values in $\mathbb{C}$ inside of each.

shows that the S_N-invariant function $A^{\zeta_1,\zeta_2}_{n_1,n_2}(v,\bar{v})$, with domain on $\mathbb{S}^2_{\text{base}}$, is decomposable as a sum of $\mathbf{H}$ *'Hurwitz blocks'*, derived from the function $A^{\zeta_1,\zeta_2}_{n_1,n_2}(x)$, with domain in the x-plane. It is crucial that all Hurwitz blocks are summed for the total function to be S_N-invariant, because each block correspond to one of the equivalence classes α. As discussed by the end of section 2.1, when one twisted operator revolves around another (cf. figure 1) the equivalence classes are shuffled. Hence a missing Hurwitz block makes the monodromies of the correlation function not well defined.

It is often possible to compute the "Hurwitz block function" $A^{\zeta_1,\zeta_2}_{n_1,n_2}(x)$ in closed form. We will do this in section 4 for a varied collection of operators. But even when this is the case, it is, in general, not possible to write the S_N-invariant function itself in closed form, because the $x_{\mathfrak{a}}(v)$ are the roots of eq. (3.20), which has order higher than 5 for almost all twists.

3.2.1 Exact Hurwitz bloks for composite fields with equal cycles

The exception is when $n_1 = n_2$. The polynomial (3.20) simplifies to

$$v = z(x) = \left(\frac{x+1}{x-1}\right)^{2n} \tag{3.23}$$

and we can find its $\mathbf{H} = 2n$ solutions exactly:

$$x_{\mathfrak{a}}(v) = -\frac{1 + v^{\frac{1}{2n}} e^{\frac{\mathfrak{a}\pi i}{n}}}{1 - v^{\frac{1}{2n}} e^{\frac{\mathfrak{a}\pi i}{n}}}, \qquad \mathfrak{a} = 0, 1, 2, \cdots, 2n-1, \tag{3.24}$$

where $v^{\frac{1}{2n}}$ is a (single) $2n$th root of v. The division of the x-plane into $\mathbf{H} = 2n$ disjoint Hurwitz regions can be clearly seen in the plot of $v(x)$, shown in figure 2 for $n = 3$. The shading of the plot follows the contours where $|v(x)| =$ constant, distinguishing the curves traced on the x-plane when v goes in circles around the origin of the base sphere. All regions meet at the two critical points $x = \pm 1$.

As stated above, each of the $\mathbf{H}$ regions of the x-plane are associated, on the one hand, to a topologically distinct ramified covering of $\mathbb{S}^2_{\text{base}}$ and, on the other hand, to a distinct

JHEP05(2022)106

class α of permutations satisfying (2.11). But in the case of $n_1 = n_2$, there is a subtlety. The functions (3.24) can be grouped in n pairs related by inversion:

$$x_{\mathfrak{a}+n} = \frac{1}{x_{\mathfrak{a}}}, \tag{3.25}$$

for $\mathfrak{a} = 0, \cdots n-1$. This is a global conformal transformation of the x-plane, which suggests that the two solutions $x_{\mathfrak{a}}$ and $x_{\mathfrak{a}+n}$ describe covering surfaces with the same topology. This is indeed the case, as illustrated in figure 3, again with the example of $n = 3$. There are $2n = 6$ solutions of $v = z(x)$ for fixed v. The values of $x_{\mathfrak{a}}$ for the panels in the bottom and upper rows are related by inversion (3.25). Surfaces in the same row are all topologically distinct. But comparing the pairs of surfaces in the same columns, we find that they are equivalent. Let us focus on the first column, with the pair $x_0 = -2$ and $x_3 = 1/x_0 = -1/2$. Rotating the upper panel 180°, we do get the same topology of the bottom panel, but with the positions of the points $t = t_0$ and $t = 0$ swapped in relation to the other ramification points. This is highlighted by the green arrows in figure 3; following the arrow in the upper panel we find the sequence $t_1 \to t_\infty \to t_0 \to x \to 0$. Rotating the plane we get an arrow in the opposite direction, to be contrasted with that indicated in the bottom panel: $t_1 \to t_\infty \to 0 \to x \to t_0$. The relative positions of every point are the same, except for $t = 0$ and $t = t_0$, which are swapped.

As ramification points, $t = 0$ and $t = t_0$ are equivalent: they are both the preimages of $z = 0$, and with equal ramification because they correspond to cycles of equal length. In this sense, swapping these two points does not matter, and the number of distinct ramified coverings is reduced to $\mathbf{H} = n$. This "reduction by half of the Hurwitz number" when $n_1 = n_2 = n$ can also be seen from the perspective of $\mathbf{H}$ as counting the number of different equivalence classes α. An explicit construction of the $2\max(n_1, n_2)$ different classes in the function (3.22) can be found in appendix B of ref. [40]. It is clear from the construction given there that when $n_1 = n_2$ the otherwise distinct $2\max(n_1, n_2)$ inequivalent classes are grouped in pairs, and only n distinct classes remain. Eq. (3.25) is the manifestation of this pairing in terms of the geometry of the covering surfaces.

But there is still one further subtlety. In (3.22) we may have different excitations of the strands n_1 and n_2, even if the strands have the same length. Then the ramification points $t = 0$ and $t = t_0$ are "decorated" with different operators, and are distinct, even though they are equivalent with regard to the twist structure.

In summary, for functions with double-cycles of the same length, the S_N-invariant four-point function (3.22) is

$$A^{\zeta_1,\zeta_2}_{n_1,n_2}(v,\bar{v}) = \frac{4n^2(N-2)!}{N!} \sum_{\mathfrak{a}=0}^{2n-1} \left|A^{\zeta_1,\zeta_2}_{n,n}(x_{\mathfrak{a}}(v))\right|^2 \tag{3.26}$$

where $x_{\mathfrak{a}}(v)$ are given in *closed form* by eq. (3.24). Furthermore, when, in addition to the twists having cycles of the same length, the excitations are also equal, i.e. $\zeta_1 = \zeta_2$, then the Hurwitz blocks have the symmetry

$$A^{\zeta,\zeta}_{n,n}(x_{\mathfrak{a}}(v)) = A^{\zeta,\zeta}_{n,n}\left(\frac{1}{x_{\mathfrak{a}}(v)}\right) \tag{3.27}$$

and only half the terms in the sum (3.26) are independent.

JHEP05(2022)106

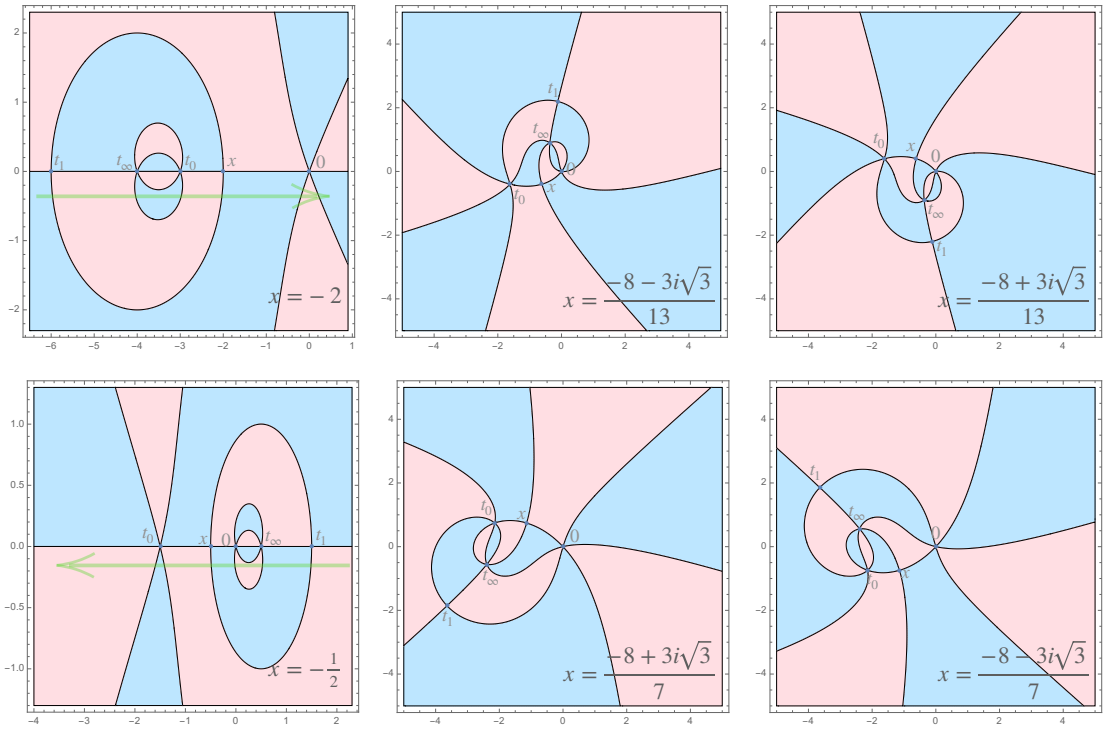

Figure 3. Covering surfaces for $n_1 = n_2 = 3$. In each panel, the horizontal axis is $\mathrm{Re}(t)$ and the vertical axis $\mathrm{Im}(t)$. Blue patches are the preimages of the upper-half plane $\mathrm{Im}(z) > 0$, and pink patches the preimages of the lower-half plane $\mathrm{Im}(z) < 0$, under the covering map (3.17). The positions of the ramification points t_0, t_1, t_∞ depend on the position of the ramification point x according to (3.18). The 6 panels correspond to the 6 solutions $x_{\mathfrak{a}}$ of eq. (3.20) for $z(x) = v = \frac{1}{729}$.

3.2.2 Composite fields with unequal cycles

The geometry of the x-plane is more complicated when $n_1 \neq n_2$. In figure 4 we show it for $n_1 = 7$, $n_3 = 3$. There are $\mathbf{H} = 2\max(n_1, n_2) = 14$ regions, $v(x)$ taking all values in $\mathbb{C}$ inside of each. (The number of regions can be found by counting, say, the different red streaks in the plot, where $\mathrm{Arg}(v) \lesssim \pi$.) The main difference from figure 2 is that in figure 4 there is an inner region with three critical points,

$$x = -\frac{n_1 - n_2}{n_2}, \quad x = -\frac{n_1 - n_2}{2n_2}, \quad x = 0, \tag{3.28}$$

which collapse into a trivial one when $n_1 = n_2$. The trefoil structure of the innermost regions (labeled 1, 5 and 14 in figure 2c) around the middle-point $x = -\frac{n_1-n_2}{2n_2}$ is the same for any values of $n_1 \neq n_2$. Increasing the difference $n_1 - n_2$ increases just the number of "petals" (labeled 2, 3 and 4) between $x = -\frac{n_1}{n_2}$ and $x = -\frac{n_1-n_2}{n_2}$, as well as the symmetric ones (labeled 11, 12 and 13) between $x = 0$ and $x = 1$. There are always $n_1 - n_2$ such petals at each side. The petals and the trefoil are associated with the twist structure of the four-point function's OPE channels.

JHEP05(2022)106

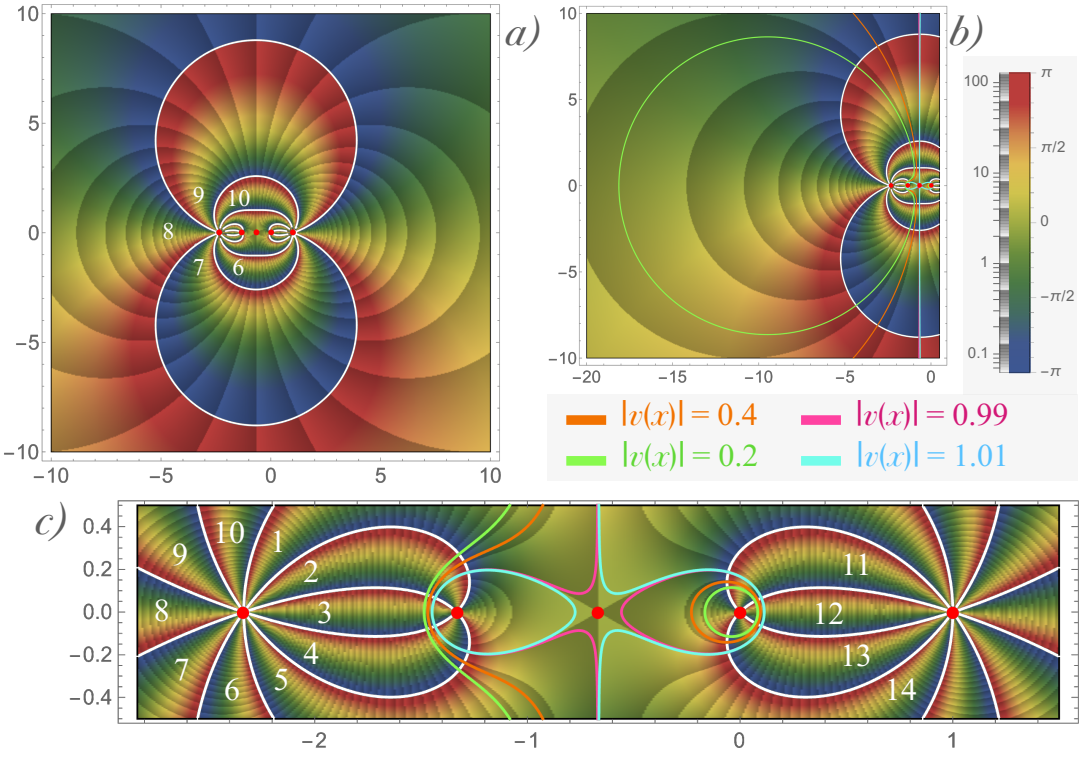

Figure 4. Plot of $v(x)$ for $n_1 = 7$, $n_2 = 3$. The frames' horizontal and vertical axes are $\mathrm{Re}(x)$, and $\mathrm{Im}(x)$, respectively. Colors depict the phase of $v(x)$, and shading follows the curves of constant $|v(x)|$, as indicated by the scales. *a)* Complete borders of the Hurwitz regions, with "outer" regions labeled. *b-c)* Four contours with $|v(x)| = \text{constant}$. *c)* Close up of the inner region near the critical points $x = -\frac{n_1}{n_2}$, $x = -\frac{n_1-n_2}{n_2}$, $x = -\frac{n_1-n_2}{2n_2}$, $x = 0$, $x = 1$ (red dots from left to right, respectively), with all 14 different regions labeled.

3.3 OPEs and Hurwitz blocks

The four-point function (3.16), there are two inequivalent OPE limits:

$$v \to 1 \qquad \text{with OPE} \qquad \bar{Z}_{[2]} \times Z_{[2]} \tag{3.29a}$$

$$v \to 0 \qquad \text{with OPE} \qquad Z_{[2]} \times \left[X^{\zeta_1}_{[n_1]} X^{\zeta_2}_{[n_2]}\right] \tag{3.29b}$$

In $v \to \infty$, the OPE is equivalent to (3.29b) in what concerns the twists, but with the double-cycle fields having opposite charges. (That is, the operators appearing in the fusion rules are different, but with the same twists discussed below.)

The critical points of $v(x)$ correspond to OPE limits. Although it is not possible to find $x_{\mathfrak{a}}(v)$ in closed form for $n_1 \neq n_2$, we can find them asymptotically for $v \approx 0, 1$. At $v = 1$, there are two critical points

$$x_{\aleph}(1) = \infty \quad \text{and} \quad x_{\beth}(1) = -\frac{n_1 - n_2}{2n_2}. \tag{3.30}$$

The root $x_{\aleph}$ has multiplicity one, and $x_{\beth}$ has multiplicity three. Explicitly, expanding $v(x)$

JHEP05(2022)106

in the vicinity of (3.30) and inverting the series,

$$x_{\aleph}(v) = -\frac{4n_1}{1-v} + \frac{n_2 - n_1 + 4n_1 n_2}{2n_2} + \left[\frac{n_1}{3} - \frac{1}{24\,n_1} - \frac{n_1}{24\,n_2^2}\right](1-v) + \left[\frac{n_1}{6} - \frac{1}{48\,n_1} - \frac{n_1}{48\,n_2^2}\right](1-v)^2 + \mathrm{O}(1-v)^3 \tag{3.31a}$$

$$x_{\beth}(v) = -\frac{n_1 - n_2}{2n_2} + \frac{3^{\frac{1}{3}}}{4}\left(\frac{(n_1^2 - n_2^2)^2}{n_1 n_2^4}\right)^{\frac{1}{3}}(1-v)^{\frac{1}{3}} - \frac{3}{40}\frac{n_1^2 + n_2^2}{n_1 n_2^2}(1-v) + \frac{1}{8\cdot 3^{\frac{2}{3}}}\left(\frac{(n_1^2 - n_2^2)^2}{n_1 n_2^4}\right)^{\frac{1}{3}}(1-v)^{\frac{4}{3}} + \mathrm{O}\,(1-v)^{\frac{5}{3}} \tag{3.31b}$$

These functions are plotted as magenta and cyan contours with $|v(x)| \approx 1$ in figure 4b-c. The contours extend to $x = \infty$ in a single direction, but move towards $x_{\beth}$ from three different directions in the inner trefoil region.

When $v = 0$, all $\mathbf{H} = 2n_1$ roots are easily found:[9]

$$x_{\beth}(0) = -\frac{n_1}{n_2} \quad \text{and} \quad x_{\gimel}(0) = 0, \tag{3.32}$$

with multiplicities $n_1 + n_2$ and $n_1 - n_2$, respectively. Expanding $v(x)$ near these points and inverting the series expansion, we find

$$x_{\beth}(v) = -\frac{n_1}{n_2} - \left(1 + \frac{n_1}{n_2}\right)\left(\frac{n_1}{n_2}\right)^{\frac{n_2 - n_1}{n_1 + n_2}} v^{\frac{1}{n_1 + n_2}} \times \left[1 + \left(\frac{n_1}{n_2}\right)^{-\frac{n_1 - n_2}{n_1 + n_2}}\left(\frac{n_1}{n_2} + \frac{n_2}{n_1} - 1\right) v^{\frac{1}{n_1 + n_2}} + \mathrm{O}\left(v^{\frac{2}{n_1 + n_2}}\right)\right] \tag{3.33a}$$

$$x_{\gimel}(v) = \left(1 - \frac{n_1}{n_2}\right)\left(\frac{n_2}{n_1}\right)^{\frac{n_1 + n_2}{n_1 - n_2}} v^{\frac{1}{n_1 - n_2}} \times \left[1 + \left(\frac{n_2}{n_1}\right)^{\frac{n_1 + n_2}{n_1 - n_2}}\left(\frac{1}{n_2} + \frac{1}{n_2} + \frac{n_1}{n_2^2}\right) v^{\frac{1}{n_1 - n_2}} + \mathrm{O}\left(v^{\frac{2}{n_1 - n_2}}\right)\right] \tag{3.33b}$$

The two functions can be visualized in figure 4b-c as the orange and green contours with $|v(x)| \approx 0$. The contours split in two closed parts. One part, given by $x_{\gimel}(v)$, circles around $x = -\frac{n_1}{n_2}$, as shown in figure 4b. They avoid $n_1 - n_2$ regions in the petals-trefoil patch in figure 4c, thus crossing a total of $\mathbf{H} - (n_1 - n_2) = n_1 + n_2$ regions. The other closed contour, given by $x_{\beth}(v)$, encircles $x = 0$, passing over the $n_1 - n_2$ remaining regions. As $v \to 0$, the contour $x_{\beth}(v)$ tightens around $x = -\frac{n_1}{n_2}$, and $x_{\gimel}(v)$ tightens (much faster) around $x = 0$.

3.3.1 Fusion rules

The twists of operators resulting from the OPEs (3.29) must appear as branches of the correlation function $A^{\zeta_1,\zeta_2}_{n_1,n_2}(v,\bar{v})$. The branches correspond to the multiplicity of roots $x_{\mathfrak{a}}$

[9] As stated before, we are assuming, without loss of generality, that $n_1 > n_2$; see [40].

JHEP05(2022)106

in the coincidence limits. The multiplicities can be read both from the leading powers in the expansions (3.31) and (3.32), and also from the number of regions around the critical points discussed above in figures 2 and 4.

For $v \to 1$, since $x_{\aleph}(v)$ has no branch cuts, the OPE has an *untwisted* field $U_{[1]}$, while the third-order branch of $x_{\beth}(v)$ indicates an operator $S_{[3]}$ of twist 3. This agrees with the composition of permutations: a product of two transpositions is either the identity or a cycle of length three,

$$[2] \times [2] = \mathrm{id} + [3]. \tag{3.34}$$

Hence the OPE (3.29a) reads

$$\bar{Z}_{[2]} \times Z_{[2]} = C_{Z\bar{Z}U}\ \{U_{[1]}\} + C_{Z\bar{Z}S}\ \{S_{[3]}\} \tag{3.35}$$

where Cs are structure constants and $\{\cdots\}$ indicates conformal families.

Similarly, in the OPE (3.29b), two types of resulting permutations contribute to the four-point function,

$$[2] \times [(n_1)(n_2)] = [n_1 + n_2] + [(n_1 - n_2)(n_2)(n_2)]. \tag{3.36}$$

In the first term in the r.h.s., a transposition (2) joins two cycles $(n_1)(n_2)$ into a single cycle of length $n_1 + n_2$; this is what we find from the branch cut of $x_{\beth}(v)$ in (3.33a). In the other type of contribution, the transposition *splits* the longer cycle in two: $(2) \times (n_1) = (n_1 - n_2)(n_2)$. The resulting cycle of length $n_1 - n_2$ is seen in the branch cut of $x_{\neg}(v)$ in (3.33b). The total fusion rule extracted from the four-point function is

$$\begin{aligned} Z_{[2]} \times [X^{\zeta_1}_{[n_1]} X^{\zeta_2}_{[n_2]}] = {} & C_{[\bar{X}\bar{X}]\bar{Z}Y}\ \{Y_{[n_1+n_2]}\} \\ & + C_{\bar{X}\bar{Z}[WX]} B_{\bar{X}X}\ \left\{[W_{[n_1-n_2]} X^{\zeta_2}_{[n_2]} X^{\zeta_2}_{[n_2]}]\right\} \end{aligned} \tag{3.37}$$

where $B_{\bar{X}X}$ is the normalization constant of a two-point function.

The appearance of the operator $W_{[n_1-n_2]}$ is an example of how there are non-trivial interactions in the fusion rules of composite, multi-cycle twisted fields, and it deserves a more detailed discussion. The terms in the r.h.s. of eq. (3.37) come from different types of equivalence classes α in the sum (3.22). Consider the following examples of representatives of classes contributing to each term, for $n_1 = 5$, $n_2 = 3$ (we label cycles by the corresponding twist position):

$$\mathrm{id} = (1,2,3,4,5)_\infty (6,7,8)_\infty \times (1,6)_1 \times (1,4)_v \times (8,7,6,5,4)_0 (3,2,1)_0 \tag{3.38a}$$

$$\mathrm{id} = (1,2,3,4,5)_\infty (6,7,8)_\infty \times (1,4)_1 \times (4,6)_v \times (8,7,6,5,4)_0 (3,2,1)_0 \tag{3.38b}$$

Taking the limit $v \to 0$ in each case,

$$(1,4)_v \times (8,7,6,5,4)_0 (3,2,1)_0 = (8,7,6,5,4,3,2,1)_* \tag{3.39a}$$

$$(4,6)_v \times (8,7,6,5,4)_0 (3,2,1)_0 = (4,5)_* (8,7,6)_* (3,2,1)_0 \tag{3.39b}$$

where new cycles resulting from the composition are marked by a star. So, keeping track of the cycles, the composite operator in the r.h.s. of (3.37) is, schematically,

$$Z_{(2)_v} \times [X^{\zeta_1}_{(n_1)_0} X^{\zeta_2}_{(n_2)_0}] = C_{\bar{X}\bar{Z}[WX]} B_{\bar{X}X}\ \left\{[W_{(n_1-n_2)_*} X^{\zeta_2}_{(n_2)_*} X^{\zeta_2}_{(n_2)_0}]\right\}. \tag{3.40}$$

JHEP05(2022)106

The branch cut of (3.33b) only "sees" the cycle of length $n_1 - n_2$ from $W_{(n_1-n_2)}$ because, in this OPE, $Z_{(2)_v}$ does not interact with $X^{\zeta_2}_{(n_2)_0}$, and $X^{\zeta_2}_{(n_2)_*}$ factorizes from the correlation function. The factorization can be seen comparing (3.38b) and (3.39b). The cycle $(n_2)_\infty$ in the composite operator at ∞, and the cycle $(n_2)_*$, resulting from the OPE, are inverses of each other, $(n_2)_\infty(n_2)_* = \mathrm{id}$. They also commute with the remaining cycles, so

$$\begin{aligned}\mathrm{id} &= (1,2,3,4,5)_\infty(6,7,8)_\infty \times (1,4)_1 \times (4,5)_*(8,7,6)_*(3,2,1)_0 \\ &= \Big[(6,7,8)_\infty \times (8,7,6)_*\Big] \times \Big[(1,2,3,4,5)_\infty \times (1,4)_1 \times (4,5)_*(3,2,1)_0\Big]\end{aligned} \tag{3.41}$$

(Note that there is no factorization of $(6,7,8)_\infty$ in (3.38b), before the OPE.) The effect of the OPE inside the four-point function is

$$\begin{aligned}&\Big\langle [\bar{X}^{\zeta_1}_{(n_1)_\infty}\bar{X}^{\zeta_2}_{(n_2)_\infty}]\bar{Z}_{(2)_1}[W_{(n_1-n_2)_*}X^{\zeta_2}_{(n_2)_*}X^{\zeta_2}_{(n_2)_0}]\Big\rangle \\ &\qquad = \Big\langle \bar{X}^{\zeta_2}_{(n_2)_\infty}X^{\zeta_2}_{(n_2)_*}\Big\rangle\Big\langle \bar{X}^{\zeta_1}_{(n_1)_\infty}\bar{Z}_{(2)_1}[W_{(n_1-n_2)}X^{\zeta_2}_{(n_2)_0}]\Big\rangle\end{aligned} \tag{3.42}$$

The factorized two-point function cannot vanish (unless the branch cut (3.33b) is absent from the four-point function expansion), which explains why the new operator with twist $(n_2)_*$ must be $X^{\zeta_2}_{(n_2)_*}$. A similar reasoning explains the product of constants in (3.37)

$$B_{\bar{X}X} \equiv \Big\langle \bar{X}^{\zeta_2}_{[n_2]}(\infty)X^{\zeta_2}_{[n_2]}(0)\Big\rangle, \quad C_{\bar{X}\bar{Z}[WX]} \equiv \Big\langle \bar{X}^{\zeta_2}_{[n_1]}(\infty)\bar{Z}_{[2]}(1)[W_{[n_1-n_2]}X^{\zeta_2}_{[n_2]}](0)\Big\rangle. \tag{3.43}$$

We assume the strands $X^{\zeta}_{[n]}$ are individually normalized, hence $B_{\bar{X}X} = 1$.

Note that classes (3.38a) and (3.38b), which differ only by the cycles $(2)_1$ and $(2)_v$, are related by channel crossing symmetry. Starting from (3.38a) and moving $(1,4)_v$ counterclockwise around $(1,6)_1$, as in figure 1, we obtain (3.38b). Hence the operators in the r.h.s. of the OPE (3.37) are intimately related.

3.3.2 Composite fields with equal cycles

When $n_1 = n_2$, the solutions in the coincidence limits are

$$\begin{aligned}\infty = x_{\aleph}(1) &= x_{\circ}(1), && \text{(multiplicity 1)} \\ 1 = x_{\beth}(0) &= x_{\mathfrak{a}}(0) \quad \forall\ \mathfrak{a} && \text{(multiplicity } 2n)\end{aligned} \tag{3.44}$$

as can be seen directly from (3.24). Solutions $x_{\gimel}(v)$ and $x_{\neg}(v)$ are missing. It follows that, for $n_1 = n_2$, there is no operator $S_{[3]}$ in the $v \to 1$ channel, and no $W_{[n_1-n_2]}$ in the $v \to 0$ channel. This can also be understood from the perspective of S_N selection rules. For example, $\sigma_{[3]}$ disappears because there is no three-point function satisfying (2.8) with a cycle of length 3 and two double-cycle twists $[(n)(n)]$.

4 Four-point functions of twisted fields in the D1-D5 CFT

We now turn to the D1-D5 CFT at the free orbifold point. Conventions for the notation of fields are given in appendix A. The holomorphic Ramond ground states of the n-twisted

JHEP05(2022)106

strands can be written in bosonized language as

$$R^{\pm}_{(n)}(z) = \exp\left(\pm\frac{i}{2n}\sum_{I=1}^{n}\left[\phi_{1,I}(z)-\phi_{2,I}(z)\right]\right)\sigma_{(n)}(z) \tag{4.1a}$$

$$R^{\dot{1}}_{(n)}(z) = \exp\left(-\frac{i}{2n}\sum_{I=1}^{n}\left[\phi_{1,I}(z)+\phi_{2,I}(z)\right]\right)\sigma_{(n)}(z) \tag{4.1b}$$

$$R^{\dot{2}}_{(n)}(z) = \exp\left(+\frac{i}{2n}\sum_{I=1}^{n}\left[\phi_{1,I}(z)+\phi_{2,I}(z)\right]\right)\sigma_{(n)}(z) \tag{4.1c}$$

All have conformal weight $h^{\rm R}_n = \frac{n}{4} = \frac{nc_{\rm seed}}{24}$, the correct weight of a spin filed in a CFT with central charge $nc_{\rm seed}$. are distinguished by their SU(2) charges $(j,\mathfrak{j})$.[10] For $R^{\pm}_{(n)}$ and $R^{\dot{A}}_{(n)}$, respectively, $(j=\pm\frac{1}{2},\ \mathfrak{j}=0)$ and $(j=0,\ \mathfrak{j}=\pm\frac{1}{2})$. NS chiral primaries can be expressed in bosonized form as

$$O^{(0)}_{(n)}(z) = \exp\left(\frac{i(n-1)}{2n}\sum_{I=1}^{n}\Big[\phi_{1,I}(z)-\phi_{2,I}(z)\Big]\right)\sigma_{(n)}(z) \tag{4.2a}$$

$$O^{(2)}_{(n)}(z) = \exp\left(\frac{i(n+1)}{2n}\sum_{I=1}^{n}\Big[\phi_{1,I}(z)-\phi_{2,I}(z)\Big]\right)\sigma_{(n)}(z) \tag{4.2b}$$

$$O^{(1\pm)}_{(n)}(z) = \exp\left(\sum_{I=1}^{n}\left[\frac{i(n\pm1)}{2n}\phi_{1,I}(z)-\frac{i(n\mp1)}{2n}\phi_{2,I}(z)\right]\right)\sigma_{(n)}(z) \tag{4.2c}$$

(see e.g. [42–44]). They have conformal weights and R-charges

$$h^{(0)}_n = \frac{1}{2}(n-1) = j^{(0)}_n; \qquad h^{(2)}_n = \frac{1}{2}(n+1) = j^{(2)}_n; \qquad h^{(1)}_n = \frac{1}{2}n = j^{(1)}_n. \tag{4.3}$$

Anti-chiral operators $\bar{O}^{(p)}_{(n)}(z)$ have opposite R-charges and the same dimensions. The labels (p) in refer to the associated cohomology of $\mathbb{T}^4$. The two middle-cohomology fields $O^{(1\pm)}_{(n)}$ have degenerate dimension and R-charge, but are distinguished by the global SU(2) charges $\mathfrak{j}^{(p)}_n$, with respect to which the other fields are neutral. There are analogous fields in the anti-holomorphic sector.

The operator that drives the theory away from the free orbifold point is a specific excitation of the 2-twisted lowest weight NS chiral with super-current modes,

$$\begin{aligned} O^{(\rm int)}_{[2]}(z,\bar{z}) &\equiv \epsilon_{AB}G^{-A}_{-\frac{1}{2}}\tilde{G}^{\dot{-}B}_{-\frac{1}{2}}O^{(0,0)}_{[2]}(z,\bar{z}) \\ &= \epsilon_{AB}\oint\frac{\mathrm{d}w}{2\pi i}\oint\frac{\mathrm{d}\bar{w}}{2\pi i}G^{-A}(w)\tilde{G}^{\dot{-}B}(\bar{w})O^{(0,0)}_{[2]}(z,\bar{z}). \end{aligned} \tag{4.4}$$

This is an exactly marginal deformation, with dimensions $h=1=\tilde{h}$, and it is a singlet of all the SU(2)s, with $j=\tilde{j}=0$, $\mathfrak{j}=\tilde{\mathfrak{j}}=0$.

From the single-cycle fields above, we can build multi-cycle, S_N-invariant fields such as the Ramond ground states of the full orbifold,

$$R_{[N^\zeta_n]} \equiv \left[\prod_{\zeta,n}(R^{\zeta}_{[n]})^{N^\zeta_n}\right] \quad \text{with} \quad h^{\rm R} = \frac{N}{4}, \quad j = \sum_{\zeta,n}N^\zeta_n\, j_\zeta. \quad \mathfrak{j} = \sum_{\zeta,n}N^\zeta_n\mathfrak{j}_\zeta, \tag{4.5}$$

[10] We denote by j and $\mathfrak{j}$ the eigenvalues of the components J^3 and $\mathfrak{J}^3$, not of the Casimirs.

JHEP05(2022)106

and also composite NS chirals

$$O_{[N_n^p]} \equiv \left[\prod_{p,n} (O_{[n]}^{(p)})^{N_n^p}\right], \quad \text{with} \quad h = j = \frac{N}{2} + \frac{\#\, O^{(2)}\text{s} - \#\, O^{(0)}\text{s}}{2} \tag{4.6}$$

where $\#O^{(p)}$ denotes the number of strands of the type p entering the composite fields. In both eqs. (4.5)–(4.6), the multiplicities form a partition of $N = \sum_{\zeta,n} n N_n^\zeta$. In the large-$N$ limit, the Ramond ground states (4.5) are heavy, $h^{\rm R} \sim N$. The multi-cycle NS chirals (4.6) can also be heavy, if the number of lowest-cohomology components is parametrically small.

4.1 Formulas for two classes of connected functions

We want to compute explicitly correlation functions of the type (3.22), using the fields above. We can do a rather generic computation, if we define the following "adjustable" operators (from which we build S_N-invariant combinations)

$$Z_{(2)}^{\{\alpha,\beta\}} \equiv \exp\left[\frac{i}{4}\sum_{I=1}^{2}\left(\alpha\phi_{1,I} + \beta\phi_{2,I}\right)\right]\sigma_{(1,2)} \tag{4.7}$$

$$\begin{aligned}\left[X_{(n_1)}^{\{\hat\sigma,\hat\varrho\}} X_{(n_2)}^{\{\check\sigma,\check\varrho\}}\right] \equiv \exp\Bigg[&\frac{i}{2n_1}\sum_{I=1}^{n_1}\left(\hat\sigma\phi_{1,I} + \hat\varrho\phi_{2,I}\right) \\ &+ \frac{i}{2n_2}\sum_{I=n_1+1}^{n_1+n_2}\left(\check\sigma\phi_{1,I} + \check\varrho\phi_{2,I}\right)\Bigg]\sigma_{(1,\cdots,n_1)}\sigma_{(n_1+1,\cdots,n_1+n_2)}\end{aligned} \tag{4.8}$$

with holomorphic conformal weights

$$h_Z = \frac{\alpha^2+\beta^2}{16} + \frac{1}{4}\left(2 - \frac{1}{2}\right) = \frac{\alpha^2+\beta^2+6}{16} \tag{4.9}$$

$$h_{XX} = \frac{\hat\sigma^2+\hat\varrho^2}{8n_1} + \frac{\check\sigma^2+\check\varrho^2}{8n_2} + \frac{n_1^2-1}{4n_1} + \frac{n_2^2-1}{4n_2} \tag{4.10}$$

The anti-holomorphic counterparts of (4.7)–(4.8) are completely analogous. Adjusting the parameters α, β, $\hat\sigma$, $\hat\varrho$, $\check\sigma$, $\check\varrho$ we obtain all the Ramond or NS chiral double-cycle fields, following table 1. We can then compute

$$A^{\alpha\beta|\hat\sigma\hat\varrho|\check\sigma\check\varrho}_{n_1,n_2}(v) \equiv \left\langle\left[\bar X_{[n_1]}^{\{\hat\sigma,\hat\varrho\}}\bar X_{[n_2]}^{\{\check\sigma,\check\varrho\}}\right](\infty)\ \bar Z_{[2]}^{\{\alpha,\beta\}}(1)\ Z_{[2]}^{\{\alpha,\beta\}}(v)\ \left[X_{[n_1]}^{\{\hat\sigma,\hat\varrho\}}X_{[n_2]}^{\{\check\sigma,\check\varrho\}}\right](0)\right\rangle, \tag{4.11}$$

and find the desired cases fixing the parameters afterwards. The twisted correlator (4.11) can be computed in the way of Lunin and Mathur [37, 38], or using conformal Ward identities to find a first-order differential equation, in what is known as the 'stress-tensor method' [33, 44, 46, 48, 51]. The computation for generic Xs, using both techniques, was done in detail in appendix B of ref. [41] for the case where $Z_{[2]} = O_{[2]}^{(\rm int)}$. The case of $Z_{[2]} = O_{[2]}^{(p,p)}$ is much simpler, and will be described now, using the Lunin-Mathur technique. Details are left to appendix C.

The fermionic exponentials in (4.11) are lifted to ramification points on the covering surface, with an appropriate factor depending on the local behavior of the map (3.17); see

JHEP05(2022)106

	$O^{(0)}_{[2]}$	$O^{(2)}_{[2]}$	$O^{(1+)}_{[2]}$	$O^{(1-)}_{[2]}$
$\{\alpha,\beta\}$	$\{1,-1\}$	$\{3,-3\}$	$\{3,-1\}$	$\{1,-3\}$
	$O^{(1+)}_{[n_1]}O^{(2)}_{[n_2]}$	$O^{(1+)}_{[n_1]}O^{(0)}_{[n_2]}$	$O^{(1+)}_{[n_1]}O^{(1+)}_{[n_2]}$	$O^{(1+)}_{[n_1]}O^{(1-)}_{[n_2]}$
$\{\hat\sigma,\hat\varrho\}$	$\{n_1+1,1-n_1\}$	$\{n_1+1,1-n_1\}$	$\{n_1+1,1-n_1\}$	$\{n_1+1,1-n_1\}$
$\{\check\sigma,\check\varrho\}$	$\{n_2+1,-1-n_2\}$	$\{n_2-1,1-n_2\}$	$\{n_2+1,1-n_2\}$	$\{n_2-1,-1-n_2\}$
	$O^{(1-)}_{[n_1]}O^{(2)}_{[n_2]}$	$O^{(1-)}_{[n_1]}O^{(0)}_{[n_2]}$	$O^{(1-)}_{[n_1]}O^{(1-)}_{[n_2]}$	$R^{\pm}_{[n_1]}R^{\mp}_{[n_2]}$
$\{\hat\sigma,\hat\varrho\}$	$\{n_1-1,-1-n_1\}$	$\{n_1-1,-1-n_1\}$	$\{n_1-1,-1-n_1\}$	$\{\pm1,\mp1\}$
$\{\check\sigma,\check\varrho\}$	$\{n_2+1,-1-n_2\}$	$\{n_2-1,1-n_2\}$	$\{n_2-1,-1-n_2\}$	$\{\mp1,\pm1\}$
	$O^{(2)}_{[n_1]}O^{(2)}_{[n_2]}$	$O^{(0)}_{[n_1]}O^{(2)}_{[n_2]}$	$O^{(0)}_{[n_1]}O^{(0)}_{[n_2]}$	$R^{\pm}_{[n_1]}R^{\pm}_{[n_2]}$
$\{\hat\sigma,\hat\varrho\}$	$\{n_1+1,-1-n_1\}$	$\{n_1-1,1-n_1\}$	$\{n_1-1,1-n_1\}$	$\{\pm1,\mp1\}$
$\{\check\sigma,\check\varrho\}$	$\{n_2+1,-1-n_2\}$	$\{n_2+1,-1-n_2\}$	$\{n_2-1,1-n_2\}$	$\{\pm1,\mp1\}$
	$R^{\dot1}_{[n_1]}R^{\pm}_{[n_2]}$	$R^{\dot2}_{[n_1]}R^{\dot2}_{[n_2]}$	$R^{\dot1}_{[n_1]}R^{\dot2}_{[n_2]}$	$R^{\dot1}_{[n_1]}R^{\dot1}_{[n_2]}$
$\{\hat\sigma,\hat\varrho\}$	$\{-1,-1\}$	$\{+1,+1\}$	$\{-1,-1\}$	$\{-1,-1\}$
$\{\check\sigma,\check\varrho\}$	$\{\pm1,\mp1\}$	$\{+1,+1\}$	$\{+1,+1\}$	$\{-1,-1\}$

Table 1. Parameters for making $Z^{\{\alpha,\beta\}}_{[2]}$ and $[X^{\{\hat\sigma,\hat\varrho\}}_{[n_1]}X^{\{\check\sigma,\check\varrho\}}_{[n_2]}]$ into different NS chirals or Ramond fields.

eqs. (C.2)–(C.3). The resulting covering-surface correlator is a *six*-point function,

$$A^{\alpha\beta|\hat\sigma\hat\varrho|\check\sigma\check\varrho}_{n_1,n_2}(x)_{\rm cover}=\Big\langle \bar X^{\{\hat\sigma,\hat\varrho\}}(\infty)\bar X^{\{\check\sigma,\check\varrho\}}(t_\infty)\bar Z^{\{\alpha,\beta\}}(t_1)Z^{\{\alpha,\beta\}}(x)X^{\{\check\sigma,\check\varrho\}}(t_0)X^{\{\hat\sigma,\hat\varrho\}}(0)\Big\rangle. \tag{4.12}$$

The relation between $A^{\alpha\beta|\hat\sigma\hat\varrho|\check\sigma\check\varrho}_{n_1,n_2}(x)_{\rm cover}$ and the base-sphere correlator $A^{\alpha\beta|\hat\sigma\hat\varrho|\check\sigma\check\varrho}_{n_1,n_2}(x)$ is

$$A^{\alpha\beta|\hat\sigma\hat\varrho|\check\sigma\check\varrho}_{n_1,n_2}(x)=e^{S_L}A^{\alpha\beta|\hat\sigma\hat\varrho|\check\sigma\check\varrho}_{n_1,n_2}(x)_{\rm cover} \tag{4.13}$$

where S_L is a Liouville action induced by the covering map [37]. In fact, e^{S_L} is the correlation function of the bare twists within (4.11), and is universal, independent of the specific excitations that define X^ζ and Z. The algorithm by Lunin and Mathur [37, 38] to derive S_L involves a careful regularization of the path integral around the ramification points. (See also [52] for a very detailed account.) An alternative, described in [41, 53], is to use the stress-tensor method to compute the bare-twist correlation function, bypassing the regularization procedure.[11] The results for $A^{\alpha\beta|\hat\sigma\hat\varrho|\check\sigma\check\varrho}_{n_1,n_2}(x)_{\rm cover}$ and S_L are given in eqs. (C.5) and (C.6), respectively, yielding our desired master formula:

$$A^{\alpha\beta|\hat\sigma\hat\varrho|\check\sigma\check\varrho}_{n_1,n_2}(x)=C_Z\;x^{K_1}\,(x-1)^{K_2}\left(x+\frac{n_1}{n_2}\right)^{K_3}\left(x+\frac{n_1}{n_2}-1\right)^{K_4}\left(x+\frac{n_1-n_2}{2n_2}\right)^{K_5} \tag{4.14a}$$

[11] Computing the functions independently in both ways also gives an important cross-check of the final results, which we have performed.

JHEP05(2022)106

with the exponents

$$
\begin{aligned}
K_1 &= \frac{(-n_1+n_2)\,(\alpha^2+\beta^2+6)}{16} - \frac{n_1(2-\check{\varrho}^2-\check{\sigma}^2)}{8n_2} - \frac{n_2(2-\hat{\varrho}^2-\hat{\sigma}^2)}{8n_1} \\
&\quad + \frac{\alpha^2+\beta^2+2\big[1-\check{\varrho}\hat{\varrho}-\check{\sigma}\hat{\sigma}-\alpha(\check{\sigma}-\hat{\sigma})-\beta(\check{\varrho}-\hat{\varrho})\big]}{8} \\
K_2 &= \frac{(+n_1+n_2)(\alpha^2+\beta^2+6)}{16} + \frac{n_1(2-\check{\varrho}^2-\check{\sigma}^2)}{8n_2} + \frac{n_2(2-\hat{\varrho}^2-\hat{\sigma}^2)}{8n_1} \\
&\quad + \frac{\alpha^2+\beta^2+2\big[1+\check{\varrho}\hat{\varrho}+\check{\sigma}\hat{\sigma}-\alpha(\check{\sigma}+\hat{\sigma})-\beta(\check{\varrho}+\hat{\varrho})\big]}{8} \\
K_3 &= \frac{(-n_1-n_2)(\alpha^2+\beta^2+6)}{16} + \frac{n_1(2-\check{\varrho}^2-\check{\sigma}^2)}{8n_2} + \frac{n_2(2-\hat{\varrho}^2-\hat{\sigma}^2)}{8n_1} \\
&\quad + \frac{\alpha^2+\beta^2+2\big[1+\check{\varrho}\hat{\varrho}+\check{\sigma}\hat{\sigma}+\alpha(\check{\sigma}+\hat{\sigma})+\beta(\check{\varrho}+\hat{\varrho})\big]}{8} \\
K_4 &= \frac{(+n_1-n_2)(\alpha^2+\beta^2+6)}{16} - \frac{n_1(2-\check{\varrho}^2-\check{\sigma}^2)}{8n_2} - \frac{n_2(2-\hat{\varrho}^2-\hat{\sigma}^2)}{8n_1} \\
&\quad + \frac{\alpha^2+\beta^2+2\big[1-\check{\varrho}\hat{\varrho}-\check{\sigma}\hat{\sigma}+\alpha(\check{\sigma}-\hat{\sigma})+\beta(\check{\varrho}-\hat{\varrho})\big]}{8} \\
K_5 &= -\frac{2+3(\alpha^2+\beta^2)}{8}
\end{aligned}
\tag{4.14b}
$$

Some constant factors involving n_1 and n_2 have been absorbed into the constant C_Z, which also takes into account the arbitrariness of normalization of the bare twists, and is fixed by the correct normalization of the correlation function in the identity OPE channel.

The function

$$
A^{\text{int}|\hat{\sigma}\hat{\varrho}|\check{\sigma}\check{\varrho}}_{n_1,n_2}(v,\bar{v}) \equiv \Big\langle \Big[\bar{X}^{\{\hat{\sigma},\hat{\varrho}\}}_{[n_1]}\bar{X}^{\{\check{\sigma},\check{\varrho}\}}_{[n_2]}\Big](\infty)\; O^{(\text{int})}_{[2]}(1)\; O^{(\text{int})}_{[2]}(v,\bar{v})\; \Big[X^{\{\hat{\sigma},\hat{\varrho}\}}_{[n_1]}X^{\{\check{\sigma},\check{\varrho}\}}_{[n_2]}\Big](0)\Big\rangle, \tag{4.15}
$$

is more complicated than (4.11) because the deformation operator $O^{(\text{int})}_{[2]}$ is not simply a fermionic exponential, but a linear combination of terms with bosonic factors and contributions from the integral defining the modes of the super-current excitation, cf. (4.4). Its computation, carried on in appendix B of ref. [41], is, nevertheless, completely analogous to the one above, including the same Liouville factor, because the twist structure is identical. In the end, we obtain

$$
A^{\text{int}|\hat{\sigma}\hat{\varrho}|\check{\sigma}\check{\varrho}}_{n_1,n_2}(x,\bar{x}) = \Big|\mathcal{A}(x)(1+\mathcal{B}(x))\Big|^2 \tag{4.16a}
$$

where

$$
\begin{aligned}
\mathcal{A}(x) &= \frac{C_{\text{int}}}{2}\;\frac{x^{P_1-Q_1}\,(x-1)^{P_2-Q_2}\left(x+\frac{n_1}{n_2}\right)^{P_3-Q_3}\left(x+\frac{n_1}{n_2}-1\right)^{P_4-Q_4}}{\left(x+\frac{n_1-n_2}{2n_2}\right)^4} \\
\mathcal{B}(x) &= x^{2Q_1}\,(x-1)^{2Q_2}\left(x+\frac{n_1}{n_2}\right)^{2Q_3}\left(x+\frac{n_1}{n_2}-1\right)^{2Q_4}
\end{aligned}
\tag{4.16b}
$$

JHEP05(2022)106

with the exponents

$$\begin{aligned}
P_1 &= +n_2 - n_1 - \frac{\check{\varrho}\hat{\varrho} + \check{\sigma}\hat{\sigma} - 6}{4} + \frac{n_2\,(\hat{\varrho}^2 + \hat{\sigma}^2 - 2)}{8n_1} + \frac{n_1\,(\check{\varrho}^2 + \check{\sigma}^2 - 2)}{8n_2} \\
P_2 &= +n_2 + n_1 + \frac{\check{\varrho}\hat{\varrho} + \check{\sigma}\hat{\sigma} + 6}{4} - \frac{n_2\,(\hat{\varrho}^2 + \hat{\sigma}^2 - 2)}{8n_1} - \frac{n_1\,(\check{\varrho}^2 + \check{\sigma}^2 - 2)}{8n_2} \\
P_3 &= -n_2 - n_1 + \frac{\check{\varrho}\hat{\varrho} + \check{\sigma}\hat{\sigma} + 6}{4} - \frac{n_2\,(\hat{\varrho}^2 + \hat{\sigma}^2 - 2)}{8n_1} - \frac{n_1\,(\check{\varrho}^2 + \check{\sigma}^2 - 2)}{8n_2} \\
P_4 &= -n_2 + n_1 - \frac{\check{\varrho}\hat{\varrho} + \check{\sigma}\hat{\sigma} - 6}{4} + \frac{n_2\,(\hat{\varrho}^2 + \hat{\sigma}^2 - 2)}{8n_1} + \frac{n_1\,(\check{\varrho}^2 + \check{\sigma}^2 - 2)}{8n_2}
\end{aligned} \tag{4.16c}$$

and

$$Q_1 = \frac{-\check{\sigma} - \check{\varrho} + \hat{\sigma} + \hat{\varrho}}{4} = -Q_4, \qquad Q_2 = \frac{-\check{\sigma} - \check{\varrho} - \hat{\sigma} - \hat{\varrho}}{4} = -Q_3 \tag{4.16d}$$

This result is, in fact, more general than the one derived in ref. [41], because in the latter case we had restricted our attention to double-cycle Ramond fields, for which $\check{\sigma}^2 = \check{\varrho}^2 = \hat{\sigma}^2 = \hat{\varrho}^2 = 1$, hence the last two terms in each exponent P_i vanishes. The present result allow us to give also the correlators for $[X^{\{\hat{\sigma},\hat{\varrho}\}}_{[n_1]} X^{\{\check{\sigma},\check{\varrho}\}}_{[n_2]}]$ made by NS chirals, using the dictionary in table 1.

Composite fields with equal cycles. In section 3.2 we showed that when $n_1 = n_2 = n$, the covering maps develop a symmetry that reflects upon the Hurwitz blocks. We can check this property, using our master formulas. The correlators (4.16) and (4.14) simplify considerably in this case,

$$A^{\alpha\beta|\hat{\sigma}\hat{\varrho}|\check{\sigma}\check{\varrho}}_{n,n}(x) = \frac{1}{(-4n)^{2h_Z}}\; x^{K_0}(x-1)^{K_-}(x+1)^{K_+} \tag{4.17a}$$

where

$$\begin{aligned}
K_0 &= \frac{(\check{\sigma} - \hat{\sigma})^2 + (\check{\varrho} - \hat{\varrho})^2}{4} - \frac{\alpha^2 + \beta^2 + 6}{8} \\
K_\pm &= \frac{\check{\varrho}\hat{\varrho} + \check{\sigma}\hat{\sigma} \pm \alpha(\check{\sigma} + \hat{\sigma}) \pm \beta(\check{\varrho} + \hat{\varrho})}{4} - \frac{\check{\varrho}^2 + \check{\sigma}^2 + \hat{\varrho}^2 + \hat{\sigma}^2}{8} + \frac{(1 \mp n)(\alpha^2 + \beta^2 + 6)}{8}
\end{aligned} \tag{4.17b}$$

and

$$A^{\mathrm{int}|\hat{\sigma}\hat{\varrho}|\check{\sigma}\check{\varrho}}_{n,n}(x) = \frac{1}{16n^2}\; x^{P_0}(x-1)^{P_- + Q}(x+1)^{P_+ - Q}\left[1 + \left(\frac{x+1}{x-1}\right)^{2Q}\right] \tag{4.18a}$$

where

$$\begin{aligned}
P_\pm &= 2(1 \mp n) - \frac{(\check{\sigma} - \hat{\sigma})^2 + (\check{\varrho} - \hat{\varrho})^2}{8}, \qquad P_0 = \frac{(\check{\sigma} - \hat{\sigma})^2 + (\check{\varrho} - \hat{\varrho})^2 - 8}{4}, \\
Q &= \frac{\check{\sigma} + \check{\varrho} + \hat{\sigma} + \hat{\varrho}}{4}
\end{aligned} \tag{4.18b}$$

JHEP05(2022)106

The symmetry (3.27) of the Hurwitz blocks can be checked explicitly. We see that $A^{\alpha\beta|\hat{\sigma}\hat{\varrho}|\check{\sigma}\check{\varrho}}_{n,n}(x) = A^{\alpha\beta|\hat{\sigma}\hat{\varrho}|\check{\sigma}\check{\varrho}}_{n,n}(1/x)$ and $A^{\text{int}|\hat{\sigma}\hat{\varrho}|\check{\sigma}\check{\varrho}}_{n,n}(x) = A^{\text{int}|\hat{\sigma}\hat{\varrho}|\check{\sigma}\check{\varrho}}_{n,n}(1/x)$ iff

$$0 = 2K_0 + K_+ + K_- = \frac{(\check{\varrho}-\hat{\varrho})^2 + (\check{\sigma}-\hat{\sigma})^2}{4} = 2P_0 + P_+ + P_-. \tag{4.19}$$

This only holds if $\check{\varrho} = \hat{\varrho}$ and $\check{\sigma} = \hat{\sigma}$, i.e. if the strands $X^{\{\hat{\sigma},\hat{\varrho}\}}_{[n]} = X^{\{\check{\sigma},\check{\varrho}\}}_{[n]}$ are identical, as expected from the discussion leading to eq. (3.27).

Since the $x_{\mathfrak{a}}(v)$ are expressible in closed form (3.24), we can write a closed formula for the correlation functions directly on the base sphere,

$$A^{\alpha\beta|\hat{\sigma}\hat{\varrho}|\check{\sigma}\check{\varrho}}_{n,n}(v) = \frac{4n^2(N-2)!}{N!}\sum_{\mathfrak{a}=0}^{n-1}\left|\frac{2^{K_+ + K_-}}{(4n)^{2h_Z}}\frac{\left(v^{\frac{1}{2n}}e^{\frac{\mathfrak{a}\pi i}{n}}\right)^{K_+}\left(1+v^{\frac{1}{2n}}e^{\frac{\mathfrak{a}\pi i}{n}}\right)^{K_0}}{\left(1-v^{\frac{1}{2n}}e^{\frac{\mathfrak{a}\pi i}{n}}\right)^{2h_Z}}\right|^2 \tag{4.20}$$

where we have used the fact that $K_0 + K_- + K_+ = 2h_Z$. When $n = 1$, there are only two inverse functions,

$$\begin{aligned}&\left\langle\left[X^{\{\hat{\sigma},\hat{\varrho}\}}_{[1]}X^{\{\check{\sigma},\check{\varrho}\}}_{[1]}\right]^\dagger(\infty)\; Z^{\{\alpha,\beta\}\dagger}_{[2]}(1)\; Z^{\{\alpha,\beta\}}_{[2]}(v)\;\left[X^{\{\hat{\sigma},\hat{\varrho}\}}_{[1]}X^{\{\check{\sigma},\check{\varrho}\}}_{[1]}\right](0)\right\rangle \\ &\qquad = 2^{2-2K_0-K_+-K_-}\left[\left|\frac{\left(v^{\frac{1}{2}}\right)^{K_+}\left(1+v^{\frac{1}{2}}\right)^{K_0}}{\left(1-v^{\frac{1}{2}}\right)^{2h_Z}}\right|^2 + \left|\frac{\left(v^{\frac{1}{2}}\right)^{K_+}\left(1-v^{\frac{1}{2}}\right)^{K_0}}{\left(1+v^{\frac{1}{2}}\right)^{2h_Z}}\right|^2\right]\end{aligned} \tag{4.21}$$

using the appropriate expression for the N-dependent factor. Note that functions with $n = 1$ scale as N^0. There are only two non-trivial twists, hence two ramification points in the covering surface of the connected correlators, so $R = 2$ in eq. (2.22).

4.2 OPE limits

We can now derive not only the twists but the conformal dimensions and structure constants of operators appearing in the OPE limits $v \to 1$ and $v \to 0$. In the channel $v \to 1$, the Huwitz blocks where $x \to x_{\aleph}(1) = \infty$, give

$$\mathscr{A}(x_{\aleph}(v)) = C_Z x_{\aleph}^{2h_Z}(v)\left[1 + \mathrm{O}(1/x_{\aleph}(v))\right] = \frac{(-4n_1)^{2h_Z}C_Z}{(1-v)^{2h_Z}}\left[1+\mathrm{O}(1-v)\right] \tag{4.22}$$

for both $A^{\alpha\beta|\hat{\sigma}\hat{\varrho}|\check{\sigma}\check{\varrho}}_{n_1,n_2}(x)$, where h_Z is given by eq. (4.9), and for $A^{\text{int}|\hat{\sigma}\hat{\varrho}|\check{\sigma}\check{\varrho}}_{n_1,n_2}(x)$, where $h_Z = 1$. Looking at the power of the leading singularity, we see that the untwisted operator $U_{[1]}$ in the OPE (3.35) is the identity. Since we have assumed that the individual cycle fields are normalized, the arbitrary constant in the correlator is now fixed to

$$C_Z = \frac{1}{(-4n_1)^{2h_Z}}. \tag{4.23}$$

The Hurwitz blocks where $x \to x_{\beth}(1)$ again have the same form for $A^{\alpha\beta|\hat{\sigma}\hat{\varrho}|\check{\sigma}\check{\varrho}}_{n_1,n_2}(x)$ and $A^{\text{int}|\hat{\sigma}\hat{\varrho}|\check{\sigma}\check{\varrho}}_{n_1,n_2}(x)$,

$$\begin{aligned}\mathscr{A}\left(x_{\beth}(v)\right) &= \text{constant} \times \left(x_{\beth}(v) + \frac{n_1-n_2}{2n_2}\right)^{-6h_L+2}\left[1+\mathrm{O}\left(x_{\beth}(v)+\frac{n_1-n_2}{2n_2}\right)\right] \\ &= \frac{\text{constant}}{(1-v)^{2h_Z-\frac{2}{3}}}\left[1+\mathrm{O}\left(1-v\right)^{\frac{1}{3}}\right]\end{aligned} \tag{4.24}$$

JHEP05(2022)106

with a constant that is readily computable but given by a cumbersome expression in general. The power of the leading singularity shows that twist-three operator $S_{[3]}$ in the OPE (3.35) is a primary with dimension $h_p = \frac{2}{3}$, that is the bare twist $\sigma_{[3]}$.

In channel $v \to 0$, the function (4.14) expands as

$$A^{\alpha\beta|\check{\sigma}\hat{\varrho}|\check{\sigma}\check{\varrho}}_{n_1,n_2}(x_{\sqsupset}(v)) = \frac{e^{i\psi}}{2^{K_5}(4n_1)^{2h_Z}} \left(\frac{n_1}{n_2}\right)^{K_1 - \frac{n_1-n_2}{n_1+n_2}K_3} \left(1+\frac{n_2}{n_2}\right)^{K_2+K_3+K_5} v^{\frac{K_3}{n_1+n_2}} + \cdots \tag{4.25a}$$

$$A^{\alpha\beta|\check{\sigma}\hat{\varrho}|\check{\sigma}\check{\varrho}}_{n_1,n_2}(x_{\neg}(v)) = \frac{e^{i\psi}}{2^{K_5}(4n_1)^{2h_Z}} \left(\frac{n_1}{n_2}\right)^{\frac{n_1+n_2}{n_1-n_2}K_1+K_3} \left(1-\frac{n_2}{n_2}\right)^{K_1+K_4+K_5} v^{\frac{K_1}{n_1-n_2}} + \cdots \tag{4.25b}$$

Here $e^{i\psi}$ simply denotes an unimportant phase that is not necesseraly the same in all functions. The leading order coefficients give the structure constants in the OPE

$$\begin{aligned} Z_{[2]} \times [X^{\zeta_1}_{[n_1]} X^{\zeta_2}_{[n_2]}] = {} & C_{[\bar{X}\bar{X}]\bar{Z}Y} \ \{Y_{[n_1+n_2]}\} \\ & + C_{\bar{X}\bar{Z}[WX]} B_{\bar{X}X} \left\{ [W_{[n_1-n_2]} X^{\zeta_2}_{[n_2]} X^{\zeta_2}_{[n_2]}] \right\} \end{aligned} \tag{4.26}$$

for the fields in table 1. We can read the conformal weights from the leading powers (4.25). For the single-cycle field $Y_{[n_1+n_2]}$,

$$h_Y = \frac{K_3}{n_1+n_2} + h_Z + h_{XX}, \tag{4.27}$$

where h_Z and h_{XX} are given in (4.9). Similarly, the dimension of the composite operator $[W_{[n_1-n_2]} X^{\zeta_2}_{[n_2]} X^{\zeta_2}_{[n_2]}]$ is $\frac{K_1}{n_1-n_2} + h_Z + h_{XX}$, but since we know the dimensions of the components $X^{\zeta_2}_{[n_2]}$, we can extract the dimension of $W_{[n_1-n_2]}$ alone,

$$h_W = \frac{K_1}{n_1-n_2} + h_Z + h_{XX} - 2\left(\frac{\check{\sigma}^2+\check{\varrho}^2}{8n_2} + \frac{n_2^2-1}{4n_2}\right) \tag{4.28}$$

The same analysis holds for the functions (4.16) with the deformation operator $O^{(\mathrm{int})}_{[2]}$, with weight $h = 1$. The leading-order expansions are

$$A^{\mathrm{int}|\check{\sigma}\hat{\varrho}|\check{\sigma}\check{\varrho}}_{n_1,n_2}(x_{\sqsupset}(v)) = e^{i\psi}(n_1+n_2)^{M_2-4} n_1^{M_1-2} n_2^{4-M_1-M_2} v^{\frac{M_3}{n_1+n_2}} + \cdots \tag{4.29a}$$

$$A^{\mathrm{int}|\check{\sigma}\hat{\varrho}|\check{\sigma}\check{\varrho}}_{n_1,n_2}(x_{\neg}(v)) = e^{i\psi}(n_1-n_2)^{M_4-4} n_1^{M_3-2} n_2^{4-M_3-M_4} v^{\frac{M_1}{n_1-n_2}} + \cdots \tag{4.29b}$$

where $M_i \equiv \max(P_i - Q_i, P_i + Q_i)$. We can read the conformal data of the OPE

$$\begin{aligned} O^{(\mathrm{int})}_{[2]} \times [X^{\zeta_1}_{[n_1]} X^{\zeta_2}_{[n_2]}] = {} & C_{[\bar{X}\bar{X}]\bar{Z}Y} \ \{Y_{[n_1+n_2]}\} \\ & + C_{\bar{X}\bar{Z}[WX]} B_{\bar{X}X} \left\{ [W_{[n_1-n_2]} X^{\zeta_2}_{[n_2]} X^{\zeta_2}_{[n_2]}] \right\} \end{aligned} \tag{4.30}$$

and find the weights

$$h_Y = \frac{M_3}{n_1+n_2} + 1 + h_{XX}, \quad h_W = \frac{M_1}{n_1-n_2} + 1 + h_{XX} - 2\left(\frac{\check{\sigma}^2+\check{\varrho}^2}{8n_2} + \frac{n_2^2-1}{4n_2}\right) \tag{4.31}$$

where h_{XX} is given in (4.9).

JHEP05(2022)106

4.3 Functions with NS chiral fields and other examples

Although the exponents (4.14b), (4.16c), (4.16d) may look complicated functions, they are, in fact, usually very simple after the parameters of table 1 are inserted. We now discuss some examples of functions and their conformal data.

4.3.1 Single-cycle NS chirals, composite Ramond

Take $Z_{[2]}$ to be a middle-cohomology NS chiral, hence $(h_Z, \tilde{h}_Z) = (1,1)$, and the composite fields be made of be R-charged Ramond fields $R^{+\dot{+}}_{[n_i]}$. The function (4.14) is the same for both $O^{(1\pm,1\pm)}_{[2]}$,

$$A^{1\pm|+|+}_{n_1,n_2}(x) = \frac{1}{16n_1^2}\frac{x^{1-n_1+n_2}(x-1)^{n_1+n_2}\left(x+\frac{n_1}{n_2}\right)^{4-n_1-n_2}\left(x+\frac{n_1-n_2}{n_2}\right)^{1+n_1-n_2}}{\left(x+\frac{n_1-n_2}{2n_2}\right)^4} \tag{4.32}$$

The expansion of the S_N-invariant function (3.22) in the channel $v \to 1$ is

$$\begin{aligned}
&\left\langle \left[\bar{R}^{+\dot{+}}_{[n_1]}\bar{R}^{+\dot{+}}_{[n_2]}\right](\infty)\bar{O}^{(1\pm,1\pm)}_{[2]}(1)O^{(1\pm,1\pm)}_{[2]}(v,\bar{v})\left[R^{+\dot{+}}_{[n_1]}R^{+\dot{+}}_{[n_2]}\right](0)\right\rangle = \\
&\frac{2n_1n_2(N-2)!}{N!}\left\{\left|\frac{1}{(1-v)^2}\left[1-\frac{1}{2}\left(\frac{1}{n_1}+\frac{1}{n_2}\right)(1-v)+\mathrm{O}(1-v)^2\right]\right|^2\right. \\
&\quad \left. +3\left|\frac{1}{(1-v)^{\frac{4}{3}}}\left[\frac{(n_1+n_2)^2}{12\left[3n_1^2n_2^2(n_1^2-n_2^2)^2\right]^{\frac{1}{3}}}+\frac{n_1+n_2}{6n_1n_2}(1-v)^{\frac{1}{3}}+\mathrm{O}(1-v)^{\frac{2}{3}}\right]\right|^2\right\} \\
&\quad + \text{Non-singular Hurwitz blocks}
\end{aligned} \tag{4.33}$$

The factor of 3 in front of the terms $\sim (1-v)^{-\frac{4}{3}}$ comes from the multiplicity of the function (3.31b). The leading coefficients give products of structure constants in $\bar{O}^{(1\pm,1\pm)}_{[2]} \times O^{(1\pm,1\pm)}_{[2]} \sim \{\mathrm{id}\} + \{\sigma_{[3]}\}$ Note that, although the NS chirals' OPEs form a ring [42–44], here the OPE is not between two chirals, but between a chiral and an anti-chiral field, which explains why the σ_3 block is not forbidden.

For the OPE $O^{(1\pm,1\pm)}_{[2]} \times [R^{+\dot{+}}_{[n_1]}R^{+\dot{+}}_{[n_2]}]$ in channel $v \to 0$, we find the following conformal weights for the operators $Y_{[n_1+n_2]}$ and $W_{[n_1-n_2]}$

$$h_Y = \frac{n_1+n_2}{4} + \frac{4}{n_1+n_2}, \qquad h_W = \frac{n_1-n_2}{4} + \frac{1}{n_1-n_2} \tag{4.34}$$

suggesting that these are fractional-mode excitations of Ramond ground states in $(n_1 \pm n_2)$-twisted strands. This should be expected, since the OPE of a NS field with a Ramond field is always in the Ramond sector.

4.3.2 Composite NS chiral and interaction modulus

In [41] we have discussed four-point functions with $O^{(\mathrm{int})}_{[2]}$ and composite Ramond fields. Here our generalized formula (4.16) allow us to take the composite fields to be made of NS

JHEP05(2022)106

chirals. For example, for highest-weight chirals we find

$$A^{\text{int}|2|2}_{n_1,n_2}(x) = \frac{1}{16n_1^2}\frac{x^{1-n_1+n_2}(x-1)^{2+n_1+n_2}\left(x+\frac{n_1}{n_2}\right)^{2-n_1-n_2}\left(x+\frac{n_1-n_2}{n_2}\right)^{1+n_1-n_2}}{\left(x+\frac{n_1-n_2}{2n_2}\right)^4} \tag{4.35}$$

and expanding the vacuum and σ_3 blocks,

$$\begin{aligned}
&\left\langle\left[\bar{O}^{(2,2)}_{[n_1]}\bar{O}^{(2,2)}_{[n_2]}\right](\infty)O^{(\text{int})}_{[2]}(1)O^{(\text{int})}_{[2]}(v,\bar{v})\left[O^{(2,2)}_{[n_1]}O^{(2,2)}_{[n_2]}\right](0)\right\rangle = \\
&\frac{2n_1n_2(N-2)!}{N!}\left\{\left|\frac{1}{(1-v)^2}\left[1-\frac{1}{192}\left(\frac{5}{n_1^2}+\frac{5}{n_2^2}+\frac{6}{n_1n_2}-16\right)(1-v)^2+\mathrm{O}(1-v)^3\right]\right|^2\right. \\
&+\left|\frac{1}{(1-v)^{\frac{4}{3}}}\left[\frac{(n_1+n_2)^2}{12\left[3n_1^2n_2^2(n_1^2-n_2^2)^2\right]^{\frac{1}{3}}}\right.\right. \\
&\qquad\left.\left.\left.-\left(\frac{(n_1^2-n_2^2)^2}{3^2n_1^4n_2^4}\right)^{\frac{1}{3}}\frac{7(n_1^2+n_2^2)-10n_1n_2}{80(n_1-n_2)^2}(1-v)^{\frac{2}{3}}+\mathrm{O}(1-v)^{\frac{3}{3}}\right]\right|^2\right\} \\
&+\text{Non-singular Hurwitz blocks}
\end{aligned} \tag{4.36}$$

An important difference between the expansion above and (4.33) is the absence of the term of order $(1-v)$ in the identity block, and of the term of order $(1-v)^{\frac{1}{3}}$ in the σ_3 block. Hence there are no operators with $h=1$ in the OPE, a confirmation that $O^{(\text{int})}_{[2]}$ is, indeed, exactly marginal — it does not couple to other operators of weight 1. This is also found in functions with Ramond ground states [41].

4.3.3 Functions with only NS chiral fields

If we take every field in the correlator to be an NS chiral, the resulting function is constrained by the NS chiral ring. Only a restricted number of three-point functions involving (single-cycle) NS chirals is non-vanishing [42–44], and the OPEs of fields in the ring are non-singular. This reflects on the structure of the functions (4.14) at $x=0$ and $x=-\frac{n_1}{n_2}$, i.e. at the $v\to 0$ channel. Namely, powers of x and $(x+\frac{n_1}{n_2})$ are positive, so that there are no singularities, or zero, when the corresponding field is absent from the OPE. These features can be seen in the list of formulas (D.1).

For example, using a schematic notation, we have

$$\left\langle\left[\bar{O}^{(2,2)}_{[n_1]}\bar{O}^{(2,2)}_{[n_2]}\right]\bar{O}^{(1+,1+)}_{[2]}O^{(1+,1+)}_{[2]}\left[O^{(2,2)}_{[n_1]}O^{(2,2)}_{[n_2]}\right]\right\rangle = \frac{1}{16n_1^2}\frac{x\left(x+\frac{n_1}{n_2}\right)^4\left(x+\frac{n_1-n_2}{n_2}\right)}{\left(x+\frac{n_1-n_2}{2n_2}\right)^4} \tag{4.37}$$

which vanishes both at $x\to 0$ and $x\to -\frac{n_1}{n_2}$. Hence the OPE $O^{(1+,1+)}_{[2]}\times[O^{(2,2)}_{[n_1]}O^{(2,2)}_{[n_2]}]$ is void. This is not surprising, as there is no OPE $O^{(1+,1+)}_{[n]}\times O^{(2,2)}_{[m]}$ in the (single-cycle) NS chiral ring.

By contrast, the function

$$\left\langle\left[\bar{O}^{(0,0)}_{[n_1]}\bar{O}^{(0,0)}_{[n_2]}\right]\bar{O}^{(0,0)}_{[2]}O^{(0,0)}_{[2]}\left[O^{(0,0)}_{[n_1]}O^{(0,0)}_{[n_2]}\right]\right\rangle = -\frac{1}{4n_1}\frac{(1-x)^2}{x+\frac{n_1-n_2}{2n_2}} \tag{4.38}$$

JHEP05(2022)106

is finite at both limits. Eqs. (4.27)–(4.28) give the dimensions $h_Y = \frac{1}{2}(n_1+n_2-1)$ and $h_W = \frac{1}{2}(n_1-n_2+1)$. The former is the correct dimension of a lowest-weight NS chiral of twist n_1+n_2, and the latter of a highest-weight chiral of twist n_1-n_2. Hence the OPE (4.26) reads

$$O^{(0,0)}_{[2]} \times \left[O^{(0,0)}_{[n_1]} O^{(0,0)}_{[n_2]}\right] = \mathscr{C}_1 \left\{O^{(0,0)}_{[n_1+n_2]}\right\} + \mathscr{C}_2 \left\{\left[O^{(2,2)}_{[n_1-n_2]} O^{(0,0)}_{[n_2]} O^{(0,0)}_{[n_2]}\right]\right\} \tag{4.39}$$

The appearance of $O^{(0,0)}_{[m]}$ and $O^{(2,2)}_{[m]}$ in the OPE with the composite field agrees with what one should expect from the single-cycle OPE of the chiral ring. The structure constants squared, $|\mathscr{C}_1|^2$ and $|\mathscr{C}_2|^2$, can be read from value of (4.38) at $x=0$ and $x=-\frac{n_1}{n_2}$, combined with the multiplicities and the "dressing" factor for N-dependence:

$$\left|\left\langle \bar{O}^{(0,0)}_{[n_1+n_2]} O^{(0,0)}_{[2]} \left[O^{(0,0)}_{[n_1]} O^{(0,0)}_{[n_2]}\right]\right\rangle\right|^2 = \frac{2n_1n_2(N-2)!}{N!}\frac{(n_1+n_2)^3}{(2n_1n_2)^2} \tag{4.40}$$

$$\left|\left\langle \bar{O}^{(0,0)}_{[n_1]} O^{(0,0)}_{[2]} \left[O^{(2,2)}_{[n_1-n_2]} O^{(0,0)}_{[n_2]}\right]\right\rangle\right|^2 = \frac{2n_1n_2(N-2)!}{N!}\frac{n_2^2}{(2n_1)^2(n_1-n_2)} \tag{4.41}$$

As a third and final example, we consider

$$\left\langle \left[\bar{O}^{(2,2)}_{[n_1]} \bar{O}^{(0,0)}_{[n_2]}\right] \bar{O}^{(0,0)}_{[2]} O^{(0,0)}_{[2]} \left[O^{(2,2)}_{[n_1]} O^{(0,0)}_{[n_2]}\right]\right\rangle = -\frac{1}{4n_1}\frac{x^2}{x+\frac{n_1-n_2}{2n_2}} \tag{4.42}$$

The function vanishes at $x=0$, so there is no composite operator with $W_{[n_1-n_2]}$ in the OPE. But it is finite at $x=-\frac{n_1}{n_2}$, with an operator of dimension $h_Y = \frac{1}{2}(n_1+n_2+1)$, i.e. the highest-weight NS chiral:

$$O^{(0,0)}_{[2]} \times \left[O^{(2,2)}_{[n_1]} O^{(0,0)}_{[n_2]}\right] = \mathscr{C}_1 \{O^{(2,2)}_{[n_1+n_2]}\} \tag{4.43}$$

The (square of the) structure constant can be read from by evaluating (4.42) at $x=-\frac{n_1}{n_2}$ and using the multiplicity and dressing factor:

$$\left|\left\langle \bar{O}^{(2,2)}_{[n_1+n_2]} O^{(0,0)}_{[2]} \left[O^{(2,2)}_{[n_1]} O^{(0,0)}_{[n_2]}\right]\right\rangle\right|^2 = \frac{2n_1n_2(N-2)!}{N!}\frac{n_1^2}{(2n_2)^2(n_1+n_2)} \tag{4.44}$$

If we take $n_2=1$ and $n_1=n>1$, the lowest-weight chiral in the composite field becomes the vacuum. The N-dependent dressing factor, which is proportional to $|\mathrm{Cent}[(n_1)(n_2)(1)^{N-n_1-n_2}| = n_1n_2(N-n_1-n_2)!$, becomes proportional to $|\mathrm{Cent}[(n)(1)^{N-n}| = n(N-n)!$, so we must multiply (4.44) by a factor of $(N-n-1)$ to obtain the result

$$\left|\left\langle \bar{O}^{(2,2)}_{[n+1]} O^{(0,0)}_{[2]} O^{(2,2)}_{[n]}\right\rangle\right|^2 = \frac{(N-2)!(N-n-1)}{N!}\frac{n^3}{2(n+1)} \tag{4.45}$$

This matches precisely with a known structure constant computed, e.g. in [43], providing a very non-trivial check of our results.

JHEP05(2022)106

4.4 The effect of spectral flow

The $\mathcal{N}=4$ superconformal algebra has an automorphism called 'spectral flow' [45]. The currents are transformed, and fermionic modes (and boundary conditions) are changed by a continuous parameter usually called spectral flow 'units'. Flow by ξ units affects the R-charge and the Virasoro currents in such a way that the weight and R-charge of a field changes as

$$h \mapsto h_\xi = h + \xi j + \frac{c}{24}\xi^2, \qquad j \mapsto j_\xi = j + \frac{c}{12}\xi, \tag{4.46}$$

while the super-currents $G^{\alpha A}(z)$ have their modes shifted by $\pm\frac{1}{2}\xi$. Since every NS chiral has $h=j$, their spectral flow by $\xi=-1$ gives a field with $h_{-1}=\frac{1}{24}c$, that is a Ramond ground state. Which NS chiral flows to which Ramond ground state is seen from the R-charges. For example, in the n-twisted sector, with $c=6n$, the lowest weight NS field $O^{(0)}_{(n)}$ has R-charge $j=\frac{n-1}{2}$, so it flows to the Ramond ground state $R^-_{(n)}$, with R-charge $j=\frac{n-1}{2}+\frac{6n}{12}\xi=-\frac{1}{2}$. Overall,

$$\begin{aligned}
&|O^{(0)}_{[n]}\rangle \xrightarrow[\xi=-1]{} |R^-_{[n]}\rangle\,, \qquad |O^{(2)}_{[n]}\rangle \xrightarrow[\xi=-1]{} |R^+_{[n]}\rangle\,, \qquad |O^{(1\pm)}_{[n]}\rangle \xrightarrow[\xi=-1]{} |R^{\dot{A}}_{[n]}\rangle \\
&|\bar{O}^{(0)}_{[n]}\rangle \xrightarrow[\xi=-1]{} |R^+_{[n]}\rangle\,, \qquad |\bar{O}^{(2)}_{[n]}\rangle \xrightarrow[\xi=-1]{} |R^-_{[n]}\rangle\,, \qquad |\bar{O}^{(1\mp)}_{[n]}\rangle \xrightarrow[\xi=-1]{} |R^{\dot{A}}_{[n]}\rangle
\end{aligned} \tag{4.47}$$

Naturally, spectral flow relates pairs of functions involving these fields. In fact, it is usual in the literature on the D1-D5 CFT to compute three-point functions with fields on the NS sector, and then relate these to functions on the Ramond sector (where SUGRA states live) via spectral flow; see for example [52, 54].

Given a state $|\Psi\rangle$, the automorphism of the Hilbert space will map it to another state $|\Psi\rangle_\xi$, while an operator $\mathscr{O}(z)$ will be mapped to $\mathscr{O}_\xi(z)$, with a linear operator U_ξ such that

$$|\Psi\rangle_\xi = U_\xi\,|\Psi\rangle\,, \qquad \mathscr{O}_\xi(z) = U_\xi \mathscr{O}(z) U_\xi^{-1}, \tag{4.48}$$

preserving amplitudes $\langle\Psi|\,\mathscr{O}\,|\Psi\rangle$. In the free orbifold CFT, the linear operator has a natural implementation in terms of the bosonized fermions, inserted at the origin (i.e. at past infinity),

$$U_\xi(z) = \exp\left(\frac{i\xi}{2}\sum_{I=1}^{N}\Big[\phi_{1,I}(z)-\phi_{2,I}(z)\Big]\right), \qquad U_\xi = U_\xi(0). \tag{4.49}$$

This is an S_N-invariant operator, including all copies $I=1,\cdots,N$ of the free bosons that bosonize the fermions. Moving U_ξ past a bare twist σ_g, for any $g\in S_N$, only has the effect of shuffling the copies, which leaves U_ξ invariant, hence $U_\xi\sigma_g=\sigma_g U_\xi$. Bosons also commute with U_ξ. Let $\mathscr{O}(z)$ be a primary fermionic field which can be written in bosonized language as an exponential of a linear combination of the $\phi_{r,I}$, multiplied (or not) by a bare twist σ_g. The most important examples of such fields are the composite NS chirals (4.6) and Ramond ground states (4.5). Commutation with U_ξ is then

$$\mathscr{O}(z)U_\xi(0) = z^{-j\xi}\,U_\xi(0)\mathscr{O}(z), \quad \text{hence} \quad \mathscr{O}_\xi(z) = U_\xi\mathscr{O}(z)U_\xi^{-1} = z^{j\xi}\mathscr{O}(z). \tag{4.50}$$

JHEP05(2022)106

Here j is the R-charge of $\mathscr{O}$. The first equation follows from the commutation of U_ξ and σ_g, along with the well-known formula (see e.g. [55]) for commuting a pair of exponentials: $e^{k_a\phi_a(z)}e^{k'_b\phi_b(z')} = e^{k_ak'_b\langle\phi_a(z)\phi_b(z')\rangle}e^{k'_b\phi_b(z')}e^{k_a\phi_a(z)}$, where $k_a, k'_b \in \mathbb{C}$, there are sums over a, b, and the c-number exponential in the r.h.s. includes the two-point function $\langle\phi_a(z)\phi_b(z')\rangle = \delta_{ab}\log(z-z')$, valid for our bosons; cf. eq. (A.3). The second equation in (4.50) also uses that $U_\xi^{-1} = U_{-\xi} = U_\xi^\dagger$, as readily seen from the explicit realization (4.49). Since U_ξ commutes with bare twists and bosons, which are R-neutral, formulas (4.50) actually hold for these fields as well.

To confirm that U_ξ in (4.49) is indeed the correct operator leading to (4.46), we can look at how it affects the weight and the charge of a state $|\mathscr{O}\rangle = \mathscr{O}(0)\,|\varnothing\rangle$ generated by an operator that transforms as (4.50). According to (4.48), we have

$$|\mathscr{O}\rangle_\xi = U_\xi\,|\mathscr{O}\rangle = \lim_{z\to 0}\left(U_\xi\mathscr{O}(z)U_\xi^{-1}\right)U_\xi\,|\varnothing\rangle = \lim_{z\to 0} z^{j\xi}\mathscr{O}(z)U_\xi\,|\varnothing\rangle\,. \tag{4.51}$$

The dimension of the state in the r.h.s. is a sum of the dimensions of $\mathscr{O}$ and U_ξ, plus a factor of $j\xi$ coming from $z^{j\xi}$. Since the exponential (4.49) has weight $h = \frac{c}{24}\xi^2$ and R-charge $j = \frac{c}{12}\xi$, $c = 6N$, the result matches (4.46). Alternatively, we can explicitly write the most general possible exponential and take the OPE with (4.49),

$$\begin{aligned}\mathscr{O}(z) &= \exp\left(\frac{i}{2}\textstyle\sum_{I=1}^N\left[\alpha_I\phi_{1,I}(z)+\beta_I\phi_{2,I}(z)\right]\right)\sigma_g(z), \quad \text{with} \quad j = \textstyle\sum\frac{1}{4}(\alpha_I-\beta_I),\\ \mathscr{O}(z)U_\xi(0) &= z^{-j\xi}\ \exp\left(\frac{i}{2}\textstyle\sum_{I=1}^N\left[(\alpha_I+\xi)\phi_{1,I}+(\beta_I-\xi)\phi_{2,I}\right]\right)\sigma_g(0).\end{aligned}$$

So the factor $z^{j\xi}$ cancels in eq. (4.51), giving

$$|\mathscr{O}\rangle_\xi = \exp\left(\frac{i}{2}\sum_{I=1}^N\Big[(\alpha_I+\xi)\phi_{1,I}(0)+(\beta_I-\xi)\phi_{2,I}(0)\Big]\right)\sigma_g(0)\,|\varnothing\rangle\,. \tag{4.52}$$

The weight and the charge of this last exponential again agree with (4.46). Further, by looking at (4.1)–(4.2), eq. (4.52) explicitly reproduces the map (4.47) between Ramond ground states and NS chiral states.

If we are considering just a specific n-twisted sector of Hilbert space generated by a bare twist $\sigma_{(n)}$, the sums over copies $I = 1, \cdots, N$ in all exponentials above can be replaced by sums over only the n copies in the corresponding cycle (n), say $I = 1, \cdots, n$. This is possible because fields in different copies commute, so the normal-ordered exponential in (4.49) can be readily factorized.[12] We can in fact repeat the argument above, using these restricted sum over copies, to derive the transformation of the single-cycle fields (4.1)–(4.2) more directly. This restricted version of the U_ξ operator also defines a notion of spectral flow on the individual n-twisted sectors (or n-twisted "strands"), where the transformations (4.46) hold with $c = 6n < 6N$. Although quite useful for some computations on the free orbifold, these individual flows are broken when the theory is deformed by $O^{(\text{int})}_{[2]}$, because its twist

[12]The factors of U_ξ made by the copies I' that do *not* enter the operator $\mathscr{O} \sim \sigma_{(n)}$, they act on $|\varnothing\rangle$ to create a tensor product of untwisted Ramond fields $|R^-_{I'}\rangle$.

JHEP05(2022)106

mixes different sectors, as discussed in [53]. Only the full spectral flow of the $c = 6N$ theory, involving all N copies simultaneously, is preserved.

In order to relate our four-point functions by spectral flow, it is convenient to regard them as two-point functions on non-trivial states. We can be rather general: consider a state $|\mathscr{X}\rangle$, created by an operator $\mathscr{X}(z)$ which transforms as in (4.50). Now consider the expectation value of a pair of conjugate operators Z and $\bar{Z}$ on the flowed state $|\mathscr{X}\rangle_\xi = U_\xi |\mathscr{X}\rangle$. Using the transposition property (4.50) twice,

$$\begin{aligned} {}_\xi\langle\mathscr{X}|\bar{Z}(1)Z(v)|\mathscr{X}\rangle_\xi &= \langle\mathscr{X}|\, U_\xi^\dagger\ \bar{Z}(1)Z(v)\ U_\xi\,|\mathscr{X}\rangle \\ &= v^{\xi j_Z}\,\langle\mathscr{X}|\, U_\xi^\dagger\ \bar{Z}(1)\ U_\xi\ Z(v)\,|\mathscr{X}\rangle \\ &= v^{\xi j_Z}\,\langle\mathscr{X}|\, U_\xi^\dagger U_\xi\ \bar{Z}(1)Z(v)\,|\mathscr{X}\rangle \\ &= v^{\xi j_Z}\,\langle\mathscr{X}|\,\bar{Z}(1)Z(v)\,|\mathscr{X}\rangle \end{aligned} \tag{4.53}$$

where j_Z is the R-charge of Z, and passing U_ξ over $\bar{Z}$ at $z = 1$ gives a trivial factor. In the last line, we used that $U_\xi^\dagger = U_{-\xi} = U_\xi^{-1}$. This computation relates correlators of the fields Z and $\bar{Z}$ on different states $|\mathscr{X}\rangle$ and $|\mathscr{X}\rangle_\xi$. But looking at the r.h.s. of the first line, we see that if we insert $\mathrm{id} = U_\xi U_\xi^{-1}$ between fields, to get $\langle\mathscr{X}|\,(U_\xi^{-1}\bar{Z}(1)U_\xi)(U_\xi^{-1}Z(v)\ U_\xi)\,|\mathscr{X}\rangle$, we can also find a relation between functions with flowed *operators* on the (fixed) state $|\mathscr{X}\rangle$. In summary,

$$\langle\mathscr{X}|\,\bar{Z}_\xi(1)Z_\xi(v)\,|\mathscr{X}\rangle = {}_\xi\langle\mathscr{X}|\bar{Z}(1)Z(v)\,|\mathscr{X}\rangle_\xi = v^{\xi j_Z}\,\langle\mathscr{X}|\,\bar{Z}(1)Z(v)\,|\mathscr{X}\rangle\,. \tag{4.54}$$

We can now apply these results to four-point functions of the type (3.1), where the Z fields carry a twist $\sigma_{[2]}$, and the states $|\mathscr{X}\rangle$ are created by the multi-cycle fields (3.2). Factorization lets us consider only the functions with double-cycle states in eq. (3.10), so we focus on the four-point functions (4.11), which are given by the master formulas computed in section 4.1. We will omit the various indices of $A^{\alpha\beta|\hat{\sigma}\hat{\varrho}|\check{\sigma}\check{\varrho}}_{n_1,n_2}(v)$ for economy:

$$A(v) = \Big\langle [\bar{X}^{\{\hat{\sigma},\hat{\varrho}\}}_{[n_1]}\bar{X}^{\{\check{\sigma},\check{\varrho}\}}_{[n_2]}]\Big|\ \bar{Z}^{\{\alpha,\beta\}}_{[2]}(1)\ Z^{\{\alpha,\beta\}}_{[2]}(v)\ \Big|[X^{\{\hat{\sigma},\hat{\varrho}\}}_{[n_1]}X^{\{\check{\sigma},\check{\varrho}\}}_{[n_2]}]\Big\rangle \tag{4.55}$$

and

$$A_\xi(v) = {}_\xi\Big\langle [\bar{X}^{\{\hat{\sigma},\hat{\varrho}\}}_{[n_1]}\bar{X}^{\{\check{\sigma},\check{\varrho}\}}_{[n_2]}]\Big|\ \bar{Z}^{\{\alpha,\beta\}}_{[2]}(1)\ Z^{\{\alpha,\beta\}}_{[2]}(v)\ \Big|[X^{\{\hat{\sigma},\hat{\varrho}\}}_{[n_1]}X^{\{\check{\sigma},\check{\varrho}\}}_{[n_2]}]\Big\rangle_\xi \tag{4.56}$$

are related as in (4.54). The R-charge of $Z^{\{\alpha,\beta\}}_{[2]}$ is $j_Z = \frac{1}{4}(\alpha-\beta)$, hence

$$A_\xi(v) = v^{\frac{(\alpha-\beta)\xi}{4}}A(v). \tag{4.57}$$

The functions (4.13) are written in terms of x, that should be related to v by the inverse covering maps $x_{\mathfrak{a}}(v)$ and eq. (3.22). Using eq. (3.19), we then have

$$\begin{aligned} A_\xi\,(x) = {}& x^{\frac{1}{4}(\alpha-\beta)(n_1-n_2)\xi}\,(x-1)^{-\frac{1}{4}(\alpha-\beta)(n_1+n_2)\xi} \\ & \times\left(x+\frac{n_1}{n_2}\right)^{\frac{1}{4}(\alpha-\beta)(n_1+n_2)\xi}\left(x+\frac{n_1}{n_2}-1\right)^{-\frac{1}{4}(\alpha-\beta)(n_1-n_2)\xi}\ A\,(x)\,. \end{aligned} \tag{4.58}$$

JHEP05(2022)106

Written this way, the shift in the exponents K_i in (4.14b) is explicit. Let us emphasize that, although eq. (4.58) is parameterized by x, we are performing a standard spectral flow on the base sphere.[13]

For example, consider the function in eq. (4.38), with only lowest weight NS chirals

$$\left\langle [\bar{O}^{(0)}_{[n_1]}\bar{O}^{(0)}_{[n_2]}]\right|\, \bar{O}^{(0)}_{[2]}\; O^{(0)}_{[2]}\, \left|[O^{(0)}_{[n_1]}O^{(0)}_{[n_2]}]\right\rangle = -\frac{1}{4n_1}\frac{(1-x)^2}{x+\frac{n_1-n_2}{2n_2}}. \tag{4.59}$$

Here $\alpha=-\beta=1$, see table 1. (We are using a schematic notation omitting the arguments of operators.) If we flow the double-cycle states by $\xi=-1$, we get the double-cycle Ramond state $|[O^{(0)}_{[n_1]}O^{(0)}_{[n_2]}]\rangle_{\xi=-1} = |[R^-_{[n_1]}R^-_{[n_2]}]\rangle$, while flowing the anti-chiral state gives the conjugate Ramond state. Hence, by eq. (4.58),

$$\begin{aligned}
&\left\langle [\bar{O}^{(0)}_{[n_1]}\bar{O}^{(0)}_{[n_2]}]\right|\, \bar{O}^{(0)}_{[2]}\; O^{(0)}_{[2]}\, \left|[O^{(0)}_{[n_1]}O^{(0)}_{[n_2]}]\right\rangle\Big|_{\text{states flowed by }\xi=-1} \\
&\quad = -\frac{1}{4n_1}\frac{x^{-\frac{n_1-n_2}{2}}(x-1)^{2+\frac{n_1+n_2}{2}}(x+\frac{n_1}{n_2})^{-\frac{n_1+n_2}{2}}(x+\frac{n_1}{n_2}-1)^{\frac{n_1-n_2}{2}}}{x+\frac{n_1-n_2}{2n_2}} \\
&\quad = \left\langle [\bar{R}^-_{[n_1]}\bar{R}^-_{[n_2]}]\right|\, \bar{O}^{(0)}_{[2]}\; O^{(0)}_{[2]}\, \left|[R^-_{[n_1]}R^-_{[n_2]}]\right\rangle
\end{aligned} \tag{4.60}$$

the same result that we find if we apply the master formula (4.14) directly to the function in the last line. As another example, take the function (4.37),

$$\left\langle [\bar{O}^{(2)}_{[n_1]}\bar{O}^{(2)}_{[n_2]}]\right|\, \bar{O}^{(1+)}_{[2]}\; O^{(1+)}_{[2]}\, \left|[O^{(2)}_{[n_1]}O^{(2)}_{[n_2]}]\right\rangle = \frac{1}{16n_1^2}\frac{x\left(x+\frac{n_1}{n_2}\right)^4\left(x+\frac{n_1}{n_2}-1\right)}{\left(x+\frac{n_1-n_2}{2n_2}\right)^4}. \tag{4.61}$$

Now $\alpha=3$, $\beta=-1$. The flowed state is $|[R^+_{[n_1]}R^+_{[n_2]}]\rangle$, and formula (4.58) gives

$$\begin{aligned}
&\left\langle [\bar{O}^{(2)}_{[n_1]}\bar{O}^{(2)}_{[n_2]}]\right|\, \bar{O}^{(1+)}_{[2]}\; O^{(1+)}_{[2]}\, \left|[O^{(2)}_{[n_1]}O^{(2)}_{[n_2]}]\right\rangle\Big|_{\text{states flowed by }\xi=-1} \\
&\quad = \frac{1}{16n_1^2}\frac{x^{1-n_1+n_2}(x-1)^{n_1+n_2}(x+\frac{n_1}{n_2})^{4-n_1-n_2}(x+\frac{n_1}{n_2}-1)^{1+n_1-n_2}}{\left(x+\frac{n_1-n_2}{2n_2}\right)^4} \\
&\quad = \left\langle [\bar{R}^+_{[n_1]}\bar{R}^+_{[n_2]}]\right|\, \bar{O}^{(1+)}_{[2]}\; O^{(1+)}_{[2]}\, \left|[R^+_{[n_1]}R^+_{[n_2]}]\right\rangle
\end{aligned} \tag{4.62}$$

which is, again, what we find using the master formula (4.14) directly.

The interaction operator is more complicated than the exponential operator for which we have derived the transformation (4.50) above, but it has been shown [57, 58] that $O^{(\text{int})}_{[2]}$ is, in fact, invariant under spectral flow,[14] hence it actually does obey (4.50), being R-neutral. Now, the first equation in the chain of equalities (4.54) tells us that four-point

[13] Variants of the original [45] automorphism of the superconformal algebra are known, e.g. the 'fractional spectral flow' related to fractional modes in twisted sectors [56], and the recently introduced "partial spectral flow" [57] that changes only two of the four fermions.

[14] Here we mean the usual, "original" spectral flow; in [57] the authors also discuss a "partial" spectral flow, under which $O^{(\text{int})}_{[2]}$ is (crucially) *not* invariant.

JHEP05(2022)106

functions including $O^{(\text{int})}_{[2]}$ and states related by spectral flow must be equal. For example, based solely on spectral flow applied to the function (4.35), we conclude that

$$\begin{aligned}
&\left\langle [\bar{O}^{(2)}_{[n_1]}\bar{O}^{(2)}_{[n_2]}] \middle| O^{(\text{int})}_{[2]}\ O^{(\text{int})}_{[2]} \middle| [O^{(2)}_{[n_1]}O^{(2)}_{[n_2]}] \right\rangle \\
&\quad = \frac{1}{16n_1^2}\frac{x^{1-n_1+n_2}(x-1)^{2+n_1+n_2}\left(x+\frac{n_1}{n_2}\right)^{2-n_1-n_2}\left(x+\frac{n_1-n_2}{n_2}\right)^{1+n_1-n_2}}{\left(x+\frac{n_1-n_2}{2n_2}\right)^4} \\
&\quad = \left\langle [\bar{O}^{(2)}_{[n_1]}\bar{O}^{(2)}_{[n_2]}] \middle| O^{(\text{int})}_{[2]}\ O^{(\text{int})}_{[2]} \middle| [O^{(2)}_{[n_1]}O^{(2)}_{[n_2]}] \right\rangle\Big|_{\text{states flowed by } \xi=-1} \\
&\quad = \left\langle [\bar{R}^{+}_{[n_1]}\bar{R}^{+}_{[n_2]}] \middle| O^{(\text{int})}_{[2]}\ O^{(\text{int})}_{[2]} \middle| [R^{+}_{[n_1]}R^{+}_{[n_2]}] \right\rangle
\end{aligned} \tag{4.63}$$

This is, indeed, the correct function for Ramond fields found by the master formula, and previously known from [40] (see eq. (61) ibid.).

5 Discussion and further developments

The present paper tries to contribute to a problem that is particularly important for the fuzzball conjecture: the complete description of the D1-D5 CFT at the free orbifold point and away from it. This requires the derivation of all three- and four-point functions involving the symmetric orbifold's Ramond and NS fields (and some of their excitations), the complete list of their OPEs and the full spectrum of the non-BPS fields that might appear at the OPE channels.

We have given here a detailed description of twisted Q-point functions in M^N/S_N orbifolds, applying a technology of [33] to correlators with multi-cycle twisted fields. We have thoroughly analyzed a special class of relatively simple four-point functions where all operators are twisted: two being composite, multi-cycle fields and two being single-cycle fields with twists of length 2. We showed how to decompose these functions into connected parts where the multi-cycle fields are reduced to double-cycle fields, then studied these connected functions, with a detailed discussion of the geometry of the genus-zero covering surfaces.

Q-point functions with multi-cycle fields are disconnected, and can become rather complicated. Even extracting the large-N dependence is a task that strongly depends on the types of twist in the composite fields. We have shown that if the fields are composite but have a finite number of cycles, i.e. if the number of cycles does not grow with $N \to \infty$, then the function scales as $\sim \sum_\chi N^{\frac{1}{2}(\chi-R)}$, which is a natural generalization of the well-known formula $\sim \sum_{\mathbf{g}} N^{-\mathbf{g}+1-\frac{1}{2}Q}$ for connected functions, the genus $\mathbf{g}$ replaced by the Euler characteristic χ. But if the number of cycles in the composite field grows with N, this generalized formula does not apply. This happens for important types of composite fields, like Ramond ground states $[(R_{[n]})^{N/n}]$, with n fixed, that source well-known Lunin-Mathur geometries [59]. In our examples of functions involving these types of field, the total N-dependence comes from computing the N-dependent number of factorizations of the total correlator into connected parts. This factorization strongly depends on the structure of

JHEP05(2022)106

the twists involved in the function. Here the non-composite fields are simple twist-2 single-cycle fields, which yield a manageable result. It would be interesting to try to find a way of determining the N-dependence in a more general way. It would also be important to explore the connection of our results with those of [14].

After reducing the factorized multi-cycle four-point function into a sum of connected functions with a finite number of cycles (in our example, the remaining composite field has at most two cycles), we can use covering surfaces methods. The full S_N-invariant correlator is a sum of 'Hurwitz blocks', each associated with one of the **H** allowed topologies of covering surfaces, where **H** is a Hurwitz number. Different types of coalescences of ramification points in these surfaces dictate the resulting twists of operators that appear in the OPE channels of the four-point function. Twists configurations can restricts the correlators to such an extent that, for special classes of functions subject to other restraints, e.g. the ring of NS chiral fields in the D1-D5 CFT, Hurwitz theory may suffice to fix the correlators completely [44]. We would like to explore the structure of Hurwitz blocks in more generality, as well as their connection with conformal blocks.

Since many four-point functions involving untwisted light fields are already known, let us mention some uses of the functions with twisted light NS fields we have calculated. One possible application is in the reconstruction of S-matrix elements of a process of absorption and emission of light (or massless) quanta from the heavy object in the bulk, as suggested in [60]. Also, our correlators can be used for deriving functions with $\frac{1}{8}$-BPS operators, relevant for 3-charge microstate solutions [61, 62]. These operators are chiral excitations of Ramond ground states, and the corresponding functions can be obtained from derivatives of the functions derived here, using Ward identities. Many particular examples of such correlators are known in the context of D1-D5-P superstrata bulk geometries. For example, in [12] it is shown that the Ward identity for the simplest Virasoro excitation L_{-1} amounts to applying a differential operator D_v to the function of unexcited fields,[15]

$$D_v = (1-v)^2 \frac{\partial}{\partial v}\left(v\frac{\partial}{\partial v}\right) + 1. \tag{5.1}$$

As our four-point functions are known in closed form only in terms of the covering-surface variables x, $\bar{x}$, the question arises of whether we could translate this Ward identity to a differential operator in terms of x instead of the base-sphere anharmonic ratio v. The answer is rather simple: since we do know the mapping function $v(x)$ explicitly, we can rewrite D_v as an operator $\tilde{D}_x$ acting on our functions $A(x,\bar{x})$,

$$\tilde{D}_x A(x,\bar{x}) = \left[\frac{\{1-v(x)\}^2}{v'(x)}\frac{\partial}{\partial x}\left(\frac{v(x)}{v'(x)}\frac{\partial}{\partial x}\right) + 1\right] A(x,\bar{x}), \tag{5.2}$$

where $v'(x) = dv/dx$. Therefore the problem of reconstructing four-point functions with excited states from our correlators — even in more complicated cases involving also other generators, say J^+_{-1} and integer powers of it — is rather straightforward. Let us note, as a last comment, that once these functions are known, the methods of [41, 53] can be used:

[15] See eqs. (5.2)-(5.4) of ref. [12]; their variable z corresponds to our v.

JHEP05(2022)106

one computes integrals of the four-point functions with the deformation $O^{(\mathrm{int})}_{[2]}$ to find the anomalous dimension of the heavy fields at second order in conformal perturbation theory. Thus we may assess the renormalization or the protection of the excited states.

Acknowledgments

The work of M.S. is partially supported by the Bulgarian NSF grant KP-06-H28/5 and that of M.S. and G.S. by the Bulgarian NSF grant KP-06-H38/11. M.S. is grateful for the kind hospitality of the Federal University of Espírito Santo, Vitória, Brazil, where part of his work was done. We would like to kindly thank an anonymous referee for comments leading to the improvement of the text, in particular the addition of a discussion about spectral flow.

A Conventions for the D1-D5 CFT

Here we gather definitions and notations for the seed $\mathcal{N} = (4,4)$ CFT. In general, we follow [41]. The R-symmetry group is $\mathrm{SU}(2)_L \times \mathrm{SU}(2)_R$. We work with $(\mathbb{T}^4)^N/S_N$, and there is an additional global group $\mathrm{SU}(2)_1 \times \mathrm{SU}(2)_2$. In the superalgebra, the R-currents $J^a_I(z)$, $\tilde{J}^{\dot{a}}_I(\bar{z})$, and supercurrents $G^{\alpha A}_I(z)$, $\tilde{G}^{\dot{\alpha}\dot{A}}_I(\bar{z})$ have indices in the SU(2) groups: $a = 1,2,3$ and $\dot{a} = \dot{1},\dot{2},\dot{3}$ are triplets of $\mathrm{SU}(2)_L$ and $\mathrm{SU}(2)_R$; $\alpha = \pm$ and $\dot{\alpha} = \dot{\pm}$ doublets of $\mathrm{SU}(2)_L$ and $\mathrm{SU}(2)_R$; $A = 1,2$ and $\dot{A} = \dot{1},\dot{2}$ doublets of $\mathrm{SU}(2)_1$ and $\mathrm{SU}(2)_2$, respectively. The index $I = 1,\cdots,N$ distinguishes the N identical copies of the seed SCFT. Each copy can be realized in terms of four real bosons plus four real holomorphic and four real anti-holomorphic fermions. They are written in complexified form as $X^{\dot{A}A}_I(z,\bar{z})$, $\psi^{\alpha\dot{A}}_I(z)$ and $\tilde{\psi}^{\dot{\alpha}\dot{A}}_I(\bar{z})$, respectively. Fermions can be conveniently bozonized by chiral bosons $\phi_r(z)$ and $\tilde{\phi}_r(\bar{z})$,

$$\begin{bmatrix}\psi^{+\dot{1}}_I(z)\\ \psi^{-\dot{1}}_I(z)\end{bmatrix} = \begin{bmatrix}e^{-i\phi_{2,I}(z)}\\ e^{-i\phi_{1,I}(z)}\end{bmatrix}, \qquad \begin{bmatrix}\psi^{+\dot{2}}_I(z)\\ \psi^{-\dot{2}}_I(z)\end{bmatrix} = \begin{bmatrix}e^{i\phi_{1,I}(z)}\\ -e^{i\phi_{2,I}(z)}\end{bmatrix} \tag{A.1}$$

and similarly for $\tilde{\psi}^{\dot{\alpha}\dot{A}}_I(\bar{z})$. Exponentials are *always* normal-ordered throughout the paper. See [58, 63] for cocycles that we ignore. The non-vanishing two-point functions are

$$\langle \partial X^{\dot{A}A}_I(z)\partial X^{\dot{B}B}_I(z')\rangle = \frac{2\epsilon^{\dot{A}\dot{B}}\epsilon^{AB}}{(z-z')^2}, \tag{A.2}$$

$$\langle \psi^{\alpha\dot{A}}_I(z)\psi^{\beta\dot{B}}_I(z')\rangle = -\frac{\epsilon^{\alpha\beta}\epsilon^{\dot{A}\dot{B}}}{z-z'}, \quad \text{or} \quad \langle \partial\phi_{r,I}(z)\partial\phi_{s,I}(z')\rangle = -\frac{\delta_{rs}}{(z-z')^2} \tag{A.3}$$

Two-point functions between fields on different copies vanish. The "magnetic-components" J^3 of the R-current and $\mathfrak{J}^3$ of the $\mathrm{SU}(2)_2$ current can be most conveniently written in bosonized form,

$$J^3_I(z) = \frac{i}{2}[\partial\phi_{1,I}(z) - \partial\phi_{2,I}(z)], \qquad \mathfrak{J}^3_I(z) = \frac{i}{2}[\partial\phi_{1,I}(z) + \partial\phi_{2,I}(z)] \tag{A.4}$$

We denote the respective eigenvalues as $j, \mathfrak{j}$, and the ones in the anti-holomorphic sector as $\tilde{\jmath}, \tilde{\mathfrak{j}}$. Note that these are "magnetic", not "azimuthal" quantum numbers.

JHEP05(2022)106

B Derivation of the N-dependence of twisted Q-point functions

We now derive the key formulas of section 2 in detail. As mentioned in the text, we use the technology of [33], but generalized for generic, multi-cycle permutations, and without recurring to diagrams.

B.1 Two-point functions

First, we derive the normalization factor $\mathscr{S}_{[g]}$ of the S_N-invariant twist $\sigma_{[g]}$ in eq. (2.4). We want to compute the two-point function

$$\langle \sigma_{[g]}(0)\sigma_{[g']}(1)\rangle \equiv \langle \sigma_{[g]}\sigma_{[g']}\rangle \equiv \frac{1}{\mathscr{S}^2_{[g]}} \sum_{h\in S_N}\sum_{h'\in S_N} \langle \sigma_{hgh^{-1}}\ \sigma_{h'g'h'^{-1}}\rangle \tag{B.1}$$

We omit the arguments $z=0$, $z'=1$ for economy of space. The functions inside the sum, which contain individual elements of S_N, vanish unless

$$(hgh^{-1})\ (h'g'h'^{-1}) = \mathrm{id}. \tag{B.2}$$

The class $[g]$ consists of all permutations with the same cycle type of g, including its inverse g^{-1}. So $\langle \sigma_{[g]}\sigma_{[g']}\rangle = 0$ if g and g' have different cycle structures, i.e. if $[g]\neq[g']$, hence we take $[g']=[g]$. Due to symmetry, all terms in the sum are equal, so we need *the number of non-vanishing terms*, i.e. terms that satisfy eq. (B.2).

For a fixed element h in the first sum in (B.1), we count the non-vanishing terms in the sum over h'. This is the number of elements $h'\in S_N$ that solve the equation

$$h'gh'^{-1} = q \quad \text{for fixed } g \text{ and fixed } q=(hgh^{-1})^{-1}\in S_N \tag{B.3}$$

Note that $q\in[g]$, hence $\exists\ k\in S_N$ such that $q=kgk^{-1}$, and

$$p^{-1}gp = g \quad \text{where } p=h'k, \text{ with fixed } k\in S_N \tag{B.4}$$

The number of elements h' which solve (B.3) is the same as the number of elements p which solve (B.4). The latter are elements of the *centralizer* of g

$$\mathrm{Cent}[g] = \{p\in S_N \mid pgp^{-1}=g\}, \tag{B.5}$$

whose order (see e.g. [47]),

$$|\mathrm{Cent}[g]| = \prod_n N_n!\ n^{N_n} \quad \text{for} \quad g=\prod_n (n)^{N_n}, \quad \sum_n N_n n = N \tag{B.6}$$

only depends on the cycle structure of $[g]$. Thus (B.1) reduces to

$$\langle \sigma_{[g]}\sigma_{[g']}\rangle = \frac{|\mathrm{Cent}[g]|}{\mathscr{S}^2_{[g]}} \sum_{h\in S_N} \langle \sigma_{hgh^{-1}}\ \sigma_{(hgh^{-1})^{-1}}\rangle = \frac{|\mathrm{Cent}[g]|\,|S_N|}{\mathscr{S}^2_{[g]}}\ \langle \sigma_g\ \sigma_{g^{-1}}\rangle \tag{B.7}$$

By construction, all the terms in this last sum over h are non-vanishing as they trivially satisfy (B.2), resulting in the factor $|S_N|=N!$. This gives the normalization factor $\mathscr{S}_{[g]} = \sqrt{N!|\mathrm{Cent}[g]}$ in eq. (2.4).

JHEP05(2022)106

B.2 Q-point functions

The Q-point function of S_N-invariant fields is a multiple sum

$$\left\langle \prod_{i=1}^{Q} \sigma_{[g_i]}(z_i) \right\rangle = \frac{1}{\prod_i \mathscr{S}_{[g_i]}} \sum_{\substack{h_1 \in S_N \\ \cdots \\ h_Q \in S_N}} \left\langle \sigma_{h_1 g_1 h_1^{-1}}(z_1) \cdots \sigma_{h_Q g_Q h_Q^{-1}}(z_Q) \right\rangle \tag{B.8}$$

We will now follow [33], but with some differences: we do not rely on the existence of diagrams; we do *not* assume that the g_i are single cycles; we do *not* assume (for now) that the functions are connected. Our goal is to extract the N-dependence of the function (B.8) which comes from the multiplicity of equivalent terms. In the r.h.s. of eq. (B.8), the correlation functions' twists are individual representatives elements $p_i = h_i g_i h_i^{-1} \in S_N$ within the conjugacy classes $[g_i]$ in the l.h.s. The non-vanishing correlators are those for which $\prod_{i=1}^{Q} p_i = \mathrm{id}$. A non-vanishing function $\langle \sigma_{p_1}(z_1) \cdots \sigma_{p_Q}(z_Q) \rangle$ will depend on how the copies inside the permutations interact. All functions whose sets $\{p_i\} = \{p_1, \cdots, p_Q\}$ are related by a *global* permutation must be equal, as that amounts to an overall relabeling of all copies, and the CFT copies are identical — only their relative positions within the cycles matter. Thus we have equivalence classes, denoted by α, of the ordered list of permutations $\{p_i\}$,

$$\alpha: \quad \{p_1, p_2, \cdots, p_Q\} \sim \{k p_1 k^{-1}, k p_2 k^{-1}, \cdots, k p_Q k^{-1}\}, \quad \text{for} \quad k \in S_N \tag{B.9}$$

and functions with $\{p_i\}$ in the same equivalence class α are equal by symmetry:

$$\langle \sigma_{p_1}(z_1) \sigma_{p_2}(z_2) \cdots \sigma_{p_Q}(z_Q) \rangle = \langle \sigma_{k p_1 k^{-1}}(z_1) \sigma_{k p_2 k^{-1}}(z_2) \cdots \sigma_{k p_Q k^{-1}}(z_Q) \rangle \tag{B.10}$$

We emphasize the difference between the functions in the r.h.s. of eq. (B.8) and that in the r.h.s. of eq. (B.10): in the former case, each twist has been conjugated by a different h_i, and in the latter all twists have undergone a global conjugation by the same element k. Let us call a representative of class α by $\{p_i^\alpha\} \in \alpha$, and the set of different equivalence classes by $\mathrm{Cl} \ni \alpha$.

It is very instructive to look at concrete examples. Take the S_N-invariant four-point function

$$\left\langle \sigma_{[(3)(2)]}(z_1) \sigma_{[(2)]}(z_2) \sigma_{[(2)]}(z_3) \sigma_{[(3)(2)]}(z_4) \right\rangle \tag{B.11}$$

and consider

$$\begin{aligned} \alpha^1_{\mathbf{5}} \ni \left\{ p_1^{\alpha^1_{\mathbf{5}}}, p_2^{\alpha^1_{\mathbf{5}}}, p_3^{\alpha^1_{\mathbf{5}}}, p_4^{\alpha^1_{\mathbf{5}}} \right\} &\sim \{(1,2,3)(4,5),\ (1,4),\ (1,4),\ (1,3,2)(4,5)\} \\ &\sim \{(1,7,3)(2,5),\ (1,2),\ (1,2),\ (1,3,7)(4,5)\} \end{aligned} \tag{B.12a}$$

$$\begin{aligned} \alpha^2_{\mathbf{5}} \ni \left\{ p_1^{\alpha^2_{\mathbf{5}}}, p_2^{\alpha^2_{\mathbf{5}}}, p_3^{\alpha^2_{\mathbf{5}}}, p_4^{\alpha^2_{\mathbf{5}}} \right\} &\sim \{(1,2,3)(4,5),\ (1,4),\ (1,3),\ (3,5,4)(1,2)\} \\ &\sim \{(1,7,3)(2,5),\ (1,2),\ (1,3),\ (3,5,2)(1,7)\} \end{aligned} \tag{B.12b}$$

$$\begin{aligned} \alpha^3_{\mathbf{5}} \ni \left\{ p_1^{\alpha^3_{\mathbf{5}}}, p_2^{\alpha^3_{\mathbf{5}}}, p_3^{\alpha^3_{\mathbf{5}}}, p_4^{\alpha^3_{\mathbf{5}}} \right\} &\sim \{(1,2,3)(4,5),\ (1,2),\ (1,3),\ (2,3,1)(4,5)\} \\ &\sim \{(1,7,3)(2,5),\ (1,7),\ (1,3),\ (7,3,1)(2,5)\} \end{aligned} \tag{B.12c}$$

JHEP05(2022)106

$$\alpha^4_{\mathbf{6}} \ni \left\{p_1^{\alpha^4_{\mathbf{6}}}, p_2^{\alpha^4_{\mathbf{6}}}, p_3^{\alpha^4_{\mathbf{6}}}, p_4^{\alpha^4_{\mathbf{6}}}\right\} \sim \{(1,2,3)(4,5),\ (1,6),\ (3,6),\ (6,2,1)(4,5)\}$$
$$\sim \{(1,7,3)(2,5),\ (1,6),\ (3,6),\ (6,7,1)(2,5)\} \tag{B.12d}$$

Here we show four different classes $\alpha^1_{\mathbf{5}}, \alpha^2_{\mathbf{5}}, \alpha^3_{\mathbf{5}}, \alpha^4_{\mathbf{6}} \in \mathrm{Cl}$ contributing to (B.11), and two representatives of each class.[16] The boldface numbers $\mathbf{c}$ in $\alpha_{\mathbf{c}}$ indicate the number of *distinct copies* entering the permutations non-trivially. Distinct copies are painted with distinct colors. The coloring emphasizes that a class is determined not by the specific copies (i.e. the algarisms) that enter the cycles, but by their *relative positions* within the cycles — that is, different orderings of the colors. *Different representatives of the same class* are different ways of filling one arrangement of relative positions with algarisms $I = 1, \cdots, N$. *Different classes* are different arrangements of the relative positions, i.e. different orderings of the colors. We can see that $\alpha^1_{\mathbf{5}} \neq \alpha^2_{\mathbf{5}}$, because $p_2^{\alpha^1_{\mathbf{5}}} = (p_3^{\alpha^1_{\mathbf{5}}})^{-1}$, while $p_2^{\alpha^2_{\mathbf{5}}} \neq (p_3^{\alpha^2_{\mathbf{5}}})^{-1}$. In classes $\alpha^3_{\mathbf{5}}$ and $\alpha^4_{\mathbf{6}}$ the double cycles p_1 and p_4 *factorize*, because they contain copies that do not appear in the other permutations. Note that the permutations in these examples might be elements of S_N with $N \gg 6$, but we omit the *trivial* cycles (of length one).

We can organize the sum in (B.8) as a sum over the different classes $\alpha \in \mathrm{Cl}$ (we are leaving the normalization factors $\mathscr{S}_{[g_i]}$ behind for a while),

$$\sum_{h_i \in S_N} \left\langle \sigma_{h_1 g_1 h_1^{-1}}(z_1) \cdots \sigma_{h_Q g_Q h_Q^{-1}}(z_Q) \right\rangle = \sum_{\alpha \in \mathrm{Cl}} \mathcal{N}_\alpha \left\langle \sigma_{p_1^\alpha}(z_1) \cdots \sigma_{p_Q^\alpha}(z_Q) \right\rangle$$
$$= \sum_{\mathbf{c}} \sum_{\alpha_{\mathbf{c}} \in \mathrm{Cl}_{\mathbf{c}}} \mathcal{N}_{\alpha_{\mathbf{c}}} \left\langle \sigma_{p_1^{\alpha_{\mathbf{c}}}}(z_1) \cdots \sigma_{p_Q^{\alpha_{\mathbf{c}}}}(z_Q) \right\rangle \tag{B.13}$$

In the first line, $\{p_i^\alpha\}$ is an arbitrary representative of class α and $\mathcal{N}_\alpha$ is the number of collections $\{p_i\} \in \alpha$. In the second line, we decompose the sum further, by cataloguing the classes $\alpha \in \mathrm{Cl}$ into subsets $\mathrm{Cl}_{\mathbf{c}} \subseteq \mathrm{Cl}$, according to the number $\mathbf{c}$ of distinct copies entering the *non-trivial* cycles of $\{p_i\}$. By construction, $\cup_{\mathbf{c}} \mathrm{Cl}_{\mathbf{c}} = \mathrm{Cl}$. For fixed $\mathbf{c}$, there is a collection of different classes $\alpha_{\mathbf{c}} \in \mathrm{Cl}_{\mathbf{c}}$, with a number $\mathcal{N}_{\alpha_{\mathbf{c}}}$ of representatives $\{p_i^{\alpha_{\mathbf{c}}}\}$, one of which is chosen to appear in the correlation function.

Let us determine $\mathcal{N}_{\alpha_{\mathbf{c}}}$. In the l.h.s. of (B.13), the sum runs over configurations of the individual permutations g_i, while in the r.h.s. there is a sum over different *collections of permutations* $\{p_i^{\alpha_{\mathbf{c}}}\}$ (not individual permutations). In summing over orbits of g_i in the l.h.s., whenever $h_1 \in \mathrm{Cent}[p_1^\alpha]$ we get the same *collection* $\{p_i^\alpha\}$;[17] whenever $h_2 \in \mathrm{Cent}[p_2^\alpha]$ we again get the same collection $\{p_i^\alpha\}$, and so on, up to $h_Q \in \mathrm{Cent}[p_Q^\alpha]$. Since in the r.h.s. of eq. (B.13) the sums over h_i are independent, the number of repeated occurrences of the collection $\{p_1^\alpha, \cdots, p_Q^\alpha\}$ is

$$|\mathrm{Cent}[p_1^\alpha]| \times \cdots \times |\mathrm{Cent}[p_Q^\alpha]| = |\mathrm{Cent}[g_1]| \times \cdots \times |\mathrm{Cent}[g_Q]| \tag{B.14}$$

[16] In all four examples, the representatives are related by $\{p_i^\alpha\} \sim \{k p_i^\alpha k^{-1}\}$ with $k = (2,4,7)$.

[17] Not just a different collection $\{p_i'^\alpha\} \sim \{p_i^\alpha\} \in \alpha$ within the same equivalence class α, but *exactly the same collection* $\{p_i^\alpha\}$.

JHEP05(2022)106

since $|\text{Cent}[p_i^\alpha]|$, only depends on the cycle structure of p_i^a, which is the same as that of g_i. The same is true for the classes $\alpha_{\mathbf{c}}$, which are special types of α, hence

$$\mathcal{N}_{\alpha_{\mathbf{c}}} = \left(\prod_{i=1}^{Q} |\text{Cent}[g_i]|\right) \times \mathcal{W}_{\alpha_{\mathbf{c}}} \tag{B.15}$$

The remaining factor $\mathcal{W}_{\alpha_{\mathbf{c}}}$ counts the number of different sequences $\{p_i^{\alpha_{\mathbf{c}}}\}$ which are *not identical but still belong to the same equivalence class* $\alpha_{\mathbf{c}}$. For example, in (B.12b) we can see two sequences $\{p_i^{\alpha_{\mathbf{5}}^2}\}$ with different individual permutations (compare each cycle in the first line with the one immediately below it in the second line) that belong to the same conjugacy class $\alpha_{\mathbf{5}}^2$ (compare the relative positions of repeated copies, i.e. the order of the colors). To find $\mathcal{W}_{\alpha_{\mathbf{c}}}$, we proceed in two steps. First, we must choose the $\mathbf{c}$ copies that will enter the non-trivial permutations out of the N copies available,

$$\mathcal{W}_{\alpha_{\mathbf{c}}} = \binom{N}{\mathbf{c}} \times w_{\alpha_{\mathbf{c}}} = \frac{N!}{(N-\mathbf{c})!\mathbf{c}!}\, w_{\alpha_{\mathbf{c}}}. \tag{B.16}$$

The final remaining factor $w_{\alpha_{\mathbf{c}}}$ counts the number of ways we can arrange the $\mathbf{c}$ copies and still find collections $\{p_i\}$ within the same class. This number $w_{\alpha_{\mathbf{c}}}$, which we will determine shortly, can depend on $\mathbf{c}$ and on the cycle structure of the $[g_i]$, but it clearly cannot depend on N. So *we have already completely determined the N-scaling dependence of the Q-point function.*

It turns out that $w_{\alpha_{\mathbf{c}}}$ has a subtle dependence on the factorization of the functions in class $\alpha_{\mathbf{c}}$. As we can see from the examples (B.12), some classes will have disconnected correlators, and note that connectedness is indeed a class property: all functions $\langle \sigma_{p_1^\alpha}(z_1)\cdots\sigma_{p_Q^\alpha}(z_Q)\rangle$ in the same class α factorize the same way. So the r.h.s. of (B.13) decomposes further,

$$\begin{aligned}
&\sum_{\alpha_{\mathbf{c}}\in \text{Cl}_{\mathbf{c}}} \mathcal{N}_{\alpha_{\mathbf{c}}} \Big\langle \sigma_{p_1^{\alpha_{\mathbf{c}}}}(z_1)\cdots\sigma_{p_Q^{\alpha_{\mathbf{c}}}}(z_Q)\Big\rangle \\
&\quad = \left(\prod_{i=1}^{Q} |\text{Cent}[g_i]|\right) \frac{N!}{(N-\mathbf{c})!\mathbf{c}!} \Bigg[\sum_{\alpha_{\mathbf{c}}\in\left[\substack{\text{fully}\\ \text{connected}\\ \text{classes}}\right]} w_{\alpha_{\mathbf{c}}} \Big\langle \cdots \Big\rangle \\
&\qquad\qquad + \sum_{\alpha_{\mathbf{c}}\in\left[\substack{\text{once}\\ \text{disconnected}\\ \text{classes}}\right]} w_{\alpha_{\mathbf{c}}} \Big\langle \cdots \Big\rangle \Big\langle \cdots \Big\rangle \\
&\qquad\qquad + \sum_{\alpha_{\mathbf{c}}\in\left[\substack{\text{twice}\\ \text{disconnected}\\ \text{classes}}\right]} w_{\alpha_{\mathbf{c}}} \Big\langle \cdots \Big\rangle \Big\langle \cdots \Big\rangle \Big\langle \cdots \Big\rangle + \cdots \Bigg]
\end{aligned} \tag{B.17}$$

The possible types of factorizations of the initial correlator will depend on the original cycle structure of the $[g_i]$, and also on $\mathbf{c}$. For example, it is possible that the cycle structure

JHEP05(2022)106

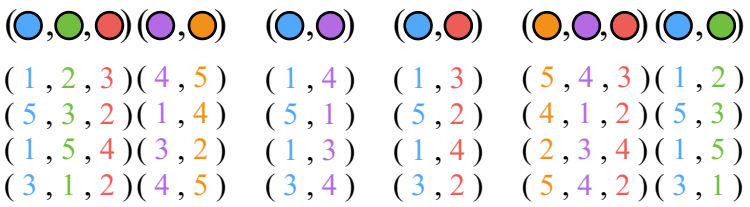

Figure 5. Four different representatives of class $\alpha^2_{\mathbf{5}}$ (the same featured in example (B.12b). All representatives have the same active copies 1, 2, 3, 4, 5 appearing in different orders, but preserving the relative positions of repeated copies.

of the $[g_i]$ be incompatible with fully connected classes — this is what happens with the functions considered in section 3 — and in this case, the first sum in the r.h.s. above is void. The factor $w_{\alpha_{\mathbf{c}}}$ is given by

$$w_{\alpha_{\mathbf{c}}} = \mathbf{c}!\,\nu_{\alpha_{\mathbf{c}}}, \quad \nu_{\alpha_{\mathbf{c}}} = \begin{cases} 1 & \text{if no two-point function factorizes} \\ 1/[\prod n_j]_{\alpha_{\mathbf{c}}} & \text{if one or more two-point function factorizes} \end{cases} \tag{B.18}$$

where the n_j are the lengths of cycles in eventual *two*-point functions that factorize in the class $\alpha_{\mathbf{c}}$.

Formula (B.18) can be obtained as follows. In eq. (B.16), we had chosen $\mathbf{c}$ copies to enter the non-trivial cycles of the set $\{p_1^{\alpha_{\mathbf{c}}}, \cdots, p_Q^{\alpha_{\mathbf{c}}}\}$. Now we start to fill the cycles of the $p_i^{\alpha_{\mathbf{c}}}$ with these copies. We choose an ordering of the copies to fill the first non-repeated slots, and then the copies in the repeated slots are fixed by the structure of the class $\alpha_{\mathbf{c}}$. So we have the freedom of choosing all $\mathbf{c}!$ orderings of $\mathbf{c}$ elements to get different collections $\{p_i^{\alpha_{\mathbf{c}}}\}$ belonging to the same class $\alpha_{\mathbf{c}}$. If no two-point functions factorize, the collections $\{p_i^{\alpha_{\mathbf{c}}}\}$ obtained in this way will all be different, yielding the first line of (B.18). But whenever the class $\alpha_{\mathbf{c}}$ has factorized two-point functions as in $\langle \sigma_{p_1^{\alpha_{\mathbf{c}}}}(z_1) \cdots \sigma_{p_Q^{\alpha_{\mathbf{c}}}}(z_Q) \rangle = \langle \cdots \rangle \prod_j \langle \sigma_{(n_j)} \sigma_{(n_j)^{-1}} \rangle$, the orderings that differ only by cyclic reorderings of the copies in the factorized cycles (n_j) will actually give the same collections $\{p_i^{\alpha_{\mathbf{c}}}\}$. There are n_j cyclic arrangements of n_j objects, and taking these into account we get the second line of (B.18).

Again, this is best understood by looking at an example. Consider class $\alpha^2_{\mathbf{5}}$ in (B.12b). In figure 5 we show different collections $\{p_i^{\alpha^2_{\mathbf{5}}}\}$, all made with the *same* copies $I = 1, 2, 3, 4, 5$. In each collection (each line), we fill the first five positions with the copies in a given ordering, and then the copies in the remaining positions cannot be chosen: they are fixed by the structure of the class, here highlighted by the coloring (positions with the same color must have the same copy). Compare the first and the last lines of figure 5, where the choices of copies differ only by a cyclic reordering of the first cycle, $(1, 2, 3) = (3, 1, 2)$. Hence, *in these two orderings, the first two cycles are the same.* Nevertheless, *the collections as a whole are not the same* because their remaining cycles are *not* equivalent. This is a consequence of the connectedness of this class. In accordance with formula (B.18), in this case there are $w_{\alpha^2_{\mathbf{5}}} = \mathbf{c}! = 5! = 120$ ways of ordering the copies $I = 1, 2, 3, 4, 5$, all of them giving different sequences $\{p_i^{\alpha^2_{\mathbf{5}}}\}$ in the same class.

JHEP05(2022)106

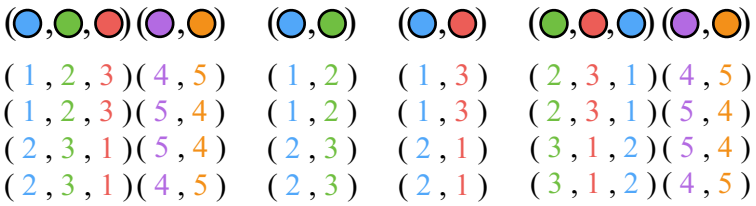

Figure 6. Different representatives of class $\alpha^3_{\mathbf{5}}$, the same featured in example (B.12c). All representatives have the same active copies 1, 2, 3, 4, 5 appearing in different orders, preserving the relative positions of repeated copies.

Now consider the analogous examination of class $\alpha^3_{\mathbf{5}}$ in (B.12c), shown in figure 6. In this class, there is a factorization of the two-cycles of p_1 and p_4, making a two-point function:

$$\begin{aligned}&\left\langle \sigma_{(\bullet,\bullet,\bullet)(\bullet,\bullet)}(z_1)\sigma_{(\bullet,\bullet)}(z_2)\sigma_{(\bullet,\bullet)}(z_3)\sigma_{(\bullet,\bullet,\bullet)(\bullet,\bullet)}(z_4)\right\rangle \\ &\quad = \left\langle \sigma_{(\bullet,\bullet,\bullet)}(z_1)\sigma_{(\bullet,\bullet)}(z_2)\sigma_{(\bullet,\bullet)}(z_3)\sigma_{(\bullet,\bullet,\bullet)}(z_4)\right\rangle \left\langle \sigma_{(\bullet,\bullet)}(z_1)\sigma_{(\bullet,\bullet)}(z_4)\right\rangle\end{aligned} \tag{B.19}$$

Now the choices of $I = 1, 2, 3, 4, 5$ that only differ by cyclic reordering of the copies entering the factorized cycles do result in *identical* collections $\{p_i^{\alpha^3_{\mathbf{5}}}\}$. As an example, consider the first two lines of figure 6: they differ by a cyclic reordering of copies 4 and 5, entering the factorized cycles, and the configuration of the remaining, non-factorized cycles is left invariant. So the two ordered choices of copies, $1, 2, 3, 4, 5$ and $1, 2, 3, 5, 4$, must not be counted as different collections $\{p_i^{\alpha^3_{\mathbf{5}}}\}$. The same happens for all other choices, for instance the ones in the third and fourth lines of figure 6. Thus, in accordance with formula (B.18), we must divide the total number $\mathbf{c}! = 5!$ of ordered choices of copies by the number $n = 2$ of cyclic reorderings of the copies entering the factorized cicles. Finally, compare the first and the last lines of figure 6, which differ by a cyclic reordering of the first, *non*-factorized cycle $(1, 2, 3) = (2, 3, 1)$. These two collections are *not* identical, as you can see that the permutations $p_2^{\alpha^3_{\mathbf{5}}} = (\bullet, \bullet)$ are not the same in the two collections, and neither are the permutations $p_3^{\alpha^3_{\mathbf{5}}} = (\bullet, \bullet)$.

B.3 Restrictions on the possible factorizations

The restricted possibilities of factorization of the function (3.3) is due to the fact that the connected functions (3.4a) and (3.4b) are implicitly multiplied by a product of factorized two-point functions

$$\langle \bar{X}^{\zeta_i}_{(n_i)}(\infty) X^{\zeta_i}_{(n_i)}(0)\rangle = 1, \tag{B.20}$$

where the fields $X^{\zeta}_{(n)}$ and $\bar{X}^{\zeta}_{(n)}$ are the ones whose cycles do not overlap with $Z_{(2)}$ nor $\bar{Z}_{(2)}$. For a hypothetical connected function with components $\bar{X}^{\zeta}_{(n)}$ and $X^{\zeta}_{(n)}$ of the original multi-cycle fields in (3.3), such that the remaining components do not *all* match into pairs like (B.20), the factorization is forbidden. For example, a factorizations leading to the connected function

$$\left\langle [\bar{X}^{\zeta_1}_{(n_1)} \bar{X}^{\zeta_2}_{(n_2)}] \bar{Z}_{(2)} Z_{(2)} X^{\zeta_3}_{(n_1+n_2-1)} \right\rangle, \tag{B.21}$$

JHEP05(2022)106

seems possible because it satisfies (2.8), but is forbidden because the factorized operators have different cycles so the analogous to (B.20) vanishes.

A more subtle case is a factorization leading to a product of three-point functions:

$$\begin{aligned}\Big\langle [\prod_{\zeta,n}(\bar{X}^{\zeta}_{(n)})^{N^{\zeta}_n}]\ \bar{Z}_{(2)}\ Z_{(2)}[\prod_{\zeta,n}(X^{\zeta}_{(n)})^{N^{\zeta}_n}]\Big\rangle \\ = \Big\langle [\bar{X}^{\zeta_1}_{(n_1)}\bar{X}^{\zeta_2}_{(n_2)}]\ \bar{Z}_{(2)}\ X^{\zeta_3}_{(n_1+n_2)}\Big\rangle\ \Big\langle \bar{X}^{\zeta_3}_{(n_1+n_2)}\ Z_{(2)}\ [X^{\zeta_1}_{(n_1)}X^{\zeta_2}_{(n_2)}]\Big\rangle.\end{aligned} \tag{B.22}$$

This is, in general, *not* forbidden. But for this factorization to occur, the original composite field must, necessarily, have at least one component with cycle length equal to the sum of other two components, i.e.

$$\Big[\prod_{\zeta,n}(X^{\zeta}_{(n)})^{N^{\zeta}_n}\Big] = \Big[X^{\zeta_1}_{(n_1)}X^{\zeta_2}_{(n_2)}X^{\zeta_3}_{(n_3)}\cdots\Big] \qquad \text{with} \qquad n_3 = n_1 + n_2.$$

So functions with fields like $\mathscr{X} = [(X^{\zeta}_{[n]})^{N/n}]$, for example, never factorize as (B.22).

Furthermore, in the concrete case of the D1-D5 CFT, the fields carry SU(2) charges — in particular, the R-charge — which must add to zero inside a non-vanishing correlation function. This imposes more selection rules. For example, if $Z_{[2]}$ is R-neutral, e.g. $Z_{[2]} = O^{(\mathrm{int})}_{(2)}$, and the $X^{\zeta}_{(n)} = R^{\zeta}_{(n)}$ are Ramond fields (4.1), all possible three-point functions like (B.22) vanish. Meanwhile, for specific configurations, e.g.

$$\Big[\prod_{\zeta,n}(X^{\zeta}_{(n)})^{N^{\zeta}_n}\Big] = \Big[R^{+}_{(n_1)}R^{+}_{(n_2)}R^{+}_{(n_1+n_2)}\cdots\Big] \quad \text{and} \quad Z_{(2)} = \bar{O}^{(0,0)}_{(2)}$$

(note that $Z_{(2)}$ is an anti-chiral field, with $j = -\frac{1}{2}$), the three-point functions in (B.22) do have zero R-charges. If all fields in (B.22) are (possibly different types of) NS chirals, there may also be non-vanishing three-point functions. For example, if

$$\Big[\prod_{\zeta,n}(X^{\zeta}_{(n)})^{N^{\zeta}_n}\Big] = \Big[O^{(0,0)}_{(n_1)}O^{(0,0)}_{(n_2)}O^{(0,0)}_{(n_1+n_2)}\cdots\Big] \quad \text{and} \quad Z_{(2)} = \bar{O}^{(0,0)}_{(2)}$$

the factorization (B.22) becomes

$$\Big\langle [\bar{O}^{(0,0)}_{(n_1)}\bar{O}^{(0,0)}_{(n_2)}]\ O^{(0,0)}_{(2)}\ O^{(0,0)}_{(n_1+n_2)}\Big\rangle\ \Big\langle \bar{O}^{(0,0)}_{(n_1+n_2)}\ \bar{O}^{(0,0)}_{(2)}\ [O^{(0,0)}_{(n_1)}O^{(0,0)}_{(n_2)}]\Big\rangle, \tag{B.23}$$

which is non-vanishing: the R-charges in the first correlator are

$$-\frac{1}{2}(n_1-1) - \frac{1}{2}(n_2-1) - \frac{1}{2}(2-1) + \frac{1}{2}(n_1+n_2-1) = 0$$

and likewise for the second correlator.

As mentioned in the main text below (3.4), *if* the factorization into three-point functions occurs, it can be dealt with using basically the same procedure we have used for the factorizations (3.4). There will be an additional contribution to the r.h.s. of eq. (3.7), with a sum over classes that factorize as (B.22). The factorized terms can then be reduced to (products of) S_N-invariant three-point functions, that will appear in the r.h.s. of eq. (3.10)

JHEP05(2022)106

multiplied by "symmetry factors". These factors are what connects the S_N-invariant three-point functions to the full four-point function with the multi-cycle composite fields. They can be found following the same type of combinatoric analysis used to derive e.g. $\mathscr{P}$, but are highly "example-sensitive": given two cycles of length n_1 and n_2 in the composite field, the symmetry factors will depend on how many components with cycle length $n_3 = n_1 + n_2$ there are in the field, on the corresponding R-charges etc. Hence it would be cumbersome to try to find a more or less generic formula — which is yet another reason why we omit these cases in the paper. Going forward, once the symmetry factors in a given case are known, there still remains to compute the S_N-invariant connected three-point functions, as we do in the paper for the connected four-point functions (3.16). But, compared with four-point functions, the analysis of twisted three-point functions is much better known. General formulas can be found in the work of Lunin and Mathur [38] and, for functions involving only NS chiral fields, many structure constants are known since they form the NS chiral ring [24, 43, 44]. We should note, yet, that the functions in (B.22) include one composite double-cycle field, and these are less studied in the literature. But this kind of structure constant is just what appears in the OPEs we have studied here, see eq. (4.26). Hence our own results can also be used to complete the computation of the special cases where the factorization (B.22) exists.

B.4 Untwisted composite fields

Let us compute the normalization factor $\mathscr{S}$ of a generic untwisted field (2.27). The symmetrization

$$\mathrm{Sym}[\otimes_{i=1}^{f}(X^{s_i}_{I_1^{(i)}} \otimes \cdots \otimes X^{s_i}_{I_{p_i}^{(i)}})] \tag{B.24}$$

is a sum of all possible configurations of the copies. A generic term in the sum is

$$\left(X^{\zeta_1}_{I_1^{(1)}} \otimes \cdots \otimes X^{\zeta_1}_{I_{p_1}^{(1)}}\right) \otimes \left(X^{\zeta_2}_{I_2^{(2)}} \otimes \cdots \otimes X^{\zeta_2}_{I_{p_2}^{(2)}}\right) \otimes \cdots \otimes \left(X^{s_f}_{I_f^{(f)}} \otimes \cdots \otimes X^{s_f}_{I_{p_f}^{(f)}}\right) \tag{B.25}$$

where the copies $I_{p_i}^{(i)}$ are all distinct. How many equivalent such terms are there? One must choose p_1 copies out of N to enter the first parenthesis (inside of which all fields are equivalent, i.e. have the same s), so there are $\binom{N}{p_1}$ options. Then one must choose p_2 copies out of the remaining $N - p_1$ copies to enter the second parenthesis, and there are $\binom{N-p_1}{p_2}$ options. And so on. The total number of equivalent terms is therefore

$$\mathscr{S} = \binom{N}{p_1} \times \binom{N-p_1}{p_2} \times \cdots \times \binom{N-\sum_{j=1}^{f-1} p_j}{p_f} = \frac{N!}{\left(N-\sum_{i=1}^{f} p_i\right)! \prod_{i=1}^{f}(p_i!)} \tag{B.26}$$

which is the result appearing in (2.27). Note that we have not required that every one of the N copies appear in each term (B.25), that is, we have not required that $\sum_i p_i = N$. If this is the case, then the expression in the last line of (B.26) simplifies

$$\frac{N!}{\left(N-\sum_{i=1}^{f} p_i\right)! \prod_{i=1}^{f}(p_i!)} = \frac{N!}{\prod_{i=1}^{f}(p_i!)} \quad \text{for} \quad \sum_{i=1}^{f} p_i = N. \tag{B.27}$$

If there are only two powers, $p_1 = q$ and $p_2 = N - q$, this formula reduces to (2.28).

JHEP05(2022)106

Factorization of four-point functions. For untwisted composite fields, since there is no sum over orbits of trivial cycles, we must redo our computations. For definiteness, consider the operator in (2.28), and the two-point function

$$\Big\langle [X^p_{[1]}Y^q_{[1]}]^\dagger(\infty)\ Z^\dagger_{[2]}(1)\ Z_{[2]}(v,\bar v)\ [X^p_{[1]}Y^q_{[1]}](0)\ \Big\rangle, \quad q=N-p. \tag{B.28}$$

There are two sums over orbits of the 2-cycles, and symmetrization of the copies in the composite fields. Leaving the normalization factors, a generic term in the sum has the following permutation structure (coordinates omitted for economy of space)

$$\Big\langle [X_{I_1}\cdots X_{I_p}Y_{I_{p+1}}\cdots Y_{I_{p+q}}]^\dagger\ Z^\dagger_{h_1(2)h_1^{-1}}\ Z_{h_v(2)h_v^{-1}}\ [X_{J_1}\cdots X_{J_p}Y_{J_{p+1}}\cdots Y_{J_{p+q}}]\ \Big\rangle. \tag{B.29}$$

The function can factorize in three ways, depending on the interaction of the cycles in the middle. If the cycles are disjoint, then the factorization is

$$\Big\langle \cdots\ Z^\dagger_{h_1(2)h_1^{-1}}\ \cdots\Big\rangle\Big\langle \cdots Z_{h_v(2)h_v^{-1}}\ \cdots\Big\rangle = 0 \tag{B.30}$$

which vanishes because the remaining correlators do not satisfy the fundamental condition (2.8). If the cycles are not disjoint, they can either compose to a three cycle, or be the inverse of each other. In the former case, if $h_1(2)h_1^{-1}h_v(2)h_v^{-1}=(3)$, then the correlator also vanishes because, again, it fails to satisfy (2.8). The final remaining possibility is that the cycles are the inverses of each other; then the factorized function does satisfy (2.8), so this is the only non-vanishing factorization.

C Derivation of the master formula

Here we give details of the derivation of the four-point function (4.11), namely

$$\Big\langle \Big[X^{\{\hat\sigma,\hat\varrho\}}_{[n_1]}X^{\{\check\sigma,\check\varrho\}}_{[n_2]}\Big]^\dagger(\infty)\ Z^{\{\alpha,\beta\}\dagger}_{[2]}(1)\ Z^{\{\alpha,\beta\}}_{[2]}(v)\ \Big[X^{\{\hat\sigma,\hat\varrho\}}_{[n_1]}X^{\{\check\sigma,\check\varrho\}}_{[n_2]}\Big](0)\Big\rangle, \tag{C.1}$$

as parameterized by the pre-image x of u on the covering surface. Near a ramification point z_*, where $z(t)\approx z_*+b_*(t-t_*)^n$, the bosonized fermionic exponentials lift to (the lifted field is in the r.h.s.) [38]

$$\exp\left[\frac{i}{2n}\sum_{I=1}^n\Big[\sigma\phi_{1,I}(z_*)+\varrho\phi_{2,I}(z_*)\Big]\right]\sigma_{(n)}(z_*)\hookleftarrow b_*^{-\frac{\sigma^2+\varrho^2}{8n}}\exp\left[\frac{i\sigma}{2}\phi_1(t_*)+\frac{i\varrho}{2}\phi_2(t_*)\right] \tag{C.2a}$$

When inserted at $z=\infty$, the exponential lifts with a *positive* power of b_*,

$$\exp\left[\frac{i}{2n}\sum_{I=1}^n\Big[\sigma\phi_{1,I}(\infty)+\varrho\phi_{2,I}(\infty)\Big]\right]\sigma_{(n)}(\infty)\hookleftarrow b_*^{+\frac{\sigma^2+\varrho^2}{8n}}\exp\left[\frac{i\sigma}{2}\phi_1(t_*)+\frac{i\varrho}{2}\phi_2(t_*)\right] \tag{C.2b}$$

JHEP05(2022)106

The coefficients at the branching points of (3.17) are

$$b_0 = x^{-n_2}(x-1)^{-n_1}\left(x+\frac{n_1}{n_2}\right)^{n_1+n_2}\left(x+\frac{n_1}{n_2}-1\right)^{-n_1} \tag{C.3a}$$

$$b_{t_0} = \left(-\frac{n_1}{n_2}\right)^{-n_2}(x-1)^{-n_2}\left(x+\frac{n_1}{n_2}\right)^{n_1+n_2}\left(x+\frac{n_1}{n_2}-1\right)^{n_2-n_1} \tag{C.3b}$$

$$b_{t_1} = -n_1(x-1)^{-2}\left(x+\frac{n_1}{n_2}\right)^{2}\left(x+\frac{n_1}{n_2}-1\right)^{-2}\left(x+\frac{n_1-n_2}{2n_2}\right) \tag{C.3c}$$

$$b_x = n_1 x^{n_1-n_2-2}(x-1)^{-(n_1+n_2)}\left(x+\frac{n_1}{n_2}\right)^{n_1+n_2}\left(x+\frac{n_1}{n_2}-1\right)^{n_2-n_1}\left(x+\frac{n_1-n_2}{2n_2}\right) \tag{C.3d}$$

$$b_{t_\infty} = \left(\frac{n_1}{n_2}\right)^{n_2} x^{n_1}(x-1)^{-(n_1+n_2)}\left(x+\frac{n_1}{n_2}\right)^{-n_2}\left(x+\frac{n_1}{n_2}-1\right)^{n_2} \tag{C.3e}$$

$$b_\infty = (-1)^{n_2}(x-1)^{-(n_1+n_2)}\left(x+\frac{n_1}{n_2}\right)^{n_1}\left(x+\frac{n_1}{n_2}-1\right)^{n_2-n_1} \tag{C.3f}$$

and the fields that we use are lifted to

$$X^{\{\hat\sigma,\hat\varrho\}\dagger}(\infty)X^{\{\check\sigma,\check\varrho\}\dagger}(t_\infty) = b_\infty^{\frac{\hat\sigma^2+\hat\varrho^2}{8n_1}} b_{t_\infty}^{\frac{\check\sigma^2+\check\varrho^2}{8n_2}} e^{-\frac{i}{2}[\hat\sigma\phi_1(\infty)+\hat\varrho\phi_2(\infty)]}\ e^{-\frac{i}{2}[\check\sigma\phi_1(t_\infty)+\check\varrho\phi_2(t_\infty)]} \tag{C.4a}$$

$$X^{\{\hat\sigma,\hat\varrho\}}(0)X^{\{\check\sigma,\check\varrho\}}(t_0) = b_0^{-\frac{\hat\sigma^2+\hat\varrho^2}{8n_1}} b_{t_0}^{-\frac{\check\sigma^2+\check\varrho^2}{8n_2}} e^{\frac{i}{2}[\hat\sigma\phi_1(0)+\hat\varrho\phi_2(0)]}\ e^{\frac{i}{2}[\check\sigma\phi_1(t_0)+\check\varrho\phi_2(t_0)]} \tag{C.4b}$$

$$Z^{\{\alpha,\beta\}\dagger}(t_1) = b_{t_1}^{-\frac{\alpha^2+\beta^2}{16}} e^{-\frac{i}{2}[\alpha\phi_1(t_1)+\beta\phi_2(t_1)]} \tag{C.4c}$$

$$Z^{\{\alpha,\beta\}}(x) = b_x^{-\frac{\alpha^2+\beta^2}{16}} e^{\frac{i}{2}[\alpha\phi_1(x)+\beta\phi_2(x)]} \tag{C.4d}$$

Lifted fields carry no twist indices because they are untwisted. Apart from the b_* factors, the function (4.12) is a six-point function of exponentials only, whose computation is immediate. Therefore,

$$\begin{aligned} A^{\alpha\beta|\hat\sigma\hat\varrho|\check\sigma\check\varrho}_{n_1,n_2}(x)_{\text{cover}} &= b_\infty^{\frac{1}{4n_1}} b_{t_\infty}^{\frac{1}{4n_2}} b_{t_1}^{-\frac{1}{8}} b_x^{-\frac{1}{8}} b_0^{-\frac{1}{4n_1}} b_{t_0}^{-\frac{1}{4n_2}} \\ &\times \left[\frac{(t_\infty-t_1)(t_0-x)}{(t_\infty-x)(t_0-t_1)}\right]^{\frac{\alpha\check\sigma+\beta\check\varrho}{4}} \left(\frac{x}{t_1}\right)^{\frac{\alpha\hat\sigma+\beta\hat\varrho}{4}} \left(\frac{t_0}{t_\infty}\right)^{\frac{\check\sigma\hat\sigma+\hat\varrho\check\varrho}{4}} (t_\infty-t_0)^{-\frac{\check\sigma^2+\check\varrho^2}{4}} (t_1-x)^{-\frac{\alpha^2+\beta^2}{4}} \end{aligned} \tag{C.5}$$

where we need to express t_1, t_0, t_∞ all in terms of x via (3.18). The final result for the base sphere four-point function, parameterized by x, is (4.13), i.e. $A^{\alpha\beta|\hat\sigma\hat\varrho|\check\sigma\check\varrho}_{n_1,n_2}(x) = e^{S_L} A^{\alpha\beta|\hat\sigma\hat\varrho|\check\sigma\check\varrho}_{n_1,n_2}(x)_{\text{cover}}$, where e^{S_L} is the bare-twist correlation function; using either the results in [52] or the stress-tensor method of [41, 53], we can find

$$\begin{aligned} S_L(x) = &-\frac{2n_2^2+(2+3n_2)(n_1-n_2)n_1}{8n_1n_2}\log x \\ &+\frac{2n_2^2+(2+3n_2)(n_1+n_2)n_1}{8n_1n_2}\log(x-1) \\ &+\frac{2n_2^2+(2-3n_2)(n_1+n_2)n_1}{8n_1n_2}\log\left(x+\frac{n_1}{n_2}\right) \\ &-\frac{2n_2^2+(2-3n_2)(n_1-n_2)n_1}{8n_1n_2}\log\left(x+\frac{n_1}{n_2}-1\right) \\ &-\frac{1}{4}\log\left(x+\frac{n_1-n_2}{2n_2}\right) \end{aligned} \tag{C.6}$$

JHEP05(2022)106

	$O^{(0)}_{[2]}$	$O^{(1+)}_{[2]}$	$O^{(1-)}_{[2]}$	$O^{(2)}_{[2]}$
$\{r,s\}$	$\{0,0\}$	$\{1,0\}$	$\{0,1\}$	$\{1,1\}$

Table 2. Parameters r, s for different NS chirals.

apart from a constant which we fix later by looking at OPE limits of the final correlator. Combining (C.5) with (4.13)–(C.6), we obtain the final result (4.14).

D List of double-cycle four-point functions

Here we list a collection of selected examples of functions $A^{\alpha\beta|\check{\sigma}\hat{\varrho}|\check{\sigma}\check{\varrho}}_{n_1,n_2}(x)$ and $A^{\text{int}|\check{\sigma}\hat{\varrho}|\check{\sigma}\check{\varrho}}_{n_1,n_2}(x)$. For economy of space, we omit the arguments of the fields.

Functions with NS chirals

$$\begin{aligned}
\left\langle\left[\bar{O}^{(0,0)}_{[n_1]}\bar{O}^{(0,0)}_{[n_2]}\right]\bar{O}^{(0,0)}_{[2]}O^{(0,0)}_{[2]}\left[O^{(0,0)}_{[n_1]}O^{(0,0)}_{[n_2]}\right]\right\rangle &= -\frac{1}{4n_1}\frac{(1-x)^2}{x+\frac{n_1-n_2}{2n_2}}\\
\left\langle\left[\bar{O}^{(2,2)}_{[n_1]}\bar{O}^{(2,2)}_{[n_2]}\right]\bar{O}^{(0,0)}_{[2]}O^{(0,0)}_{[2]}\left[O^{(2,2)}_{[n_1]}O^{(2,2)}_{[n_2]}\right]\right\rangle &= -\frac{1}{4n_1}\frac{\left(x+\frac{n_1}{n_2}\right)^2}{x+\frac{n_1-n_2}{2n_2}}\\
\left\langle\left[\bar{O}^{(1\pm,1\pm)}_{[n_1]}\bar{O}^{(1\pm,1\pm)}_{[n_2]}\right]\bar{O}^{(0,0)}_{[2]}O^{(0,0)}_{[2]}\left[O^{(1\pm,1\pm)}_{[n_1]}O^{(1\pm,1\pm)}_{[n_2]}\right]\right\rangle &= -\frac{1}{4n_1}\frac{\left(x+\frac{n_1}{n_2}\right)(x-1)}{x+\frac{n_1-n_2}{2n_2}}\\
\left\langle\left[\bar{O}^{(2,2)}_{[n_1]}\bar{O}^{(0,0)}_{[n_2]}\right]\bar{O}^{(0,0)}_{[2]}O^{(0,0)}_{[2]}\left[O^{(2,2)}_{[n_1]}O^{(0,0)}_{[n_2]}\right]\right\rangle &= -\frac{1}{4n_1}\frac{x^2}{x+\frac{n_1-n_2}{2n_2}}\\
\left\langle\left[\bar{O}^{(1\pm,1\pm)}_{[n_1]}\bar{O}^{(1\mp,1\mp)}_{[n_2]}\right]\bar{O}^{(0,0)}_{[2]}O^{(0,0)}_{[2]}\left[O^{(1\pm,1\pm)}_{[n_1]}O^{(1\mp,1\mp)}_{[n_2]}\right]\right\rangle &= -\frac{1}{4n_1}\frac{x\left(x-1+\frac{n_1}{n_2}\right)}{x+\frac{n_1-n_2}{2n_2}}\\
\left\langle\left[\bar{O}^{(0,0)}_{[n_1]}\bar{O}^{(0,0)}_{[n_2]}\right]\bar{O}^{(1+,1+)}_{[2]}O^{(1+,1+)}_{[2]}\left[O^{(0,0)}_{[n_1]}O^{(0,0)}_{[n_2]}\right]\right\rangle &= \frac{1}{16n_1^2}\frac{x(x-1)^4\left(x+\frac{n_1-n_2}{n_2}\right)}{\left(x+\frac{n_1-n_2}{2n_2}\right)^4}\\
\left\langle\left[\bar{O}^{(2,2)}_{[n_1]}\bar{O}^{(2,2)}_{[n_2]}\right]\bar{O}^{(1+,1+)}_{[2]}O^{(1+,1+)}_{[2]}\left[O^{(2,2)}_{[n_1]}O^{(2,2)}_{[n_2]}\right]\right\rangle &= \frac{1}{16n_1^2}\frac{x\left(x+\frac{n_1}{n_2}\right)^4\left(x+\frac{n_1-n_2}{n_2}\right)}{\left(x+\frac{n_1-n_2}{2n_2}\right)^4}
\end{aligned} \tag{D.1}$$

Functions with Ramond ground states and NS chirals. With parameters (r,s) such that the NS chirals are given by the choices in table 2,

$$A^{\zeta_1\zeta_2;(p)}_{n_1,n_2}(v,\bar{v}) = \left\langle [R^{\zeta_1}_{[n_1]}R^{\zeta_2}_{[n_2]}]^\dagger(\infty)O^{(p,p)\dagger}_{[2]}(1)O^{(p,p)}_{[2]}(v,\bar{v})[R^{\zeta_1}_{[n_1]}R^{\zeta_2}_{[n_2]}](0)\right\rangle \tag{D.2}$$

is given by formula (4.14) as

$$\begin{aligned}
A^{++(p)}_{n_1,n_2}(x) = C\,x^{-\frac{n_1-n_2}{2}}(x-1)^{\frac{n_1+n_2-2(r+s)}{2}}\left(x+\frac{n_1}{n_2}\right)^{-\frac{n_1+n_2-4-2s+s}{2}}\\
\times\left(x-1+\frac{n_1}{n_2}\right)^{\frac{n_1-n_2}{2}}\left(x+\frac{n_1-n_2}{2}\right)^{-1-r(r+1)-s(s+1)}
\end{aligned} \tag{D.3}$$

JHEP05(2022)106

$$A^{+-(p)}_{n_1,n_2}(x) = C\,x^{-\frac{n_1-n_2-4-2(r+s)}{2}}(x-1)^{\frac{n_1+n_2}{2}}\left(x+\frac{n_1}{n_2}\right)^{-\frac{n_1+n_2-2r(r+1)-2s(s+1)}{2}} \times\left(x-1+\frac{n_1}{n_2}\right)^{\frac{n_1-n_2-2(r+s)}{2}}\left(x+\frac{n_1-n_2}{2}\right)^{-1-r(r+1)-s(s+1)} \tag{D.4}$$

$$A^{\dot{1}+(p)}_{n_1,n_2}(x) = C\,x^{-\frac{n_1-n_2-2r}{2}}(x-1)^{\frac{n_1+n_2-2s}{2}}\left(x+\frac{n_1}{n_2}\right)^{-\frac{n_1+n_2-2r(r+1)-2s(s+1)}{2}} \times\left(x-1+\frac{n_1}{n_2}\right)^{\frac{n_1-n_2+2+2r}{2}}\left(x+\frac{n_1-n_2}{2}\right)^{-1-r(r+1)-s(s+1)} \tag{D.5}$$

$$A^{\dot{1}-(0)}_{n_1,n_2}(x) = C\,x^{-\frac{n_1-n_2-2-2s}{2}}(x-1)^{\frac{n_1+n_2+2}{2}}\left(x+\frac{n_1}{n_2}\right)^{-\frac{n_1+n_2-2r(r+1)-2s(s+1)}{2}} \times\left(x-1+\frac{n_1}{n_2}\right)^{\frac{n_1-n_2-2s}{2}}\left(x+\frac{n_1-n_2}{2}\right)^{-1-r(r+1)-s(s+1)} \tag{D.6}$$

$$A^{\dot{1}\dot{1}(0)}_{n_1,n_2}(x) = C\,x^{-\frac{n_1-n_2}{2}}(x-1)^{\frac{n_1+n_2+2+2(r-s)}{2}}\left(x+\frac{n_1}{n_2}\right)^{-\frac{n_1+n_2-2}{2}} \times\left(x-1+\frac{n_1}{n_2}\right)^{\frac{n_1-n_2}{2}}\left(x+\frac{n_1-n_2}{2}\right)^{-1-r(r+1)-s(s+1)} \tag{D.7}$$

$$A^{\dot{1}\dot{2}(0)}_{n_1,n_2}(x) = C\,x^{-\frac{n_1-n_2-2}{2}}(x-1)^{\frac{n_1+n_2}{2}}\left(x+\frac{n_1}{n_2}\right)^{-\frac{n_1+n_2}{2}} \times\left(x-1+\frac{n_1}{n_2}\right)^{\frac{n_1-n_2+2}{2}}\left(x+\frac{n_1-n_2}{2}\right)^{-1} \tag{D.8}$$

References

[1] S. Giusto, R. Russo and C. Wen, *Holographic correlators in AdS_3*, *JHEP* **03** (2019) 096 [arXiv:1812.06479] [INSPIRE].

[2] S. Giusto, R. Russo, A. Tyukov and C. Wen, *Holographic correlators in AdS_3 without Witten diagrams*, *JHEP* **09** (2019) 030 [arXiv:1905.12314] [INSPIRE].

[3] L. Rastelli, K. Roumpedakis and X. Zhou, *$AdS_3 \times S^3$ Tree-Level Correlators: Hidden Six-Dimensional Conformal Symmetry*, *JHEP* **10** (2019) 140 [arXiv:1905.11983] [INSPIRE].

[4] L. Eberhardt and M.R. Gaberdiel, *String theory on AdS_3 and the symmetric orbifold of Liouville theory*, *Nucl. Phys. B* **948** (2019) 114774 [arXiv:1903.00421] [INSPIRE].

[5] L. Eberhardt, M.R. Gaberdiel and R. Gopakumar, *The Worldsheet Dual of the Symmetric Product CFT*, *JHEP* **04** (2019) 103 [arXiv:1812.01007] [INSPIRE].

[6] L. Eberhardt, M.R. Gaberdiel and R. Gopakumar, *Deriving the AdS_3/CFT_2 correspondence*, *JHEP* **02** (2020) 136 [arXiv:1911.00378] [INSPIRE].

[7] M.R. Gaberdiel, R. Gopakumar, B. Knighton and P. Maity, *From symmetric product CFTs to AdS_3*, *JHEP* **05** (2021) 073 [arXiv:2011.10038] [INSPIRE].

JHEP05(2022)106

[8] A. Galliani, S. Giusto, E. Moscato and R. Russo, *Correlators at large c without information loss*, *JHEP* **09** (2016) 065 [arXiv:1606.01119] [INSPIRE].

[9] A. Galliani, S. Giusto and R. Russo, *Holographic 4-point correlators with heavy states*, *JHEP* **10** (2017) 040 [arXiv:1705.09250] [INSPIRE].

[10] A. Bombini, A. Galliani, S. Giusto, E. Moscato and R. Russo, *Unitary 4-point correlators from classical geometries*, *Eur. Phys. J. C* **78** (2018) 8 [arXiv:1710.06820] [INSPIRE].

[11] J. Tian, J. Hou and B. Chen, *Holographic Correlators on Integrable Superstrata*, *Nucl. Phys. B* **948** (2019) 114766 [arXiv:1904.04532] [INSPIRE].

[12] A. Bombini and A. Galliani, *AdS_3 four-point functions from $\frac{1}{8}$ -BPS states*, *JHEP* **06** (2019) 044 [arXiv:1904.02656] [INSPIRE].

[13] S. Giusto, R. Russo, A. Tyukov and C. Wen, *The CFT_6 origin of all tree-level 4-point correlators in $AdS_3 \times S^3$*, *Eur. Phys. J. C* **80** (2020) 736 [arXiv:2005.08560] [INSPIRE].

[14] N. Ceplak, S. Giusto, M.R.R. Hughes and R. Russo, *Holographic correlators with multi-particle states*, *JHEP* **09** (2021) 204 [arXiv:2105.04670] [INSPIRE].

[15] O. Lunin and S.D. Mathur, *AdS/CFT duality and the black hole information paradox*, *Nucl. Phys. B* **623** (2002) 342 [hep-th/0109154] [INSPIRE].

[16] K. Skenderis and M. Taylor, *The fuzzball proposal for black holes*, *Phys. Rept.* **467** (2008) 117 [arXiv:0804.0552] [INSPIRE].

[17] K. Skenderis and M. Taylor, *Fuzzball solutions and D1-D5 microstates*, *Phys. Rev. Lett.* **98** (2007) 071601 [hep-th/0609154] [INSPIRE].

[18] I. Kanitscheider, K. Skenderis and M. Taylor, *Fuzzballs with internal excitations*, *JHEP* **06** (2007) 056 [arXiv:0704.0690] [INSPIRE].

[19] I. Kanitscheider, K. Skenderis and M. Taylor, *Holographic anatomy of fuzzballs*, *JHEP* **04** (2007) 023 [hep-th/0611171] [INSPIRE].

[20] M. Taylor, *Matching of correlators in AdS_3/CFT_2*, *JHEP* **06** (2008) 010 [arXiv:0709.1838] [INSPIRE].

[21] S. Giusto, E. Moscato and R. Russo, *AdS_3 holography for 1/4 and 1/8 BPS geometries*, *JHEP* **11** (2015) 004 [arXiv:1507.00945] [INSPIRE].

[22] S. Rawash and D. Turton, *Supercharged AdS_3 Holography*, *JHEP* **07** (2021) 178 [arXiv:2105.13046] [INSPIRE].

[23] S. Giusto, S. Rawash and D. Turton, *Ads_3 holography at dimension two*, *JHEP* **07** (2019) 171 [arXiv:1904.12880] [INSPIRE].

[24] J. Garcia i Tormo and M. Taylor, *Correlation functions in the D1-D5 orbifold CFT*, *JHEP* **06** (2018) 012 [arXiv:1804.10205] [INSPIRE].

[25] A.L. Fitzpatrick, J. Kaplan and M.T. Walters, *Universality of Long-Distance AdS Physics from the CFT Bootstrap*, *JHEP* **08** (2014) 145 [arXiv:1403.6829] [INSPIRE].

[26] A.L. Fitzpatrick, J. Kaplan and M.T. Walters, *Virasoro Conformal Blocks and Thermality from Classical Background Fields*, *JHEP* **11** (2015) 200 [arXiv:1501.05315] [INSPIRE].

[27] A.L. Fitzpatrick and J. Kaplan, *Conformal Blocks Beyond the Semi-Classical Limit*, *JHEP* **05** (2016) 075 [arXiv:1512.03052] [INSPIRE].

JHEP05(2022)106

[28] A.L. Fitzpatrick, J. Kaplan, D. Li and J. Wang, *On information loss in AdS_3/CFT_2*, *JHEP* **05** (2016) 109 [arXiv:1603.08925] [INSPIRE].

[29] E. Hijano, P. Kraus and R. Snively, *Worldline approach to semi-classical conformal blocks*, *JHEP* **07** (2015) 131 [arXiv:1501.02260] [INSPIRE].

[30] E. Hijano, P. Kraus, E. Perlmutter and R. Snively, *Semiclassical Virasoro blocks from AdS_3 gravity*, *JHEP* **12** (2015) 077 [arXiv:1508.04987] [INSPIRE].

[31] K.B. Alkalaev and V.A. Belavin, *Classical conformal blocks via AdS/CFT correspondence*, *JHEP* **08** (2015) 049 [arXiv:1504.05943] [INSPIRE].

[32] B. Carneiro da Cunha and M. Guica, *Exploring the BTZ bulk with boundary conformal blocks*, arXiv:1604.07383 [INSPIRE].

[33] A. Pakman, L. Rastelli and S.S. Razamat, *Diagrams for Symmetric Product Orbifolds*, *JHEP* **10** (2009) 034 [arXiv:0905.3448] [INSPIRE].

[34] R. Cavalieri and E. Miles, *Riemann Surfaces and Algebraic Curves: A First Course in Hurwitz Theory*, London Mathematical Society Student Texts, Cambridge University Press, Cambridge, U.K. (2016), [DOI].

[35] J.R. David, G. Mandal and S.R. Wadia, *Microscopic formulation of black holes in string theory*, *Phys. Rept.* **369** (2002) 549 [hep-th/0203048] [INSPIRE].

[36] S.G. Avery, B.D. Chowdhury and S.D. Mathur, *Deforming the D1D5 CFT away from the orbifold point*, *JHEP* **06** (2010) 031 [arXiv:1002.3132] [INSPIRE].

[37] O. Lunin and S.D. Mathur, *Correlation functions for M^N/S_N orbifolds*, *Commun. Math. Phys.* **219** (2001) 399 [hep-th/0006196] [INSPIRE].

[38] O. Lunin and S.D. Mathur, *Three point functions for M^N/S_N orbifolds with $N = 4$ supersymmetry*, *Commun. Math. Phys.* **227** (2002) 385 [hep-th/0103169] [INSPIRE].

[39] A. Dei and L. Eberhardt, *Correlators of the symmetric product orbifold*, *JHEP* **01** (2020) 108 [arXiv:1911.08485] [INSPIRE].

[40] A.A. Lima, G.M. Sotkov and M. Stanishkov, *Correlation functions of composite Ramond fields in deformed D1-D5 orbifold $SCFT_2$*, *Phys. Rev. D* **102** (2020) 106004 [arXiv:2006.16303] [INSPIRE].

[41] A.A. Lima, G.M. Sotkov and M. Stanishkov, *On the dynamics of protected ramond ground states in the D1-D5 CFT*, *JHEP* **07** (2021) 120 [arXiv:2103.04459] [INSPIRE].

[42] A. Jevicki, M. Mihailescu and S. Ramgoolam, *Gravity from CFT on S^N_X: Symmetries and interactions*, *Nucl. Phys. B* **577** (2000) 47 [hep-th/9907144] [INSPIRE].

[43] A. Dabholkar and A. Pakman, *Exact chiral ring of AdS_3/CFT_2*, *Adv. Theor. Math. Phys.* **13** (2009) 409 [hep-th/0703022] [INSPIRE].

[44] A. Pakman, L. Rastelli and S.S. Razamat, *Extremal Correlators and Hurwitz Numbers in Symmetric Product Orbifolds*, *Phys. Rev. D* **80** (2009) 086009 [arXiv:0905.3451] [INSPIRE].

[45] A. Schwimmer and N. Seiberg, *Comments on the $N = 2$, $N = 3$, $N = 4$ Superconformal Algebras in Two-Dimensions*, *Phys. Lett. B* **184** (1987) 191 [INSPIRE].

[46] L.J. Dixon, D. Friedan, E.J. Martinec and S.H. Shenker, *The Conformal Field Theory of Orbifolds*, *Nucl. Phys. B* **282** (1987) 13 [INSPIRE].

JHEP05(2022)106

[47] B. Sagan, *The symmetric group: representations, combinatorial algorithms, and symmetric functions*, vol. 203 of *Graduate Texts in Mathematics*, 2 ed., Springer-Verlag, New York, U.S.A. (2001).

[48] G.E. Arutyunov and S.A. Frolov, *Virasoro amplitude from the S^N R^{24} orbifold sigma model*, *Theor. Math. Phys.* **114** (1998) 43 [hep-th/9708129] [INSPIRE].

[49] A. Pakman, L. Rastelli and S.S. Razamat, *A Spin Chain for the Symmetric Product CFT(2)*, *JHEP* **05** (2010) 099 [arXiv:0912.0959] [INSPIRE].

[50] I. Bena, S. Giusto, R. Russo, M. Shigemori and N.P. Warner, *Habemus Superstratum! A constructive proof of the existence of superstrata*, *JHEP* **05** (2015) 110 [arXiv:1503.01463] [INSPIRE].

[51] G.E. Arutyunov and S.A. Frolov, *Four graviton scattering amplitude from S**N R^8 supersymmetric orbifold sigma model*, *Nucl. Phys. B* **524** (1998) 159 [hep-th/9712061] [INSPIRE].

[52] S.G. Avery, *Using the D1D5 CFT to Understand Black Holes*, other thesis, (2010) [arXiv:1012.0072] [INSPIRE].

[53] A.A. Lima, G.M. Sotkov and M. Stanishkov, *Renormalization of twisted Ramond fields in D1-D5 SCFT$_2$*, *JHEP* **03** (2021) 202 [arXiv:2010.00172] [INSPIRE].

[54] S.G. Avery, B.D. Chowdhury and S.D. Mathur, *Emission from the D1D5 CFT*, *JHEP* **10** (2009) 065 [arXiv:0906.2015] [INSPIRE].

[55] P. Francesco, P. Mathieu and D. Sénéchal, *Conformal field theory*, Springer Science & Business Media, Germany (2012).

[56] T. De Beer, B.A. Burrington, I.T. Jardine and A.W. Peet, *The large N limit of OPEs in symmetric orbifold CFTs with $\mathcal{N} = (4, 4)$ supersymmetry*, *JHEP* **08** (2019) 015 [arXiv:1904.07816] [INSPIRE].

[57] B. Guo and S. Hampton, *Partial Spectral Flow in the D1D5 CFT*, arXiv:2112.10573 [INSPIRE].

[58] B.A. Burrington, A.W. Peet and I.G. Zadeh, *Operator mixing for string states in the D1-D5 CFT near the orbifold point*, *Phys. Rev. D* **87** (2013) 106001 [arXiv:1211.6699] [INSPIRE].

[59] O. Lunin and S.D. Mathur, *Metric of the multiply wound rotating string*, *Nucl. Phys. B* **610** (2001) 49 [hep-th/0105136] [INSPIRE].

[60] O. Lunin and S.D. Mathur, *A toy black hole S-matrix in the D1-D5 CFT*, *JHEP* **02** (2013) 083 [arXiv:1211.5830] [INSPIRE].

[61] S. Giusto, S.D. Mathur and A. Saxena, *Dual geometries for a set of 3-charge microstates*, *Nucl. Phys. B* **701** (2004) 357 [hep-th/0405017] [INSPIRE].

[62] S. Giusto, S.D. Mathur and A. Saxena, *3-charge geometries and their CFT duals*, *Nucl. Phys. B* **710** (2005) 425 [hep-th/0406103] [INSPIRE].

[63] B.A. Burrington, A.W. Peet and I.G. Zadeh, *Bosonization, cocycles, and the D1-D5 CFT on the covering surface*, *Phys. Rev. D* **93** (2016) 026004 [arXiv:1509.00022] [INSPIRE].

JHEP05(2022)106